Online incipient detection and localisation for low voltage faults in oil impregnated paper cables

van Luijk, N.G.

Award date:
2002

technische universiteit eindhoven

Capaciteitsgroep Elektrische Energietechniek
Electrical Power Systems

Online Incipient Detection and Localisation for Low Voltage Faults in Oil Impregnated Paper Cables

door: N.G. van Luijk
EPS.02.A.165

Afstudeerwerk verricht o.l.v.:

prof.dr.ir. E.F. Steennis
dr. P.A.A.F. Wouters

juli 2002

/ faculteit elektrotechniek

Abstract

Low voltage mass impregnated paper insulated cables have well surpassed their life expectancy and are still widely in use today. Replacement of these cables is a long term project as there is a vast amount installed in the London network (more than 20.000km). A large part of the cables are still in healthy condition and so from a financial point of view, keeping these cables in operation so long as they remain healthy, is more cost effective than replacing when unnecessary. Managing these assets becomes crucial to the network performance as oil impregnated cables start to cause faults more often than the more recently installed extruded cables. A better understanding is needed of the behaviour of low voltage oil impregnated paper cables in fault conditions caused by a failure in the cable itself, to develop ways for monitoring these cables online.

Most faults in low voltage paper insulated cables are a result of moisture ingress, which is caused by damage to the water protective sheath. The moisture will cause the properties of the insulation to change slowly and at some point will result in a sudden breakdown of the insulation, causing a low voltage arc. This arc tends to exist only for a short period of time, which is not sufficient to cause the fuse protection to react. In time the fault will develop further and will allow the low voltage arc to become repetitive, eventually leading to a fuse trip. This consequently results in a low voltage fault.

To understand the behaviour of the low voltage arc, experiments were conducted on a test circuit to see what the effects are of an arc on the system. Besides the arcing phenomena, another phenomenon, sparking, was detected. Moisture causes sparking in the same way that it can cause an arc to ignite. The sparking is a continuous event for as long as there is an organic substance polluting the fault location, and sparking can deteriorate the insulation significantly. Although sparking suggests a fault presence and development, it does not indicate or predict the failure of the insulation or the ignition of an arc.

The results of the simulated tests show that arc detection is possible even on long distance circuits, making incipient fault detection possible. Using the recording data to detect the low voltage arc it is even possible to make a localisation of the fault with an accuracy of better than 10%. Sparking is not detectable though, as the discharges are too small to be measured on a long circuit with numerous T-joints.

Using the found results it is possible to detect arcing and localise the fault using impedance calculations by means of low cost recording equipment. This makes it viable to implement an inexpensive way of asset management and improving the networks performance.

Samenvatting

Sinds de uitvinding van olie geïmpregneerde papieren kabel zijn er tienduizenden kilometers van deze kabel geïnstalleerd (in Londen alleen al 20.000 km). Het merendeel van deze kabels is zijn verwachte levensduur al ruim gepasseerd en vervanging is een lange termijn project. Het is dus van belang om deze onderdelen van het netwerk te monitoren om een bedrijfszeker netwerk te kunnen garanderen. Vanuit een financieel oogpunt is het interessant om deze kabels tot het uiterste van hun levensduur te exploiteren om zo het maximale uit de investeringskosten te halen. Om dit te bereiken is beter inzicht nodigvan het gedrag gedurende een fout in de kabel.

De meeste fouten in olie geïmpregneerde papieren kabels worden veroorzaakt door het indringen van water. Dit is direct het gevolg van een beschadiging aan de waterwerende mantel. Het indringen van water veroorzaakt een verandering in diëlektrische eigenschappen van de isolatie, wat kan leiden tot onmiddellijke doorslag in de vorm van een laagspanningboog. Smeltveiligheden zullen vaak niet aanspreken omdat de tijdsduur van de boog zeer kort is (enkele milliesecondes), waardoor er geen onderbreking in de elektriciteitsvoorziening plaats vindt. De fout zal in de tijd langzaam ontwikkelen tot een repeterende fout, die op den duur een smeltveiligheid zal aanspreken. Het aanspreken van een beveiliging veroorzaakt een onderbreking in de elektriciteitsvoorziening, in dit geval wordt er gesproken van een laagspannings fout

Om een beter idee te krijgen in het gedrag van laagspanningsfouten is het nodig om het effect van een laagspanningsboog in olie geïmpregneerde papieren kabel te onderzoeken. Door verschillende experimenten uit te voeren is het mogelijk het gedrag van laagspanningsfouten te simuleren in een gecontroleerde omgeving. Dit heeft niet alleen geleid tot het detecteren van laagspanningsbogen maar ook tot het waarnemen van een vonk fenomeen. Het vonken en de laagspanningsbogen wordt hoofdzakelijk veroorzaakt door de aanwezigheid van water of vocht in de papieren isolatie. In tegenstelling tot de laagspanningsbogen is het vonk fenomeen een continu process, zolang er vocht aanwezig is in de isolatie. Het vonken geeft aan dat er een fout in de kabel aan het ontwikkelingen is, maar heeft geen relatie tot het voorspellen van een laagspanningsboog. Het ontsteken van een boog is dan ook niet dereikt gecolleleerd met het vonk fenomeen.

De resultaten van de gesimuleerde experimenten tonen aan dat het mogelijk is om laagspanningsbogen te detecteren, zelfs in circuits met lange kabellengtes. Dit maakt het mogelijk om een beginnende fout te detecteren voordat deze een smeltveiligheid aanspreekt. Het vonk effect daarentegen is niet detecteerbaar op lange kabels, door hun lage amplitude en de aanwezigheid een grote hoeveelheid T-splitsingen.

Uit de data gemeten tijdens de laagspanningsboog is het mogelijk om een lokalisatie van de fout op de kabel te geven met behulp van impedantie berekeningen met een foutmarge van beter dan 10%. Het toepassen van de resultaten maakt het mogelijk om laagspanningsbogen te detecteren en te lokaliseren met behulp van goedkope meetapparatuur, wat het mogelijk maakt om tegen geringe investeringskosten het netwerk goedkoper en bedrijfszekerder te bedrijven.

Content

1 Introduction

1.1 Background

Underground electrical distribution cables are one of the most vital components in a metropolitan electricity network, and utility companies are even keener to find and apply techniques to monitor these cables as most of the existing electrical cables have passed their expected life span.

Electricity became available as a commercial product in the nineteenth century, and distribution was limited to overhead lines. In the late eighteen hundreds the first underground electrical power cable was introduced which changed the way electricity was supplied and made underground distribution possible in a reliable way in London and other major cities around the world. Oil impregnated paper lead sheath cable (PILC/PILS) was later introduced and thousands of kilometres have subsequently been installed. Through the years construction and properties of oil impregnated paper cables have changed quite considerably making high dielectric losses as experienced in the early days belong to the past. Although PILC and PILS are still made today, London Electricity took the decision in the beginning of 1970 to install a different type of paper cable, the oil impregnated paper aluminium sheath cable (CONSAC) and extruded XLPE cable. However, only a limited amount of CONSAC was installed, as preference was given to extruded cables (XLPE). The choice to go for XLPE turned out to be a good decision as the CONSAC cables started to have failures as a result of the brittle aluminium sheath caused by natural corrosion. The time line of the installation of different type of 240/415 Volts distribution is detailed below.

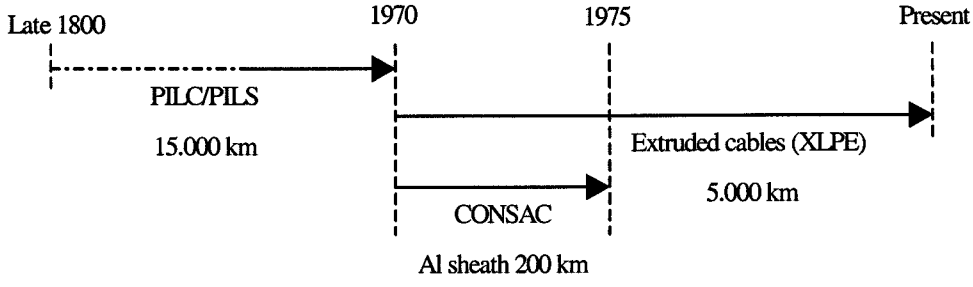

Figure 1-1 Timeline of low voltage cables used in London with their installed kilometres.

The paper cable installed in the early nineteen hundreds lasted well past its lifetime expectation and some of the cable dates back as far as the first oil impregnated cable. Whilst most of the oil impregnated paper cable is still performing reasonably well, the number of faults on low voltage oil impregnated paper cables is increasing.

If the failure rate is allowed to increase further, it will demand a greater stress on resources to keep the network performance within the targets, increasing the network operation costs significantly. A fault can usually be recovered fairly quickly because of the way the network has been built, using automated control systems, but this is only the case on the high and medium voltage part of the network at present.

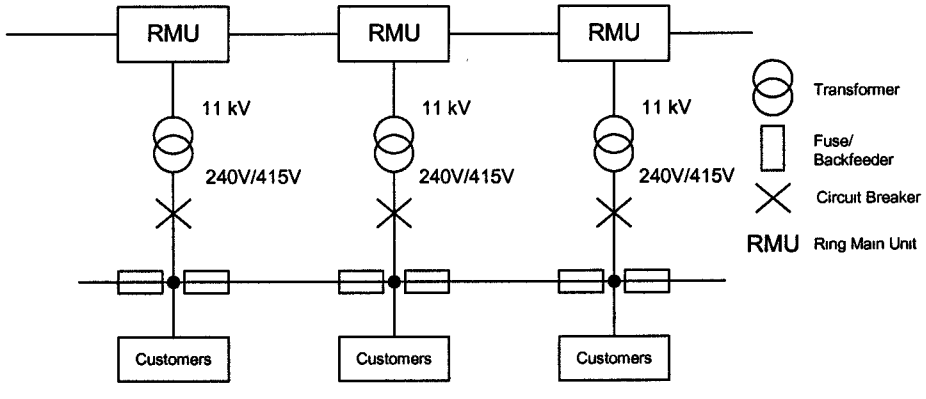

Figure 1-2 Build up of distribution network in London, the medium and low voltage side.

The network in London consists of 11 kV rings supplied from a 132 kV mains circuit. By using Ring Main Units (RMU) the supply sides to the low voltage transformers can be switched at the 11 kV side, giving a faster restoration time in the event of a fault. In a limited way the low voltage network is built up in the same way, only the ring is formed by back feeders from other circuits. Back feeding is not designed for continuous loading and therefore only gives limited time to restore the faulty circuit, see Figure 1-2

The fault recovery time at the medium voltage side has been improved in the last five years by using automated switching. At the low voltage side the recovery time is still lengthy since the substation needs to be visited and the fuse needs to be replaced manually. The fault cause at the low voltage side cannot normally be found immediately and often only the fuse is replaced.

Depending on the fault situation the fuse can blow again, either after a short time or a longer time. This process is repeated until there is a clear idea of what is causing the fault, leading to disruption on these circuits for customers. Although medium voltage faults cause disruption for more customers than low voltage faults, the number of faults and recovery time is much less. By improving the low voltage network performance, the reliability of the network can be improved and customer minutes lost can be kept down, as at present most of the disruptions occur on low voltage networks.

1.2 Aim of the work

The goal of this work is to find a solution for detecting and predicting low voltage faults in underground mass impregnated oil filled paper distribution cables at an affordable cost. This report contains the research work aimed to understand the behaviour of low voltage faults and of any incipient phenomena. Studies involved research into the behaviour of faults in low voltage oil impregnated paper cable in order to establish the relationships between the phase voltages, the phase current and any incipient phenomena before, during and after a low voltage fault.

1.3 Plan of approach

A better understanding of oil impregnated paper cables and their properties first need to be established, this data is widely available in literature. It is also important to have an understanding of fault location and pinpointing techniques that are currently available that could be of use or partly of use in this project.

To acquire data from low voltage faults, a test network has to be set up with the proper recording equipment to measure low voltage fault and incipient phenomena. The test network should contain 500 metres of cable to simulate long supply line and its effect. Oil impregnated paper cable samples are needed and prepared to make low voltage fault simulations. Additionally, recording units will be installed in the field to record real low voltage fault as comparison data to the simulated faults.

1.4 Outline of this report

Chapter 2 gives an overview of the properties of oil impregnated cables based on information that is available in literature. Also the influence of moisture and temperature on the insulation is considered.

A brief description of available fault monitoring, location and pinpointing techniques is given in Chapter 3, which is an important factor for the localisation of low voltage faults.

A description of the test network used and the results of the simulations conducted on the cable samples are given in Chapter 4.

In Chapter 5, background is given on incipient phenomena detected during the tests conducted in Chapter 4.

Recommendations to apply the findings on the networks are given in Chapter 6

Chapter 7 brings together the conclusion regarding the complete report.

Some ideas on future directions of research are summed up in Chapter 8.

2 Properties of Paper Cable

2.1 Cable build up

To manufacture oil impregnated cable, the copper or aluminium conductor will be wound with layers of paper. After this process, air and moisture needs to be removed separately by means of heat and vacuum both from the impregnant and the paper insulation. The cable is then wound on a steel drum and placed in a pressurised tank. The impregnant (oil) is fed into the tank at 125°C. This temperature will be maintained during the process. The pressure is raised in the tank and after the impregnation period, the tank is allowed to cool very slowly. After the impregnation period the metal sheathing and armour is added, finishing the cable either with a plastic or bitumised outer sheath.

There is a wide variety of installed low voltage oil impregnated paper cables, most of which are Paper Insulated Lead Covered (PILC) or Concentric Sheath Aluminium Conductor (CONSAC). There are a number of other types which are based on either PILC or CONSAC, for example, Paper Insulated Lead Sheathed (PILS) and Paper Insulated Aluminium Sheathed (PIAS). These cables may vary in build up but it can be assumed that their behaviour would be the same.

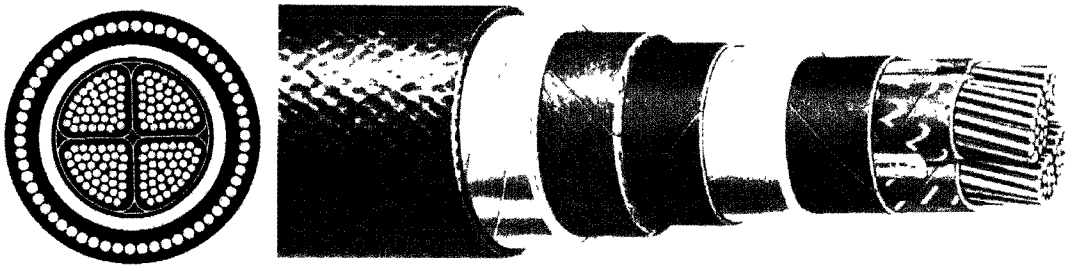

Figure 2-1 Cross section of a PILC cable.

The first oil impregnated PILC cable was based on a lead earth sheath. It was introduced as aluminium stranded four-core cable with a lead earth shield which could either be solid or sheathed. Figure 2-1 illustrates the cable build up. In this occurrence the armour consists of a steel tape but it can also be a steel wire variant. To prevent water ingress, the armour is imbedded in bitumised textiles.

Figure 2-2 Cross section of a CONSAC cable.

The CONSAC cable as shown in Figure 2-2 was introduced as a solid aluminium three-core cable with a solid aluminium earth shield which was used as combined earth and neutral. To prevent water ingress a bitumen layer is coated onto aluminium and concealed in a PVC outer sheath.

With the introduction of plastic extruded cables like XLPE, oil impregnated paper cables are not used for voltage ranges of 240 to 1000 Volts. These types are only be used in voltage ranges between 10 kV and 35 kV at present.

Appendix A and B give an overview of the properties of typical paper insulated distribution cable at different conductor areas.

2.2 Dielectric properties

All cables are subjected to dielectric losses. This is usually described by introducing complex dielectric properties as in equation 2-1. The real component causes the cable to behave as a capacitor; the imaginary component causes resistance like losses as illustrated in vector diagram Figure 2-3. The imaginary component acts like a conductivity of the dielectric. The complex dielectric permittivity can be written as [1]:

$$\varepsilon(\omega) = \varepsilon'(\omega) - j\varepsilon''(\omega) \tag{2-1}$$

To understand how the complex dielectric permittivity influences the current, the current is divided into two components, a pure capacitive component I_C, which is 90 degrees ahead of the applied voltage U, and a resistive component I_R which is in phase with the voltage U, shown in Figure 2-3.

$$\hat{I}(\omega) = j\omega\hat{U}(\omega)C_0\,[\varepsilon'(\omega) - j\,\varepsilon''(\omega)] \text{ or } I = I_R + jI_C \tag{2-2}$$

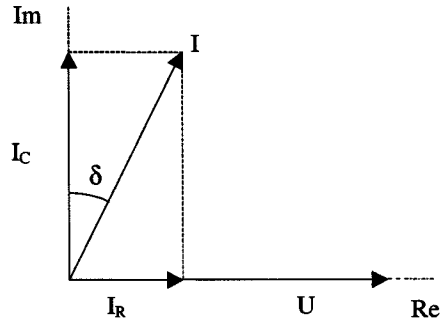

Figure 2-3 Vector diagram of voltage and current in a cable.

The angle between imaginary and real components is called the loss angle (tanδ) and can be written either as a function of the dielectric property or current as equation 2-3 shows.

$$\tan\delta = \frac{I_R}{I_C} = \frac{\varepsilon''(\omega)}{\varepsilon'(\omega)} \tag{2-3}$$

As equation 2-1 shows, changes in the dielectric permittivity will change the behaviour of the cable, and the condition of the cable can be determined by measuring the capacitive and resistive component of the current waveform using equation 2-3 from which the loss angle can be calculated.

In the following sections the effect of moisture and temperature on the dielectric are explained. In chapter 3.5.2 a brief explanation is given about the tanδ method to determine the state of a cable. Table 2-1 summarises typical dielectric values for electrical power cables.

Table 2-1 Overview of typical relative permittivity (ε) values of electrical insulation used in power cables [2].

Typical dielectric (ε) values	
PVC	3,3-4,5
EPR	3
PE	2,3
XLPE	2,5-3
Oil-Impregnated Paper	3,7-4,0

2.3 Influence of moisture

Impregnation of oil is a basic approach to protect cellulose paper from external moisture. It may be permanently effective if the oil-paper is isolated from ambient and other sources of moisture. Moisture in impregnated paper reacts in the same way as in unimpregnated paper, and since the main part of the total moisture content is held by the paper, only a small amount is dissolved in oil. Increased dielectric losses, increased conductivity and lowered breakdown strength are instant consequences of moisture in the cable. Besides the electrical changes in properties of the cable, moisture causes faster decomposition of cellulose. As illustrated in Figure 2-4, an increase in temperature increases the dielectric losses significantly at higher moisture contents.

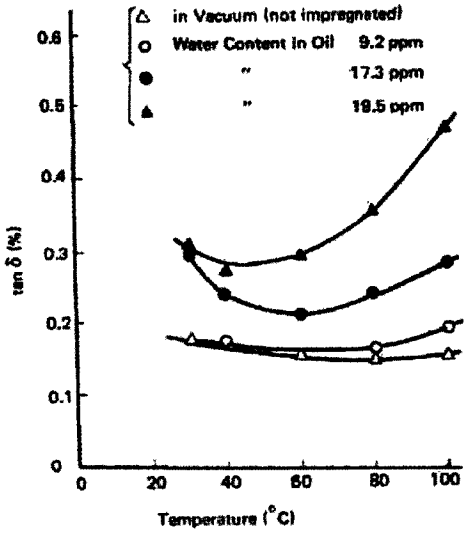

Figure 2-4 Effect of water content on the loss tangent of paper system at 50 Hz [3].

2.4 Influence of temperature

Temperature in oil impregnated paper cables is a very important aspect for their life expectation and failure rate. As the demand for electricity has increased significantly in the last hundred years, low voltage oil impregnated paper cables have seen their loads increase rapidly, resulting in higher operating temperatures. The conductor losses that cause the main temperature increase can be written as:

$$P = I^2 R \tag{2-4}$$

Higher operating temperatures have a positive effect on repelling moisture as Figure 2-5 shows. Papers affinity to water is lowered and is pressed out of the paper into the oil. The ability of oil to dissolve water increases at higher temperatures and therefore water rejected by the paper can be dissolved to some extent. However, this only lasts until the solubility of oil is reached [3]. Furthermore, oil will expand ten times more than copper when temperature increases. This will lead to pressurising of the cable, repelling water out of the cable. When the cable cools down, the pressure will drop in the cable and moisture can penetrate the cable easier. This explains why many failures happen after a cable have been taken off line and is re-energised.

Increased temperature also has negative impacts as the lead or aluminium sheath can be stretched permanently by the pressure of the expanding oil, causing a tiny empty volume between the paper insulation and the earth sheath when the temperature decreases. This gap will have a lower pressure than outside the cable surroundings and can lead to partial discharges at higher voltages, but also to pressures below atmosphere causing the cable to suck in water via leaking joints for instance.

Besides deformation of the cable itself, a rise in temperature also increases the dielectric loses. Although these loses are insignificant in the case of a healthy modern cable, in a cable with increased moisture content a rise in temperature has a considerable affect on the dielectric losses, see Figure 2-4. Equation 2-5 gives the power dissipation in the dielectric:

$$P = U^2 \omega C_0 \varepsilon_r \tan\delta \qquad (2\text{-}5)$$

Where U is the applied voltage, ω the angular frequency, C_0 is the geometric capacitance of the electrodes and tanδ is the loss angle. The power dissipation is proportional to the loss angle tanδ and the square root of the applied voltage U. As the loss angle tanδ is closely related to the moisture content in the cable, the power loss is a direct result of moisture ingress.

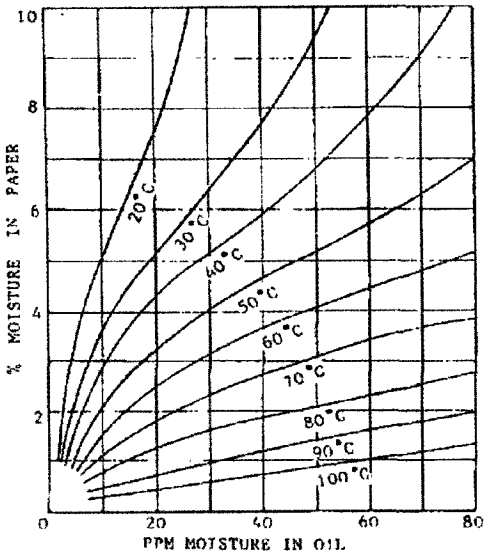

Figure 2-5 Moisture distribution in oil- paper insulation.

The increase in dielectric losses and dissipation losses results in a higher temperature which in itself will cause further degradation. If this process continues it may end in thermal breakdown of the insulation as Figure 2-6 illustrates. Within thermal stability limits, elevated temperatures still contribute to thermal ageing of the insulation. Oil impregnated cables have operation temperatures between 10°C and 80°C, but normally operate below 65°C. Operating at higher temperatures causes more rapid degradation of the cellulose chains. Normally this is a very slow process, but H_2O (Water) and O_2 (Oxygen) accelerate the chemical reactions two times faster for every 6°C increase [5].

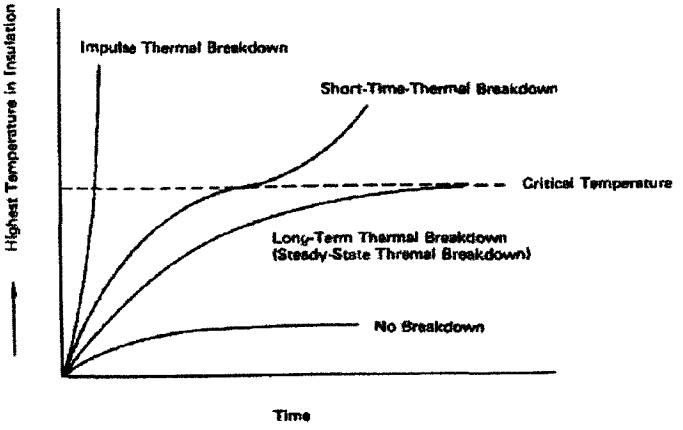

Figure 2-6 Representation of temperature increase(s) leading to insulation failure.

3 Fault monitoring and location

There is a wide variety of different methods available on the market for monitoring and pre-location of electrical faults in cables. Unfortunately, most of them are off-line methods, specifically those for extruded cables like XLPE or high voltage cables. In the event of a low voltage fault it is very difficult to use most of the methods mentioned below as the cables are permanently loaded with customers. To use any of the methods either all customers must be disconnected, or the method must lend itself to be used on loaded circuits without exceeding the limitations of the low voltage network.

In order to have a general definition of the state of a low voltage fault, faults can be divided into four categories, which make it easier to understand the condition a cable is in. A classification scheme of defined faults [5] can be set-up as followed:

- **High resistance fault:** A fault where the impedance of the fault from either the conductor to ground or conductor to another conductor is greater than 200 Ω.
- **Low resistance fault:** A fault where the impedance of the fault from either the conductor to ground or conductor to another conductor is less than 200 Ω.
- **Shunt fault:** A fault where the fault path is from the conductor to ground. In most cases the conductors and neutral are still intact (no interruption).
- **Series fault:** A fault where the conductors, neutral or both have been burned open (interruption).

Depending on the cable type and fault current the damage done by a fault can range from a small pinhole to complete destruction of the conductor(s). The type of fault will eventually result in a high or low resistance fault.

Low voltage fault location or pinpointing will always be limited by the presence of customers connected to the circuit. Disconnecting these customers physically from the circuit is virtually impossible as connection boxes are inside residential houses. Therefore a method to detect low voltage faults needs to be able to detect and localise faults without disturbing the network specifications.

The following sections will discuss a variety of detection, pre-localisation and pinpointing techniques which can be of significance for detecting low voltage fault or incipient fault behaviour. Although many techniques may not be applicable for low voltage fault and incipient detection, the fundamentals of these methods may be of use in low voltage detection, location and analysis equipment.

3.1 Partial discharge

Partial discharges are breakdown phenomena that do not completely bridge the distance between electrodes. Generally, three types of partial discharges can be distinguished [6]:

- **Internal discharges:** Occur in cavities in a solid dielectric, which are usually gas-filled.
- **Surface discharges:** Occur along dielectric interfaces where substantial tangential field strength is present. The interface is either gas or liquid bound.
- **Corona discharges:** Occur at sharp metallic points in an electric field.

The partial discharge method is based upon detection of small discharges in the insulation of the cable. As the dielectric is never without minor defects, these discharges will always occur, especially in medium voltage cables (PILC) or accessories of PILC and XLPE medium voltage cable systems. For XLPE cable these discharges usually occur in accessories or in aged cables. Small gas filled cavities can cause partial discharges. In these defects there will be an increased field strength. Apart from that, in a gas filled environment the breakdown voltage is lower than in a solid dielectric. At some point the defect will discharge, damaging the cavity and making it bigger.

The number of such inclusions has a tendency to increase during service operation for oil impregnated paper due to cellulose ageing, discharge activity, moistening as well as drying of insulation. At present this technique is only applied off-line, but is being developed further to use on live circuits.

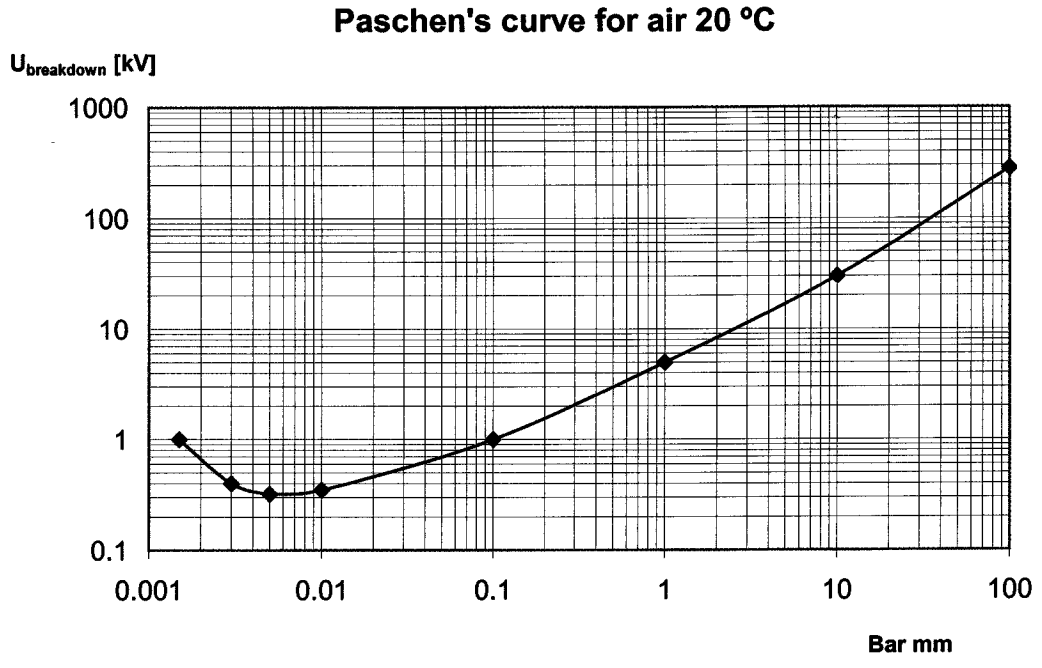

Figure 3-1 Paschen's Curve.

As Figure 3-1 shows, the Paschen curve gives the breakdown voltage of air as a function of pressure. In low voltage cables the field strength is too low to cause partial discharges even taking into account field enhancements in voids. However, moisture and the presence of carbon particles may increase the field strength above the partial discharge inception level, allowing discharges. This can also occur in low voltage cables, which could make discharge detection possible as well at this voltage level.

3.2 Pulse Echo/Time Domain Reflection

The pulse echo or time domain reflection method is based upon injecting a pulse into the cable and measuring the reflection of the fault. This reflection occurs when the fault has a low impedance Z_f with respect to the cable characteristic impedance Z_0. To do this type of measurement, the propagation speed of signals in the cable must be known.

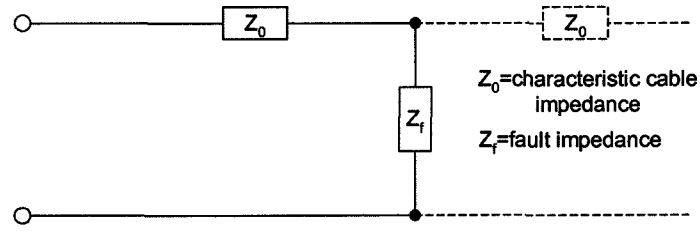

Figure 3-2 Simple circuit of a cable with a fault.

The propagation velocity v can be determined by injecting a pulse into a cable with known length s and measuring the time t between injection and reflection, as in equation 3-1. The distance needs to be divided by two, because the pulse travels up and down the cable.

$$s = \frac{v\,t}{2} \tag{3-1}$$

In practice the exact cable length is usually not known, but the dielectric constant ε may be sufficiently accurate as it is specified by the cable manufacturer, see Table 2-1. Using equation 3-2 the propagation velocity can then be calculated, in which v_c is the speed of light (300m/μs). The propagation velocity in a paper cable is about 180m/μs.

$$v = \frac{v_c}{\sqrt{\varepsilon}} \tag{3-2}$$

Knowing the propagation speed and the time between the pulse and its reflection, the distance of the fault in the cable can be determined.

To understand the propagation behaviour of a pulse a cable/line model is needed. In general, distribution lines and cables can be described in a four-parameter model: resistance (*R*), inductance (*L*), capacitance (*C*) and conductance (*G*) per length unit. Figure 3-3 illustrates the cable/line model.

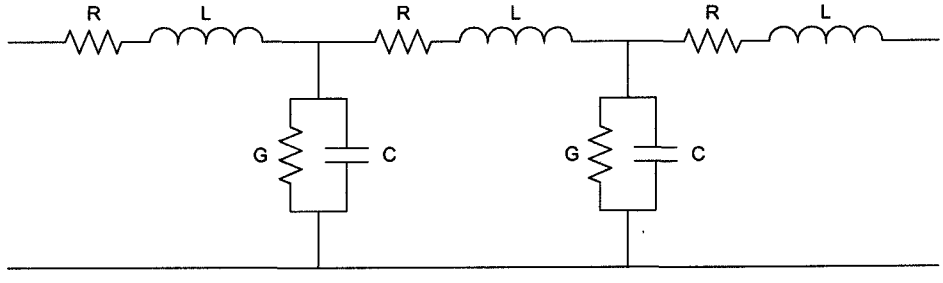

Figure 3-3 Electrical circuit of a transmission line.

To calculate the characteristic impedance Z_0 of the cable, equation 3-3 is used. For high frequency pulses the characteristic impedance can be simplified to equation 3-4.

$$Z_0 = \sqrt{\frac{R + j\,\omega\,L}{G + j\,\omega\,C}} \tag{3-3}$$

$$Z_0 = \sqrt{\frac{L}{C}} \tag{3-4}$$

When the pulse wave is reflected, a reverse wave is created. Both forward and reverse wave can be described as $u_{forward}$ and $u_{reverse}$. The same applies for the current. On the point of reflection the equation 3-5 and 3-6 are valid, which are based up on the law of Kirchoff.

$$u_0 = u_{forward} - u_{reverse} = i\,Z_0 \tag{3-5}$$

$$i = i_{forward} - i_{reverse} \tag{3-6}$$

When the equation for voltage as a function of current is formed for both waveforms, the results as in equation 3-7 and 3-8, show that the current of the reverse waveform will be of opposite polarity to the current of the forward waveform. An illustration of the forward and reverse waveforms is given in Figure 3-4. For a forward waveform both voltage and current are of the same polarity, for a reverse waveform the voltage and current are of opposite polarity.

$$u_{forward} = i_{forward}\,Z'_f \quad \text{or} \quad u_{forward} = u_0\,t_r \tag{3-7}$$

$$u_{reverse} = -i_{reverse}\,Z_0 \quad \text{or} \quad u_{reverse} = u_0\,r \tag{3-8}$$

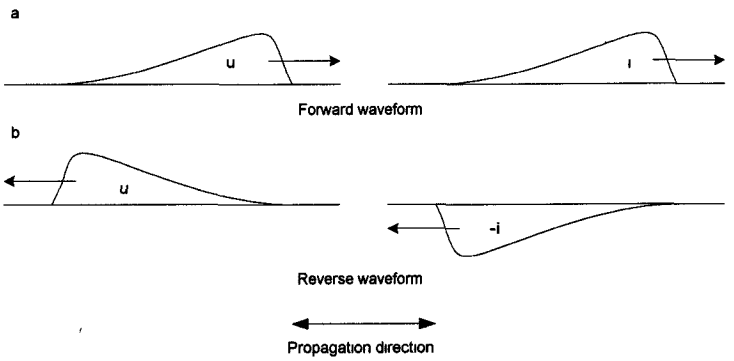

Figure 3-4 Representation forward waveform (a) and a reverse waveform (b)

An illustration of a waveform is shown in Figure 3-5. In reality there will often be multiple reflections from joints and T-joints. Also, the pulse is subjected to attenuation of the cable which filters out higher frequencies when the pulse(s) travel up and down the cable. This makes it more complicated to locate a fault, especially for low voltage networks as they have many T-joints.

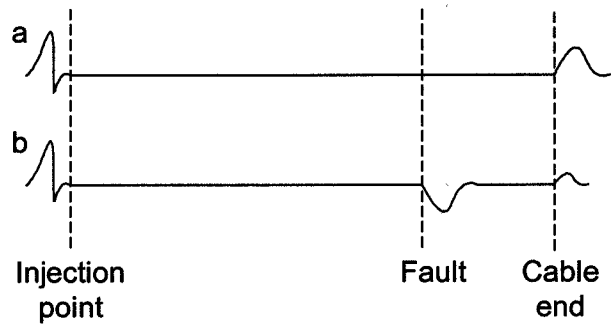

Figure 3-5 Example of measured waveform at injection point in event of an open circuit (a) and for a fault condition (b).

A pulse injected in a circuit will have reflection and transmission coefficients dependant on differences in impedance in the circuit, and can be described in equation 3-9 and 3-10 using [1, 7]. An illustration is given in Figure 3-6. Both fault impedance and characteristic impedance of the cable need to be taken into account when calculating the transmission and reflection.

$$r = \frac{Z'_f - Z_0}{Z'_f + Z_0} \tag{3-9}$$

$$t_r = \frac{2\,Z'_f}{Z'_f + Z_0} \tag{3-10}$$

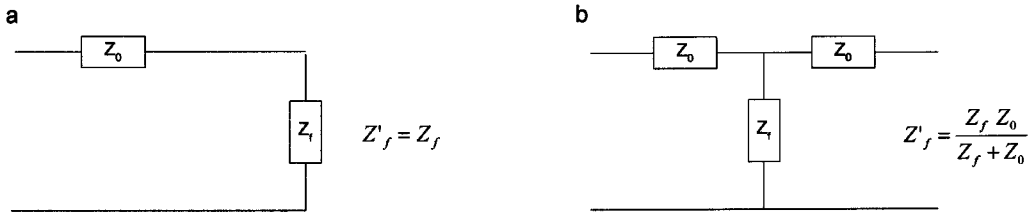

Figure 3-6 (a) Open end or termination at the end of a cable, (b) change in impedance at any point in the cable. In which Z_0 is the characteristic impedance, Z_f the fault impedance Z'_f the substitution impedance.

When there is an open circuit, the fault impedance Z'_f is 'infinite', resulting in a reflection that has the same polarity as the incoming pulse. Due to the propagation characteristics of the cable, the pulse will be filtered from its high frequencies. In the event of a short circuit fault, the fault impedance is zero; the pulse will be completely reflected with an opposite polarity.

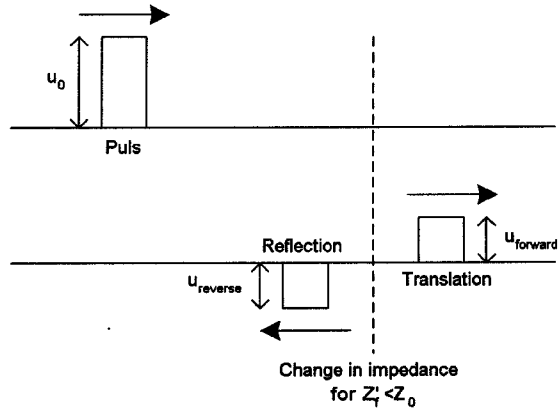

Figure 3-7 Voltage pulse behaviour at impedance discontinuity.

3.3 Arc reflection

The arc reflection method is based on the Pulse Echo/Time Domain reflection method, but in this case a high voltage source has been introduced which sends high voltage pulses into the cable. The pulse detection equipment is protected from these high voltage pulses by means of a filter. This method allows a high resistance fault to breakdown causing an arc. The reflection of the injected pulse (injected during breakdown of the fault) can be measured during the arc. This method should only be used as a last resort as it damages the fault even further. It has the same effect as a burn: a fault that becomes a series fault or a shunt fault by means of forcing large currents through the fault.

3.4 Resistance bridge

The resistance bridge is usually applied when there is a high resistance fault where neither Pulse echo/Time Domain reflection or Transient methods can be applied. The principle behind this method is illustrated in Figure 3-8.

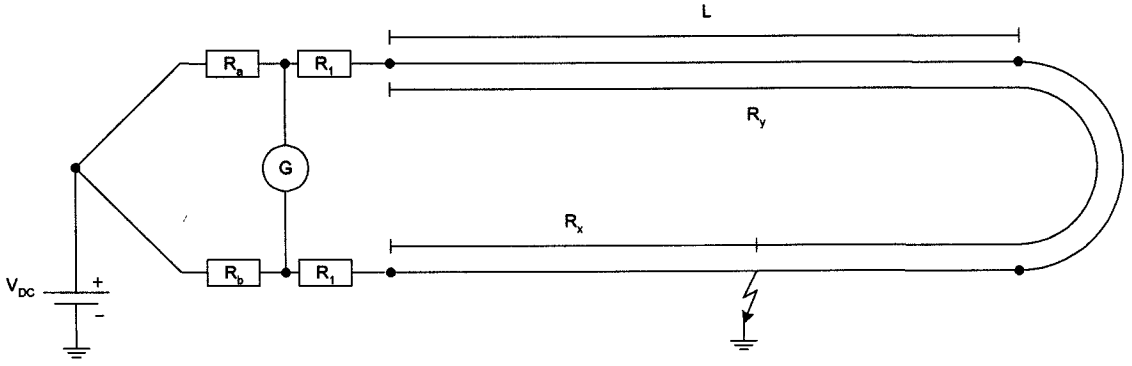

Figure 3-8 Schematic for set up of a Murray loop test

By making a connection at the end of the cable between a healthy core and the fault core, a loop is created. This configuration is called the Murray loop test. The balancing resistors (R_a) and (R_b) are adjusted in such a way that no current can be measured by the galvanometer/multimeter (G). The resistor value either determines the fault location by using the resistance per kilometre value of the cable supplied by the cable manufacturer, or by determining the loop resistance over a healthy core. The resistance of the test leads (R_1) from galvanometer/multimeter (G) must be taken into account as they can have a big influence on low resistance cables. Although this method is straightforward, accurate data needs to be known about the cable, the length of any cross sections and the resistance value, as these values determine the accuracy. Return paths due to the earth are also an unknown factor and can influence the measurement. Using equation 3-11 the resistance (R_x) to the fault can be calculated.

$$R_x = \frac{R_b(R_1 + R_y) - R_a R_1}{R_a} \tag{3-11}$$

To determine the distance to the fault, the resistance per metres is calculated from the loop resistance divided by the total length. Alternatively, it can be determined from the specification of the cable manufacturer and equation 3-12 in which R_{pm} is the resistance per metres.

$$x = \frac{R_x}{R_{pm}} \tag{3-12}$$

Besides this method there are other methods applicable, e.g. using more than one healthy core. All of these methods use the same basics of a balancing bridge as described above and all of them require an off-line network without any connected customers.

3.5 Dielectric measurements

3.5.1 DC leakage current method

DC leakage current measurements can be done off-line, or on-line using a more complex system (which uses the superposition principle). By applying a DC voltage between conductors or between conductor and screen, the leakage current can be measured. The healthy part of the cable will not contribute to the measured value. Local deterioration will cause a significantly larger current than the healthy part of the insulation. For a low voltage system the applied DC voltage is too high and the leakage currents of loads causes a problem.

3.5.2 Tanδ method

The most common method of dielectric response diagnostic is the tanδ method. A signal, variable in frequency, is applied to the cable. Current and voltage are then measured at different frequencies. The frequency can vary between very low (0.0001 Hz) to high (kHz).

Using equation 2-3 the loss factor tanδ can be calculated. An increase in dielectric dissipation will result in a bigger tanδ. This method can also be used online with a more complex way combined with DC leakage current measurement. Localised changes in dielectric properties are not detected. Therefore if this method is applied, the total cable length needs to be effected by degradation. This is often the case with water treeing in XLPE cable, for example. Water intrusion in oil impregnated paper cable, is always very localised and therefore hardly detectable with the tanδ method on long cables.

3.5.3 Other methods

There are many other varieties of techniques for measuring changes in the dielectric properties. Most of which are based on the tanδ method, DC leakage current, or a combination of both [9].

3.6 Transients

The transient method is a technique where a pulse is injected and the reflections measured which makes it possible to determine the fault distance. The following sections will describe the two methods of applying this technique.

3.6.1 Impulse voltage

The impulse voltage method for fault location is normally only used for flashing faults where fault burning has been unsuccessful [10]. An oscilloscope is connected through a high voltage coupling capacitor C_c see Figure 3-10. When the impulse generator is fired the voltage pulse will propagate along the cable at a velocity v, as in equation 3-2. When the impulse reaches the fault, the fault starts breaking down and generates a voltage step of equal instantaneous magnitude and opposite polarity. The pulse travelling back to the impulse generator is then recorded by means of an oscilloscope. A series choke L_c is used as high impedance to the reflecting pulse returning from the fault. The transient will now travel backwards and forwards between the surge generator and the fault. Using the measured voltage as shown in Figure 3-9, the reflection time τ_i can be determined. Using equation 3-1 the distance to the fault can be calculated.

There are two major sources of errors using this method, namely the ionisation delay time of the fault and the distortion of the impulse front during transmission. The ionisation error can be reduced or eliminated by progressively increasing the impulse voltage amplitude and observing that the fault position seemingly moves forward with each increment.

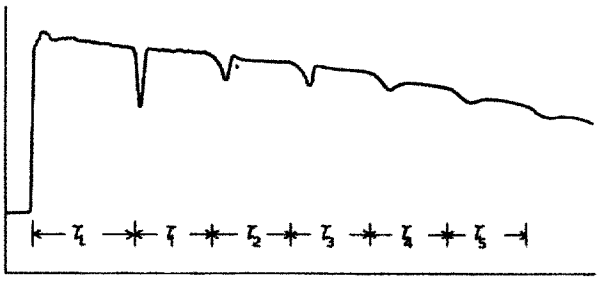

Figure 3-9 Output (voltage) waveform of impulse generator[10].

As the impulse travels along the cable it is subjected to attenuation and distortion which reduces the peak amplitude of the wave and increases the slope of the leading edge. This also increases the ionisation delay.

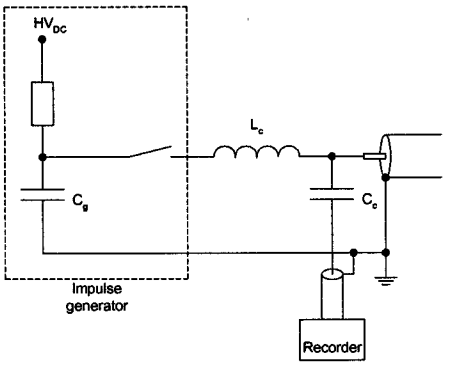

Figure 3-10 Set up for impulse voltage method

3.6.2 Impulse current

The impulse current method [10] uses a linear coupler to detect current impulses instead of voltage impulses. The linear coupler comprises a short length of insulated wire, a transformer consisting of the secondary winding in close proximity to the earth shield and the primary winding. The flux due to the current flowing in the primary winding induces a voltage in the secondary winding proportional to the rate of change of the primary current. A pulse is injected and reflects at the fault position and will start propagating forwards and backwards between the impulse generator and the fault. A switch in Figure 3-11 represents the spark gap or triggered contact.

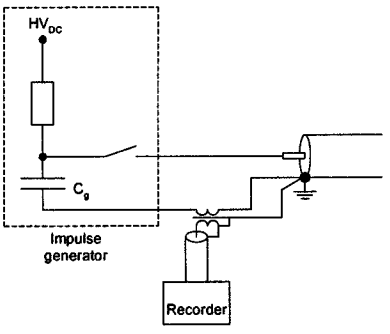

Figure 3-11 Set up for impulse current method.

When the arc is created by a DC source over the spark gap or triggered contact, it will not extinguish until the DC voltage drops below the minimum threshold voltage. As the arc exists for a short time (but much longer than the transition time of the pulses, see Figure 3-9), reflected pulses will see the capacitor C_g as a short circuit because of their high frequency components.

Typical waveforms obtained [10] are illustrated in Figure 3-12 by means of the linear coupler which is a differentiating element. The time intervals marked as τ_i contain some ionisation delay time for the fault to breakdown, whereas the intervals marked as τ_f are pure transit times to the fault. Figure 3-12a shows the waveform of a very low resistance short circuit fault $R_f << Z_0$. During this fault the pulse will effectively propagate between two short circuits, causing the voltage to change polarity at the short circuit points, the current of the waveform will change accordingly to figure 3-6 for a forward and reverse waveform. In Figure 3-12b the oscillation caused by an open-circuit fault is shown. During this fault the pulse will propagate between an open circuit and a short circuit causing the current to alternate. Figure 3-12c shows the waveform obtained from a fault where the fault breaks down with an ionisation delay. The effect of ionisation delay is very apparent as the time between the injected pulse and the first returning pulse is much longer than the time between the following pulses. When the pulse reaches the fault point, the fault will not breakdown instantly at the beginning of the rising flank, but instead later at the rising flank or even at the falling flank.

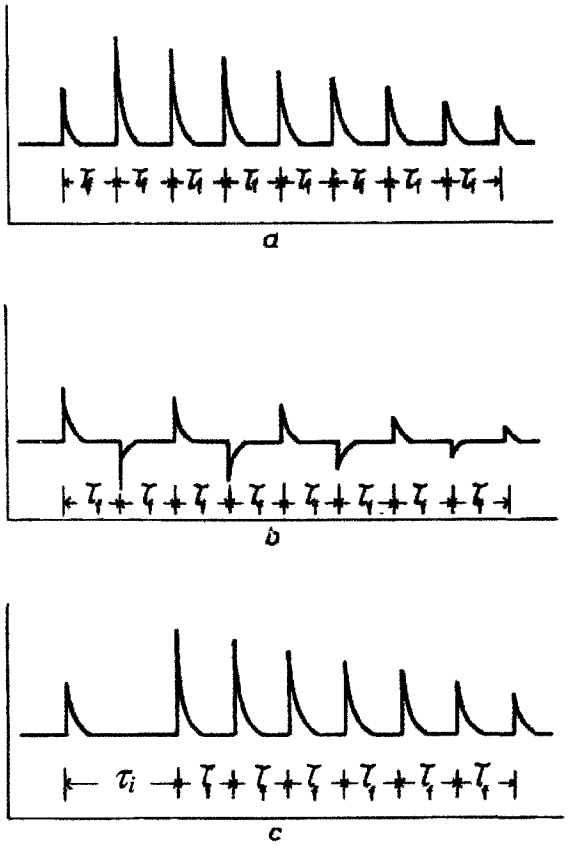

Figure 3-12 Output waveforms from linear coupler for various types of fault
a) Low resistance fault
b) Open circuit fault
c) High resistance fault

The advantage of using the current impulse method, as opposed to the voltage impulse method, is that high frequency current transients are recorded. The high frequencies see the capacitors of the pulse generator as a short circuit, resulting in small pulse voltages. The current will remain large and easy to measure. Furthermore it is cheaper to measure the current as there is no need for a high voltage divider and it is safer as the measurements are taken from the earth shield.

This technique is not applicable for high resistance on low voltage cables, as it requires a high voltage to breakdown the fault, which means that no loads may be connected to the cable.

3.7 Low voltage method

A method to detect and pre-localise a low voltage fault on a life cable is based on detecting a reflection from the actual fault, by using the pulse reflection method to inject a pulse into the cable. The time of reflection from the fault will then determine its location. Injecting a pulse in an intact cable will return the characteristic echo of the cable and show any T-joints and open ends, which can be used to compare with the echo during a fault. This method can only localise a fault in the main distribution cable and not in any supply cables on long circuits as the attenuation of the cable and T-joints affects the pulse too much. The device also needs to monitor the cable for some length of time until the fault reoccurs. A buffer coil must be installed to have a high impedance for pulses at the start of the supply cables and thus to prevent reflections from other cables when injecting the pulse. This means that the circuit needs to be taken off-line while installing the buffer coil. As a result, it will take customers off line, but at present it is the only method used to locate low voltage faults aside from trial and error diggings. Figure 3-13 illustrates the set-up of the device.

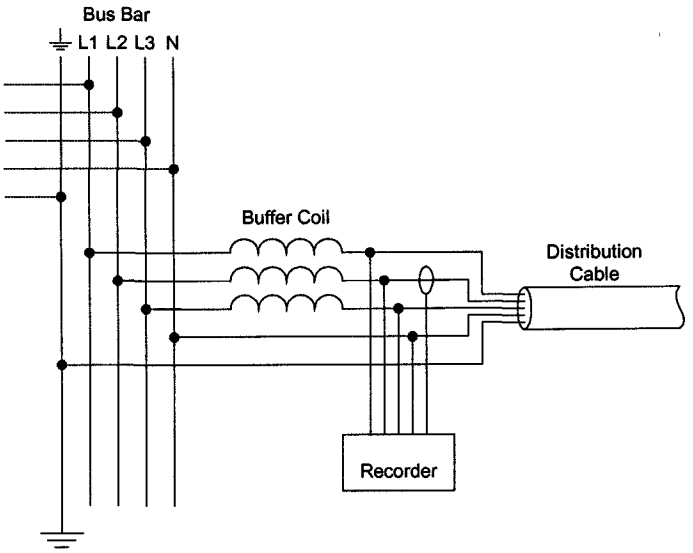

Figure 3-13 Set-up of low voltage disturbance recorder.

The device is connected to the three phase conductors and a current sensor is placed on the suspected phase. The recorder will wait for disturbances in the voltage waveform. If a disturbance is detected, a pulse train is injected and the echo is recorded. Both echo, current and three phase voltage waveforms are digitally stored over a period of typically ten cycles. The data can then be remotely acquired for further analysis to determine the cause of the disturbance and its location. This gives operators flexibility to monitor suspicious substations.

3.8 Fault pinpointing

Application of the location tools decreases the area in which to search for the fault. However, it is not necessarily accurate enough to excavate the faulty part of the cable. More accurate techniques are needed to pinpoint faults and physical mechanics which fault pinpointing can be based on are [5]:

- Change in magnitude of voltage
- Change of polarity voltage
- Change of current (low frequency)
- Modification of magnetic field
- Emission of sound/ultra-sound
- Temperature rise
- Chemical changes
- Visual changes
- Partial discharge
- Emission of electromagnetic signals (high frequency)
- Physical movement

The following sections will explain in more detail which fault pinpointing techniques are available.

3.8.1 Acoustic

In most cases a surge generator is used to pinpoint a fault. This device consists of a variable high voltage DC source and a high voltage capacitor bank. The capacitor bank is charged by the DC source and is discharged over a spark gap (or by triggered contacts to the output). The pulse repetition rate of the source can be once in every set time period.

The steep wave fronts generated by the surge generator will breakdown the fault and the energy dissipated at the fault location will create noise and vibration. The surrounding matter in which the cable is buried will act as a conductor for these acoustic signals. The conductance is dependant on the type of earth matter e.g. clay, lime, concrete, etc in which the cable is buried. To detect the signals a sensitive microphone is used. The operator is able to scan a retain length of cable, designated by the pre-location technique(s), for acoustic signals caused by the fault.

3.8.2 Electromagnetic disturbance

To detect an eccentric effect the sensor is moved around the cable to detect a maximum and minimum in the electromagnetic field caused by the forward and returning current. The eccentric distribution of magnetic field lines are caused by the eccentric build up of the cable as Figure 3-14a and b show. In practical terms this means that the cables must be installed in ducts. A surge generator injects a steep wave front into the cable causing the fault to break down. The pick up coil will detect an eccentric effect at point C in Figure 3-14b for a 3-core cable prior to the fault as current is flowing through the faulty conductor and earth shield. At a certain distance behind the fault for example point D in Figure 3-14b there will only be current in the earth shield producing a uniform magnetic field. Detection of electromagnetic fields extending outside the cable has limited use, as the sensor needs to be placed directly onto the cable as this method makes use of the eccentric position of the conductors of a 3-core cable.

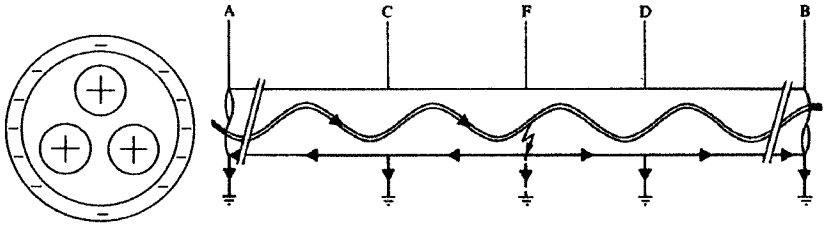

Figure 3-14 (a) Three core cable (b) Currents in a multicore cable run in ducts with manholes.

The same a applies for a one core cable only the field prior to the fault is small caused by cancellation of forward and return current. A much larger field is detected after the fault as here only the return current is flowing. This type of pinpointing has certain limitations and is best used for very low resistance faults.

3.8.3 Pool of Potential

A cable that is in physical contact with the earth in which it is buried makes galvanic contact. The conductor therefore has a connection to ground at the fault position. A DC voltage is applied between the faulty conductor and the earth to allow detection of the fault. The current from the DC voltage will flow partly through the earth. The corresponding potential disturbance in the earth allows detection of the fault.

As Figure 3-15 illustrates, a voltage gradient occurs at the fault location, which has the highest density at the fault point. Using a sensitive voltmeter connected to two ground spikes, the difference in potential can be measured at different points along the cable. A change in polarity will tell that the fault point has been passed. This method can pinpoint the fault with an accuracy of less than 10 centimetres.

3.8.4 Magnetic Field

The magnetic field method detects the magnetic field using a magnetometer. A DC current, which is high enough to be detected by the magnetometer, is applied to the faulty conductor, and the disturbance in the magnetic field can be found around the fault point.

The magnetometer will detect magnetic field caused by the return sheath current. By walking along the cable within a designated area defined by pre-location, the changes in the magnetic field are detected when the deflection of the signal as Figure 3-15 shows. The magnetic field method is easier and faster in use than the pool of potential method but less accurate. Therefore both methods complement each other.

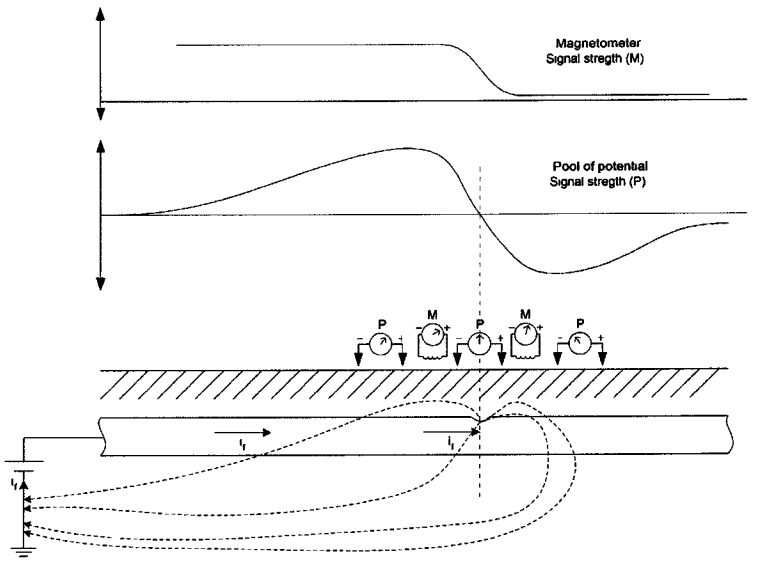

Figure 3-15 Location of fault using pool of potential and magnetic field method.

3.8.5 Audio frequency

Audio frequency can be used with the pool of potential method. Instead of using a DC source now an AC source (b) is used to generate audio frequencies. The audio tone is detected between two points, similar to the pool of potential method. Just around the fault location the waveforms will have the highest amplitude (F), see Figure 3-16. A gradually decreasing amplitude can be detected with the audio receiver when moving away from the fault location.

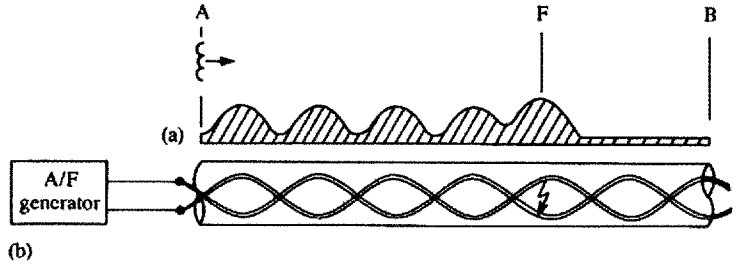

Figure 3-16 Audio location using twist of cores

Another method is using the twist of the cores in the cable. The fault needs to be low resistance to make it work. Using an audio generator (b) an audio signal can be detected because the conductors are twisted, the forward and return current will produce magnetic fields and due to the twist there will be minimum and maximum, this is illustrated in Figure 3-16. An operator will walk along the cable with the audio receiver searching for the audio signal (a). After the fault point there will be a steady audio tone, which makes it possible for the operator to pinpoint the fault.

3.8.6 Smell detection

Electrical faults create smells/odours in the ground. A gas analyser can be used to detect these smells, in the same way that utility companies detect underground gas leaks with special gas detectors that are put into the ground. At first this technique was tested using trained dogs to detect smells, but this experiment failed as the dogs became distracted by more interesting things happening on the street. Currently a new technique with a gas sensor can be put into the ground and using a computer to analyse the ground for any faults, this product is still in the development phase and has not yet been properly tested.

3.9 Conclusion

Most of the location methods are not applicable for finding fault on low voltage networks due to the constant connection of customers. This makes online testing difficult, as the voltage has to be kept within the regulator specifications. Pulse echo techniques are useful and are already applied on low voltage networks to locate faults. However the circuit needs to be taken offline to install the equipment that prevents reflection from other parts of the network.

It is difficult to pinpoint fault on low voltage systems, as most of the methods require a high voltage impulse generator. One promising method is smell detection which, as mentioned above, is currently in development.

At present it is only possible to find a fault on underground low voltage networks using pulse echo methods, which can give reasonable accuracy. However, pinpointing a fault is still very hard and usually requires disconnection of customers.

Even making use of the mentioned methods in the previous sections, pinpointing of faults remains difficult and needs skilled operators to find them.

4 Test Objects and Results

To conduct proper research on low voltage faults, data of voltage and current behaviour is necessary. As it is currently not known which phenomena occur during low voltage faults it was necessary to simulate faults in controlled condition to allow similar conditions for faults and easy access for measuring voltage at the fault point.

4.1 Test set up

To simulate a real low voltage fault, a number of cable samples were used. Two types of oil impregnated paper cable were selected, namely four-core PILC/PILS and three-core CONSAC. The samples were connected to 500 metres of four-core XLPE cable to simulate the effect of a fault on longer lengths of cable. In most cases in London the maximum length from the substation to the customer is limited to 500 - 600 metres.

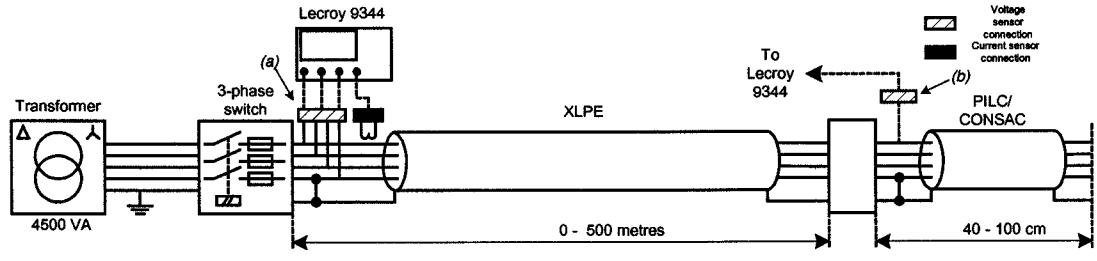

Figure 4-1 Set-up of measurement system to simulated low voltage faults.

The XLPE cable has been cut at a length of 200 metres, in order to simulate variation of the fault location. The cable is fed from a three-phase isolating transformer through a three-phase circuit breaker with a fuse box. Neutral and armour are bonded together to simulate a combined neutral and earth system. A four-channel digital scoop (LeCroy 9344) records the voltage and current waveforms at a maximum sample rate of 500 kHz.

The voltage at the fault point see (b) in Figure 4-11,is measured by means of high frequency probes. At the supply side, (a) in Figure 4-1, the voltage is measured by means of isolating transformers. The reason for taking isolating transformers instead of high frequency probes is to isolate both points from each other thus preventing a parallel current path along the oscilloscope. This problem does not exist when measuring at only one point along the circuit.

The current is recorded through a current clamp with a range from DC to maximum 5 kHz. Specifications can be found in appendix C. To confirm that the frequency response is sufficient, a high frequency (DC to 50 MHz) current probe was used in the first measurements to verify the results. In all measurements the responses of both current clamps were similar.

The choice to use the lower frequency current clamp was made since it can handle larger short circuit currents, which the available high frequency probe did not allow. Also, a large number of these current probes have been installed in substations to monitor load currents. Another factor that needed to be considered was the high price of high frequency probes, which at the same time can handle the large peak currents.

4.2 Test specifications and calculations

The transformer and cable used to feed the cable samples are specified in Table 4-2 and Table 4-3. Using these values the short circuit power and currents can be calculated for the test system. Appendices D and E detail the equations required to calculate these short circuit values. Table 4-1 shows the results for the test system. A typical low voltage circuit in London is given in appendix F as comparison. It is difficult to make precise calculations, as the zero sequence impedance of the cable has to be known, which in many cases is not supplied by the cable manufacturer. In the case of the test network with XLPE cable and transformer this was not known. The following assumption were made, $\underline{Z}_0=3\ \underline{Z}_1$ and $\underline{Z}_1=\underline{Z}_2$ for the XLPE cable and $\underline{Z}_0=3\ \underline{Z}_1$ and $\underline{Z}_1=\underline{Z}_2$ for the transformer [7]. In which $\underline{Z}_1$ is the positive sequence impedance, $\underline{Z}_2$ the negative sequence impedance and $\underline{Z}_0$ the zero sequence impedance

Table 4-1 Short circuit values for test network at different fault location, neglecting the cable inductance due to its low value as compared to the cable resistance (see appendix F equations F-2 to F-5).

Short circuit parameters	0 metres fault	200 metres fault	500 metres fault
I_{k1} [A] using F-2	125	73	35
I_{k2} [A] using F-3	216	112	51
I_{k3} [A] using F-4	250	130	59
S_k [kVA] (3-phase) using F-5	90	53	25

The results shown are based on a normal short circuit event. In the event of a low voltage fault causing an arc the short circuit calculations need to include arc impedance in the equation. It is important to note that the cable length mainly determines the magnitude of the fault current. This will cause low voltage arcs in the cable nearer to the supply to be more volatile, resulting in a faster trip of the fuse and more damage to the cable.

In the test network used, the high DC resistance of the XLPE cable will prevent high short circuit currents to occur in the system compared to a distribution system. This is also the case with supply cables (cables to a customer) branched from a low voltage distribution cable in the field. Supply cables are of much smaller diameter and therefore will have a high DC resistance. The differences in parameters like impedance and resistance for different core diameters are shown in appendices A and B.

Table 4-2 Specifications isolating transformer.

Details Transformer	Value
Nominal Power (S_n) [kVA]	4,5
Primary Voltage (U_{pri}) [V]	415
Secondary Voltage (U_{sec}) [V]	415
Primary Current (I_{pri}) [A]	7
Secondary Current (I_{sec}) [A]	6,5
Reactance (x) [%]	2,5
X_{tr} [Ohm] using F-1(app F)	0,96
Coil configuration	Delta/Star

Table 4-3 Measured cable properties for 2.5mm² 4-core XLPE supply cable.

Plastic cable properties at 20°C	Value
Resistance (R'_c) [mOhm/m]	7,8
Inductance[1] (L'_c) [μH/m]	0,78
Capacitance phase to phase ($C'_{c\_p\text{-}p}$) [pF/m]	~85
Capacitance phase to earth ($C'_{c\ p\text{-}earth}$) [pF/m]	~132
Discharge current[2] ($I_{c\_p\text{-}p}$) [A]	~4
Discharge current[2] ($I_{c\_p\text{-}earth}$) [A]	~3

[1]Factory specification [2]Using equation 4-5

When taking the capacitance of the cable into account, the cable can supply an additional current to the fault for a short time. This current is called here the discharge current and can be determined from the energy that is stored by the capacitance of the cable [8]:

$$W = \frac{1}{2} C_c \, u^2 \tag{4-1}$$

During the short circuit no energy will be dissipated of the resistance of the arc is assumed to be zero. This means the capacitive energy is converted into inductive energy through equation 4-2 and this process will continue vice versa (oscillating waveform) [8]:

$$W = \frac{1}{2} L_c \, I_c^{\,2} \tag{4-2}$$

From equation 4-1 and 4-2 the discharge current can be calculated as:

$$I_c = \sqrt{\frac{C_c}{L_c}} \, u = \frac{u}{Z_c} \tag{4-3}$$

The result in Table 4-3 show that the magnitude of the discharge current is low compared to the 50Hz short circuit current. Therefore the discharge current will be ignored in further calculations.

4.3 Cable samples

Oil impregnated paper cable samples were used to simulate a low voltage fault. These samples consisted of two main types of cable, namely four-core PILC/PILS or three-core CONSAC. To create the fault, the outer sheath is damaged by drilling a large hole in the earth sheath. A very small hole is drilled in the oil impregnated paper insulation to the conductor. This allows the injection of water into the hole and oil impregnated paper insulation. It is necessary to damage the paper as it takes a very long period (months) for water to penetrate the oil and paper, if not damaged, causing a conducting path. A picture of a prepared cable sample is shown in Figure 4-2

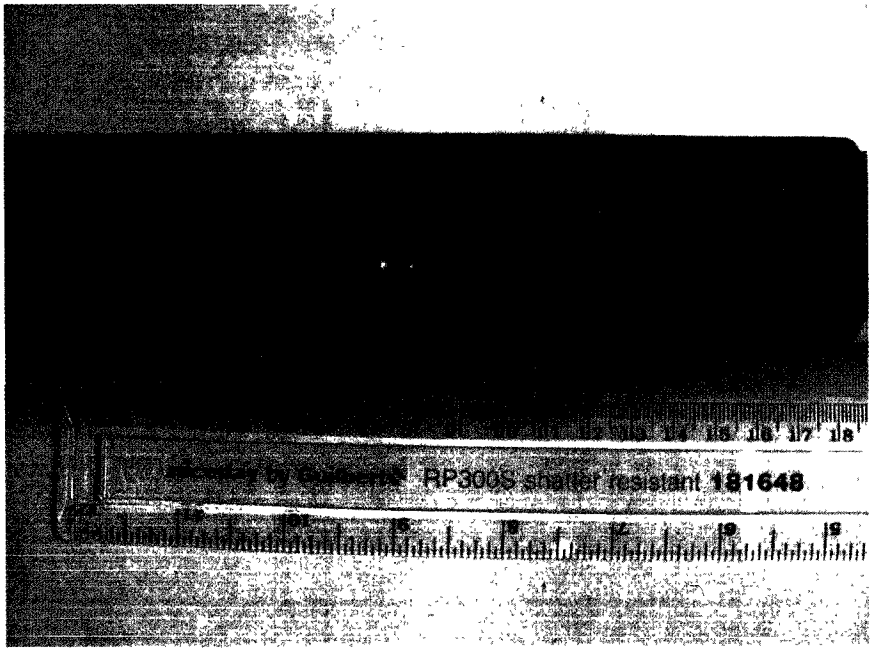

Figure 4-2 Prepared CONSAC cable.

For a realistic simulation of the fault in its natural environment, the groundwater conductivity has to be known. Groundwater samples were taken from two locations in London and their conductivity was measured. These results, including tap water conductivity are shown in Table 4-4.

As there is no major difference in conductivity between the samples, tap water was used and injected into the cable sample. Salt was added to increase the conductivity of the water to speed up the process for the first breakdown of the fault. After the first flashover, carbon and metal particles are deposited in the insulation facilitating the next flashover easier with normal tap water.

Table 4-4 Specific conductivity and resistance of ground- and tap water in London

Location London	Conductivity [S m]	Resistance [Ohm/m]
Osborne street	0,085	11,8
White Chapel High Street	0,075	13,3
London tap water at 21°C	0,09	11,1

4.4 Results of simulated low voltage faults

4.4.1 Phase to neutral/earth fault

Several faults have been created at different distances from the supply source to obtain a picture of the effect of the cable impedance on the fault. Figure 4-3 shows the result of a low voltage arc at a distance of 500 metres from the supply source. The voltage is measured close to the fault. When the insulation breaks down the voltage almost drops instantly to the minimum arc voltage, the current rises steeply and at this point the inductance of the cable plays a role due to the large *di/dt*. The current will reach its maximum and then starts to drop, according to the source voltage.

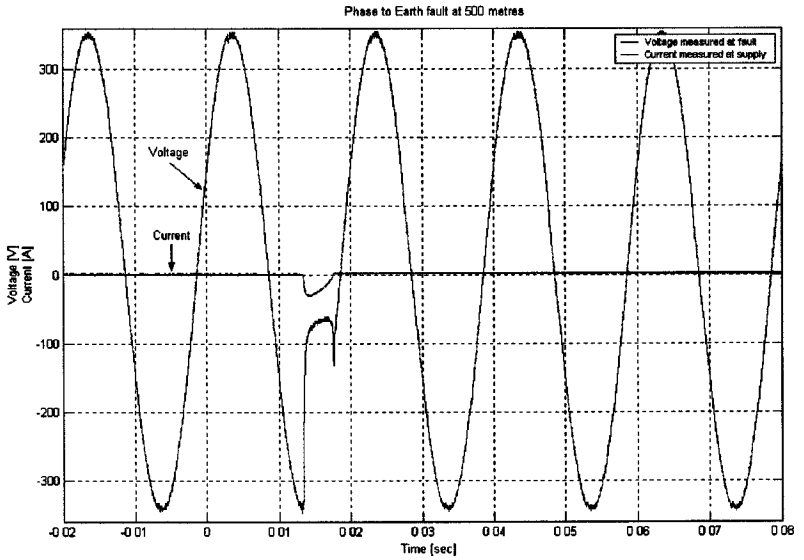

Figure 4-3 Current and voltage before, during and after a low voltage arc at a cable length of 500 metres using a PILC cable sample. Current amplitude is 30.6A and arc voltage amplitude is 65V.

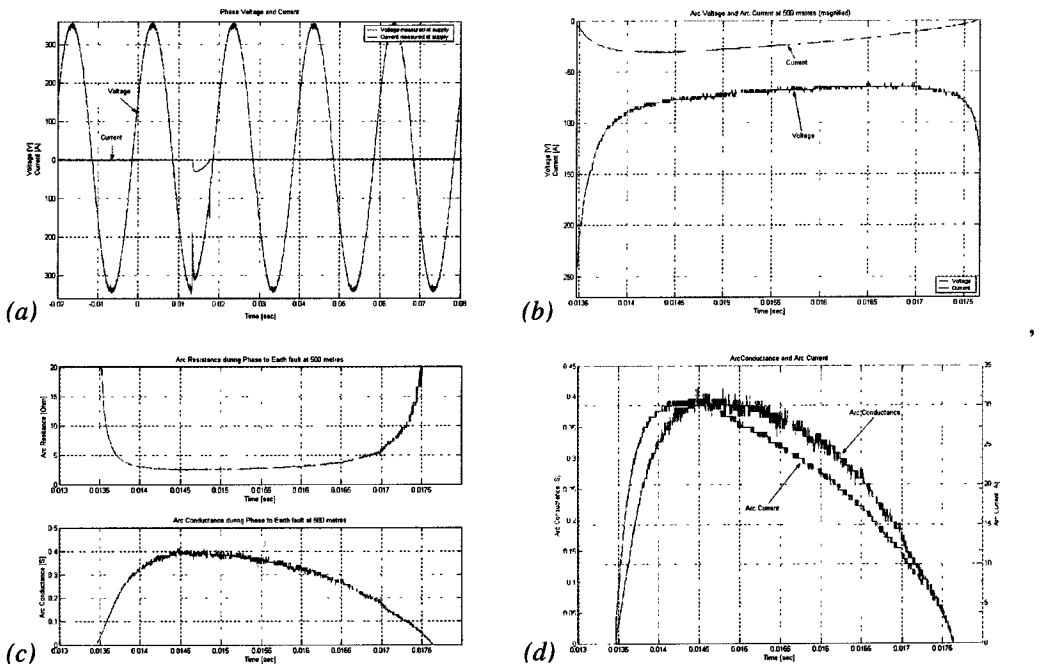

Figure 4-4 (a) Voltage and current at supply, (b) Arc voltage and arc current at fault, (c) Arc resistance and arc conductivity, (d) Arc conductivity and arc current.

At a certain point the current will be low enough to cause the minimum threshold voltage of the arc to rise. When the supply voltage becomes lower than the required arc voltage, the arc will be unable to sustain itself and will extinguish. At this point no current will flow and the supply voltage will return to normal.

The result of an arc at the fault point is a drop in voltage, which is usually noticed by flickering lights at customers sides [11]. The effect of this arc on the voltage at the supply is less, only the large *du/dt* are picked up, is seen at the moment of ignition and extinguishing of the arc. Figure 4-4a shows this, a detailed picture can be found in appendix G, figure G.1. The difference between the voltage waveform in Figure 4-3 and in Figure 4-4a is the voltage over the cable impedance, which masks the nearly constant arc voltage when the voltage is measured at the supply side.

Figure 4-4b is a close-up of 4-3 and shows the effect of the arc voltage increase when the current decreases. From the arc current and arc voltage the arc conductance and arc resistance can be derived resulting in Figure 4-4c. These figures also show that a decrease in current implies a decrease in conductivity and therefore an increase in resistance. A plot of both arc current and arc resistance as in Figure 4-4d shows that arc current and arc conductivity is almost linear dependant on each another. Except for the slight phase shift, which suggests the arc, is not completely resistive.

Similar plots were acquired for faults at 200 metres and 0 metre distances of the source supply. To make comparison easier, all waveforms are plotted for negative cycle arcs. Results for positive cycle arcs are comparable.

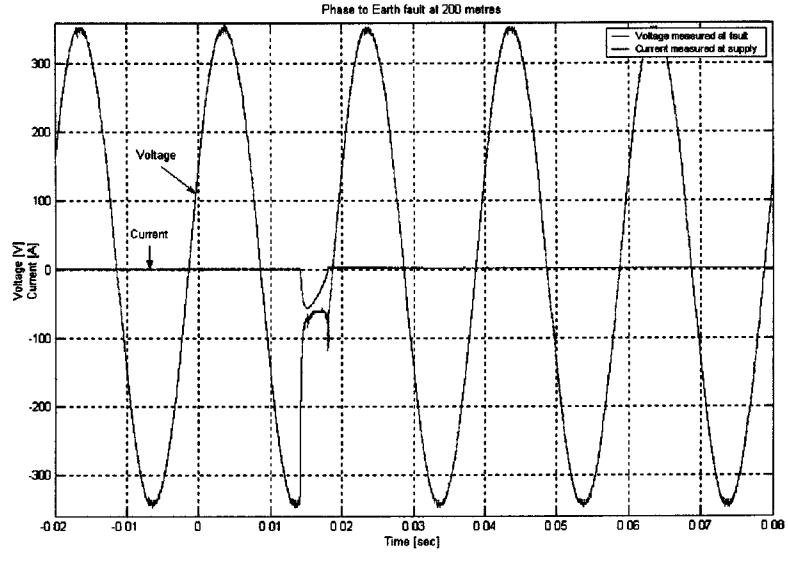

Figure 4-5 Current and voltage before, during and after a low voltage arc at a cable length of 200 metres using a PILC cable sample. The peak current is 56.5A and arc voltage amplitude is 54V.

Corresponding waveform plots can be found in Figure 4-5 and Figure 4-6 and in appendix H and I. The major difference for different fault locations is the magnitude of the current flowing through the arc. A shorter distance will result in a lower arc voltage. Also higher arc currents cause the arc to be more volatile and therefore clear themselves faster due to the bigger blast.

Comparing the known current values during an arc event with the calculated short circuit values in Table 4-1 shows that the calculated values are realistic and gives an indication of the short circuit currents during an arc event. This knowledge can give a rough idea of magnitude of the arc voltage. It is important to note that the current given in the fault calculations is the root mean square value. Also the arc voltage is neglected in Table 4-1.

The effect of the constant arc voltage becomes more evident as the fault position is closer to the supply, this will cause the measurement transformers to start to saturate due to the DC component in the voltage waveform. Therefore it is inadvisable to measure these phase voltages with voltage transformers; instead a resister or capacitor divider is recommended.

The fast Fourier transformations in appendix G to J show that most of the frequency content is below 10 kHZ. At 9.8 kHz there is another peak in the spectrum, which is caused by a frequency component of the extinguishing arc. Therefore if the complete disturbance needs to be recorded a sample frequency of at least 20 kHz is required.

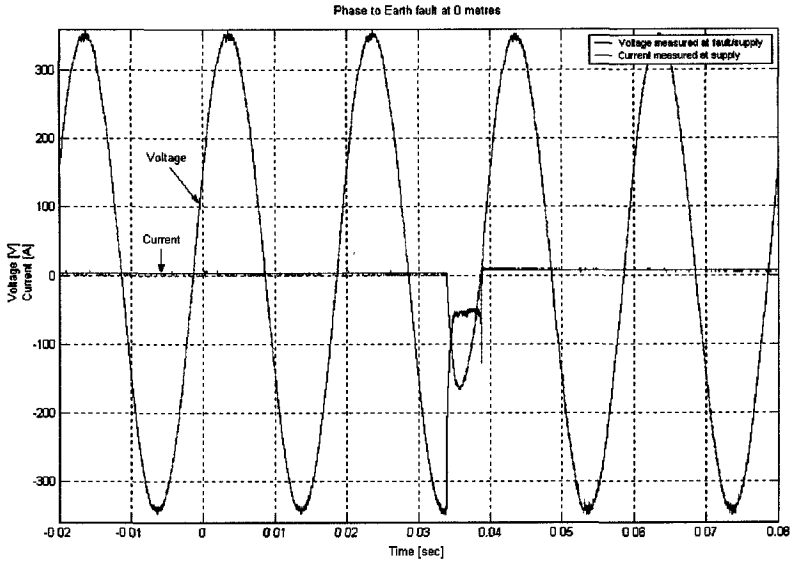

Figure 4-6 Current and voltage before, during and after a low voltage arc at a cable length of 0 metres using a PILC cable sample. The peak current is 166A and arc voltage amplitude is 53V.

4.4.2 Phase to phase fault

Phase to earth faults are more likely to happen as moisture will penetrate the cable, usually through a defect in the earth sheath. This does not detract from the fact that these faults can still develop into phase to phase fault. In some events it is possible to develop a phase to phase fault straight away. Phase to phase arcs tend to be much more volatile than phase to neutral/earth arcs because of their larger potential differences. Figure 4-7 shows the larger potential difference between both phases allowing larger short circuit currents. Detailed figures can be found in appendix J where arc conductance and resistance are plotted. The higher potential difference will make re-strikes more common in both negative and positive half cycle. Figure J.1b shows the phase voltages at fault location, interesting is to see how the voltage in phase one rises with phase two. When this kind of waveforms is recorded, the fault must be close to he point of measurement.

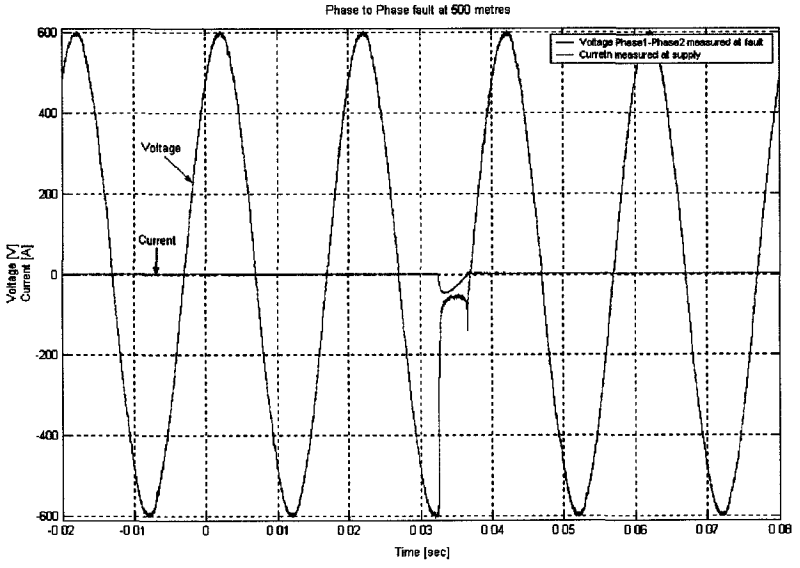

Figure 4-7 Current and voltage before, during and after a low voltage arc at a cable length of 500 metres using a PILC cable sample. The current amplitude is 47A and arc voltage amplitude is 55V. The voltage is obtained by subtracting the separately measured phase voltages.

4.5 Intermittent faults

The ignition of an arc will at first be confined to one cycle but as the fault starts to develop the arcs starts to ignite in multiple cycles. These intermittent faults will in most events blow the fuse, due to repetitive stress. Figure 4-8 shows the plot of a repeating arc where the arc current varies between 29 Ampere and 40 Ampere and the absolute arc voltage varies between 35 Volt and 60 Volt. From Figure 4-8 it can be seen that a repeat of an arc causes higher currents to flow and a significant drop in ignition voltage from 345 Volt to 170 Volt. The main source for changes in these values is the current, which determines the minimum arc voltage and extinguishing voltage. A possible explanation is the ionisation of air and other gases or moisture near the fault due to the previous strike, making it easier for the next cycle to develop an arc. A more likely cause for lower ignition voltages of the arc though, are carbon particles created in the previous strike in combination with any remaining moisture and possibly the localised increase in temperature. In both events the conductivity increases and hence also the arc current. This process will continue until the fault clears itself or a permanent fault is created

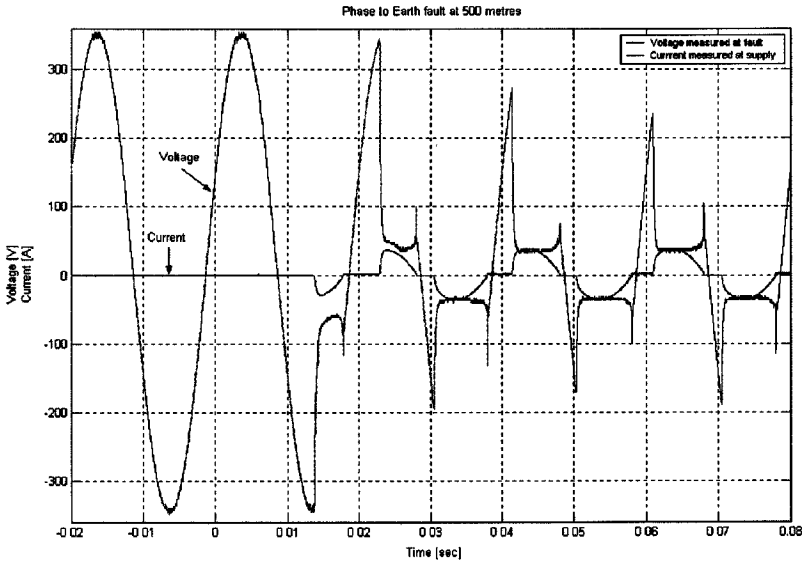

Figure 4-8 Current and voltage before, during and after a low voltage arc during a phase to earth fault at a cable length of 500 metres using PILC cable sample.

4.6 Results in the field

To verify the result of the laboratory tests, data from several substations, which are feeding through oil impregnated paper cable was gathered. Although the data acquired from the field has more disturbances due to load influences, the voltage recorded at the supply source show similar characteristics as for a simulated fault. Large changes in voltage *(du/dt)* are not detected with the recorders due to the limited sample rate of 4 kHz. Consequently this also prevents the detection of voltage disturbance when the arc extinguishes. Analysis of the frequency spectrum of the voltage waveform at supply side show frequency components up to 10 kHz during the simulated arc, see the fast Fourier transformations shown in appendices G to J.

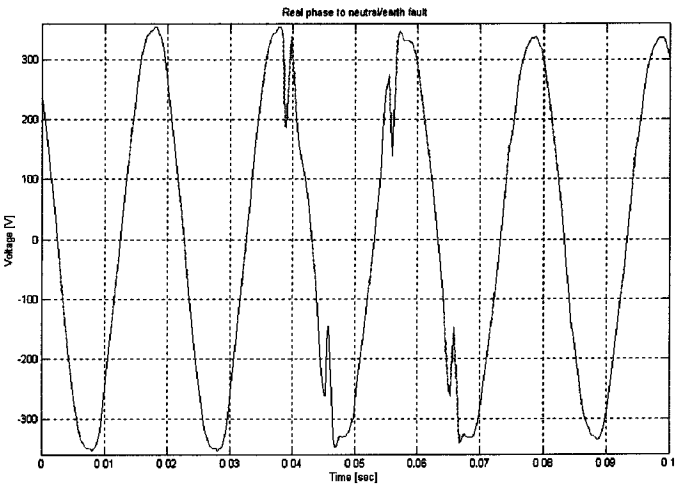

Figure 4-9 Voltage before, during and after a in the field low voltage arc. No current signal was available.

4.7 Conclusion

The data gathered gives conclusive insights into the behaviour of low voltage arcs and can be summarised in a number of points:

- Magnitude of fault current is dependent on system impedance. Therefore the place of the arc in the cable determines the maximum fault current.
- Low voltage arcs seem to clear faster at larger fault currents due to the blast created by the arc.
- Arc voltage reaches a nearly steady value when maximum fault current has been reached.
- A phenomena called sparking occurs at the fault location.
- Intermittent arcs tend to have a lower arc ignition voltage and larger fault currents.
- Phase to phase arcs are more likely to ignite faster due to the potential differences and as a result will show more intermittent behaviour.
- Fuses can sustain a large number of low voltage arcs before they trip.
- The voltage over impedance of the cable will (caused by the arc current) make an arc less noticeable in the voltage waveform at supply side.
- No difference observed in behaviour between different tested types of oil impregnated paper insulated cables
- The drop in arc voltage as a result of an arc event causes disturbances, which can be noticed for example by light flickering.

Measurements taken with CONSAC cable show similar behaviour as PILC/PILS cable as expected. Both types of cables use the same insulation material only they differ in outer sheet material.

The data gathered shows some characteristics that will need further explanation.

1. The arc voltage is non linear to the arc.
2. From visual data there is a spark phenomena occurring at the fault point.
3. The arcing seems to have a preference for the negative cycle of the voltage waveform.

These occurrences will be described in chapter 5.

The effects of a low voltage fault (arc) can be clearly noticed as a chopped sinusoidal waveform. The behaviour of fuses during these arcs show that it is possible for a fault to develop over a long time span before a fuse trips. It can be concluded that a low voltage fault will only be noticed if it disturbs the supply voltage enough to be noticed e.g. light flickering at customers side or when a fuse is blown. It may be assumed that there are a large number of faults developing in the low voltage network without being noticed.

Phase to phase arcs are the most volatile arcs, because of the larger potential difference between the phases. This will lead to a quicker fault development and to more volatile behaviour of the fault.

Due to the voltage drop over the cable impedance, the effect of a low voltage arc is less noticeable at the supply side see Figure 4-3 and Figure 4-4a. However using the cable impedance voltage, impedance calculations can be made to localise faults if the arc voltage can be established within reasonable accuracy. When the arc occurs closer to the supply source, the constant arc voltage becomes more evident because of the lower voltage build up due to the cable impedance. This will cause a larger DC component, which can saturate voltage transformers used to measure the waveforms.

To capture the complete distortion on the voltage waveform at extinguishing of the arc, a minimum sample rate of 20 kHz is necessary as the typical frequency component of the extinguishing lies around 9.8 kHz. Although higher sample frequency will allow a better recording of the arc extinguishing event. Sampling at 20 kHz will allow an oscilloscope to capture the voltage disturbance caused by the arc extinguishing in the voltage waveform at the supply side.

5 Incipient phenomena

Prior to a fault, incipient phenomena occur that suggest a fault is developing or has developed. Any phenomena happening before the fuse blows e.g. sparking or low voltage arcing will be handled as incipient behaviour. This is important as it defines the bases of incipient fault detection research used throughout this report.

5.1 Fault process

The fault process usually begins with damage to the water protective sheath of the cable. The damage will allow outside influences such as water, to penetrate the cable and change the dielectric properties of the insulation material. Many cables can lie for long periods of time submerged in water as the ground in London is mainly clay which acts as a barrier for rain water. Also the ground water levels can be high in some places causing cables to be almost permanently submerged in water. This constant presence of water and water pressure will cause a fault to develop in the event of damaged sheaths or leaking joints

At a certain point the insulation material, which includes both paper and oil, becomes conductive enough to allow sparking/tracking between the conductors or conductor(s) to neutral or earth. The sparking or tracking will result in further deterioration of the insulating material. At some point the insulation fails and a flashover will occur, cleaning the fault area from moisture but creating carbon particles. The fault will clear itself and the repeating process of water intrusion restarts. At some point however, the arcing will have caused enough carbon residues to create a fault that will not clear itself. At this point the fault will be permanent. This complete process can be described in a flowchart as shown in appendix K.

The process leading to a low voltage arc can be described in three steps as followed:

- Protective sheath has been damaged and insulation material is starting to change its properties due to outside influences e.g. water intrusion.
- Insulation material has changed its properties to a point where it starts being conductive, resulting in sparking or tracking in the insulation material.
- Insulation material has become conductive enough to develop a flashover, resulting in a low voltage fault arc.

5.2 Low voltage arc behaviour

Although a low voltage arc is a dynamic short circuit, it does not always blow the fuse. This is because the arc will extinguish itself when the applied voltage falls below the minimum threshold voltage for the arc to exist. This is seen as incipient behaviour before a low voltage fault occurs. Eventually an arc will cause the fuse to blow when the fault develops further.

5.2.1 Arc conductance

Taking a closer look at the relationship between arc conductance and arc current it suggests that the arc conductance can be written, as in equation 5-1, in which k is a constant value [12].

$$\frac{1}{g} = \frac{k}{i_{arc}} \tag{5-1}$$

When plotting the arc conductance as a function of the arc current, Figure 5-1, it becomes evident that there is not a constant linear behaviour between both parameters. For an arc ignition the behaviour of the arc conductance will be linear to the arc current and equation 5-1 is applicable. However as soon as the current starts to drop the relationship between current and conductance starts to become non linear and equation 5-1 is invalid. The figure also shows that the graphs for different fault currents are reasonably similar to each other, suggesting that there is a scaling factor.

The situation even becomes more complicated if there are more strikes, which can be seen in a plot of a re-striking arc as illustrated in Figure 5-2 using the data from the fault presented in Figure 4-8. In this case the conductance curve changes in steepness from the first strike to the second, making a general scaling coefficient not applicable. First strikes and second strikes have similar slope angles that are different from slope angles of re-strikes.

An important conclusion can be drawn from these figures. The slope angle of the conductance is directly related to the current for ignition of the arc. The non linear part is dependent on the ignition voltage of the arc, a high ignition voltage will result in a larger 'belly' as the first en second strike shows in Figure 5-2, the lower the ignition voltage the closer the 'belly' will be to the linear ignition line.

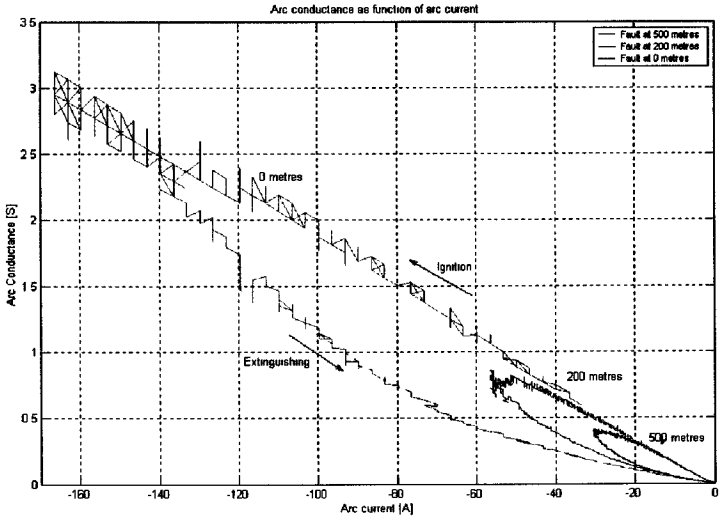

Figure 5-1 Arc conductance as function of arc current for different faults.

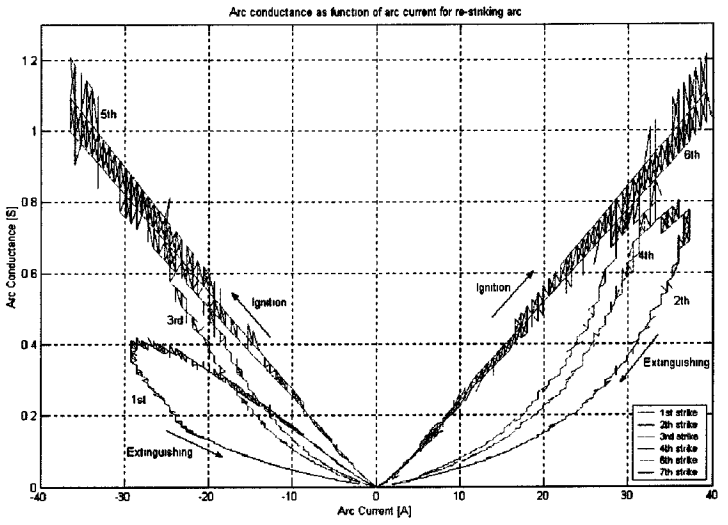

Figure 5-2 Arc conductance for re-striking arc.

Ignition of the arc could roughly be described by one slope angle, except the curve will stop being linear near the point where the current starts to drop. This is the point needed to determine the minimum arc voltage. More statistical data from arcs would be needed to determine slope angles, although this would not be a solution for all low voltage arcs, as they are a very unpredictable phenomena.

The arc conductance strongly depends on the current flowing through the arc. A limiting factor for the arc current is the system impedance, which consists of the transformer (Z_{tr}), cable to (Z_c) and from (Z_r) the fault and the fault impedance (Z_f). Additionally there is the impedance of the cable to (Z_{c_load}) and from (Z_{r_load}) the load. These impedances effect the system in such a way that there will be a current flowing through the load as well as the short circuit current caused by the arc. An illustration is given of this impedance schematic in Figure 5-3.

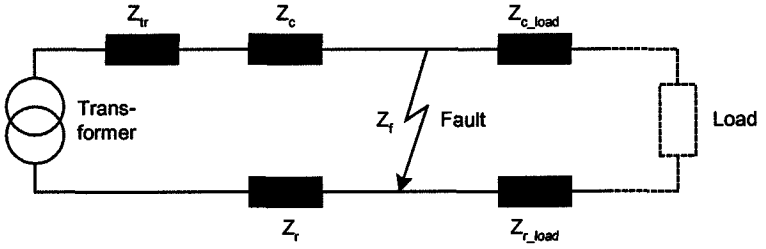

Figure 5-3 Impedance illustration of circuit with low voltage fault

To have a better understanding of a fault, a low voltage fault can be interpreted as a circuit element with a spark gap and a parallel resistor as shown in Figure 5-4 [10]. The resistance of the arc is non-linear and dependent on the current. This interpretation may seem very simplistic for a complex phenomenon like an arc, but for this purpose it gives a reasonable description of the system.

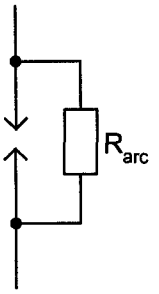

Figure 5-4 Representation schematic of a low voltage arc

To predict the behaviour of the arc over time, a model of the arc conductance is needed. In literature there are a number of models that can be used. A widely used model to determine arc conductivity is the Mayr model, as described in equation 5-2 [13].

$$\frac{1}{g}\frac{dg}{dt} = \frac{1}{\tau}\left[\frac{u_{arc}\, i_{arc}}{P_0} - 1\right] \tag{5-2}$$

where g is the arc conductance, u_{arc} is the arc voltage, i_{arc} is the arc current, P_0 is the lost power or cooling power to the ambient environment (assumed constant), and τ is the time constant of the arc. To evaluate this equation a number of factors need to be known, like cooling power, arc voltage and time constant, to calculate the arc conductance. This leads to assumptions making the Mayr model inappropriate to determine the arc conductance for an arc in a underground cable.

A simpler method is to use the measured arc current and arc voltage as in equation 5-3, to determine the arc conductance. However, this will still require measurements of the arc voltage.

$$g = \frac{i_{arc}}{u_{arc}} \tag{5-3}$$

Both 5-2 and 5-3 show that determining the arc conductance requires knowledge of the arc voltage over a period of time. One option to model the arc is to keep the arc voltage constant over a period of time, by making an assumption or by using predefined slope angles acquired from e.g. Figure 5-1 and Figure 5-2. In reality as the measurements in Chapter 4.4 show, the arc voltage will vary to some extent over time. Assuming the arc voltage constant will introduce a slight error in conductivity calculations. In general the arc's plasma determines the arcs conductance.

5.2.2 Arc voltage behaviour

The data acquired from the fault simulations suggests non-linear behaviour of the voltage. When the supply voltage reaches the critical ignition arc voltage, the arc ignites and the voltage over the arc will drop as a function of the current. Assuming the applied voltage is a sinusoidal waveform, the applied voltage will start to drop after reaching its peak and at a certain stage the arc current will then start dropping as well. This will cause the arc voltage to rise following a different path to the ignition curve. The arc will remain until the applied voltage falls below the arc threshold voltage needed to sustain itself.

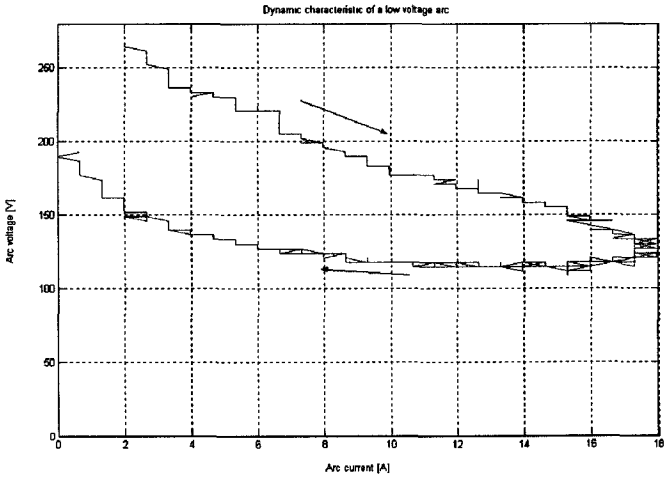

Figure 5-5 Dynamic characteristic of a simulated low voltage arc. Both arc voltage and current are taken as absolute value, to make comparison easier with Figure 5-6.

In Figure 5-3 the arc voltage is plotted as a function of the arc current, for the simulated arc. The figure suggests a hysteresis effect, as the arc voltage has different values during ignition and extinguishing at the same arc current.

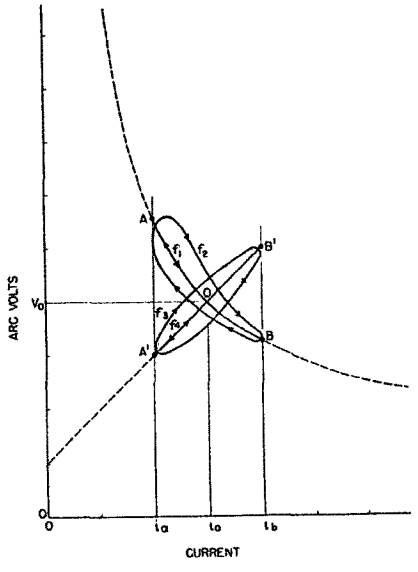

Figure 5-6 A dynamic characteristic of an arc with current pulsating at successively higher frequencies, $f_1<f_2<f_3<f_4$ [14].

The hysteresis effect is supported in a publication by T.E. Browne [14]. When the current changes slowly the arc will have a static characteristic. When there is a more rapidly changing current, the hysteresis effect becomes evident in such a way that the voltage departs from the static characteristic.

This behaviour is illustrated in Figure 5-6 where the static curve is given by the hyperbolic curve AB, the steady current is given by i_o for a steady arc voltage v_o.

The current will oscillate between i_a and i_b with a frequency f_1 of a few cycles per hour. In this case the voltage will follow the static characteristics. For somewhat higher frequencies, the arc voltage will start to follow an elliptical curve making the hysteresis effect evident. At an even higher frequency f_3, the elliptical curve will start to rotate clockwise and change its shape in a way that the major axis approaches a straight line A'B'. At frequencies f_4, above 100 kHz, the arc can follow A'B' closely.

The basics of a similar behaviour can be seen in Figure 5-5. Due to the bit noise of the oscilloscope A/D converter on the voltage and current channel, the curve is not as smooth as in Figure 5-6, but it shows the hysteresis effect, which the arc voltage is subjected too. Similar plots for different conditions can be found in appendices G to J. These clearly show the hysteresis effect, it also becomes more evident that the larger the arc peak current cause the arc voltage will stay longer constant.

5.2.3 Negative cycle effect

In general, the arc seems to have a preference to ignite during the negative cycle of the voltage for a phase to earth or a phase to neutral fault. There may be a number of reasons for is this preference, but there is no definite answer at this point, because the phenomenon depends on many factors.

One possible explanation may be the polarity effect, which is based on a charge building up in the gas, also moisture in the paper could cause the same effect of building up space charge in the cable.

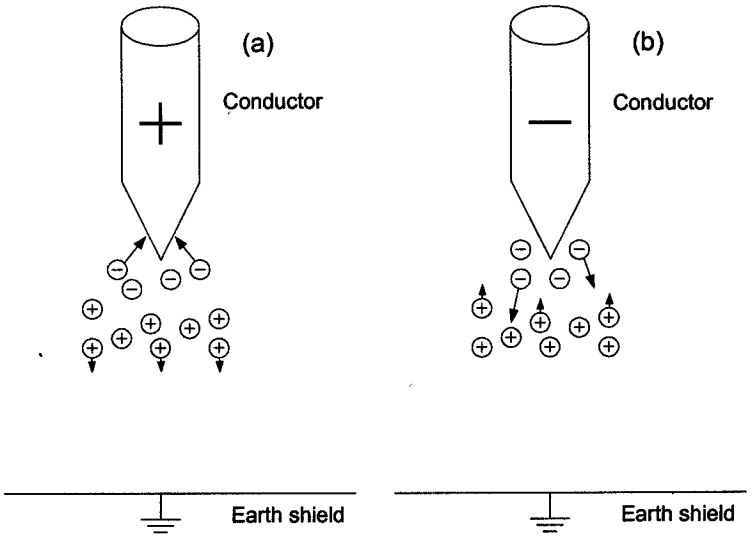

Figure 5-7 (a) Space charge build up in positive point plane gap.
(b) Space charge build up in negative point plane gap.

When the voltage is in its positive half cycle, ionisation occurs due to the collisions caused by the electrons in the field close to the point of the conductor, because field stress is high there. The high mobility of the electrons will draw them into the anode leaving a positive charge behind as these have a lower mobility (Figure 5-7a). This will decrease the field strength in the near vicinity of the conductor, but an increase in the field strength further away from the conductor. In the negative half cycle (Figure 5-7b) the electrical field lines have changed direction. Because of the positive charges left behind during the negative cycle, the field stresses around the conductor are enhanced sufficiently to initiate a breakdown [15]. Although the conductor in a cable is not as sharp as in Figure 5-7 the principle of electrons having a higher mobility than a positive charge remains the same, only the field stress for a sharp object is higher than a cylindrical object as a conductor.

5.2.4 Even harmonic distortion due to electrical arcs

When a low voltage fault develops, the arc tends to concentrate in the negative half cycle of the voltage waveform and it is that later due to increased damage, the arcing occurs in the positive cycle as well.

When the arc occurs at only one half of a cycle, strong even harmonics, especially the second harmonic are created [16]. This may serve as a tool to verify the state of a developing low voltage fault. However, large supply networks especially industrial sites and office blocks, converters, half way rectifiers and three phase half controlled bridges generate even harmonics as well. Nevertheless, it is an important effect that should be taken into consideration.

5.2.5 Fuse behaviour during low voltage arc conditions

Most substations are protected from short circuit currents on the bus bar by means of low voltage fuses. Appendix L shows the characteristics of different fuse ratings. Basically a fuse is a thermal device. The power dissipated by the fuses will determine whether the fuse will blow in a certain time as is formulated in equation 5-4.

$$W_{fuse} = \int_0^t I^2 R_{fuse}\, dt \qquad (5\text{-}4)$$

Low voltage arcs will tend to ignite in the top of the sinusoidal and extinguish when the voltage drops below the minimum arc threshold voltage. Yet low voltage arcs can ignite at lower voltages than the top of a sinusoidal when the fault has developed far enough.

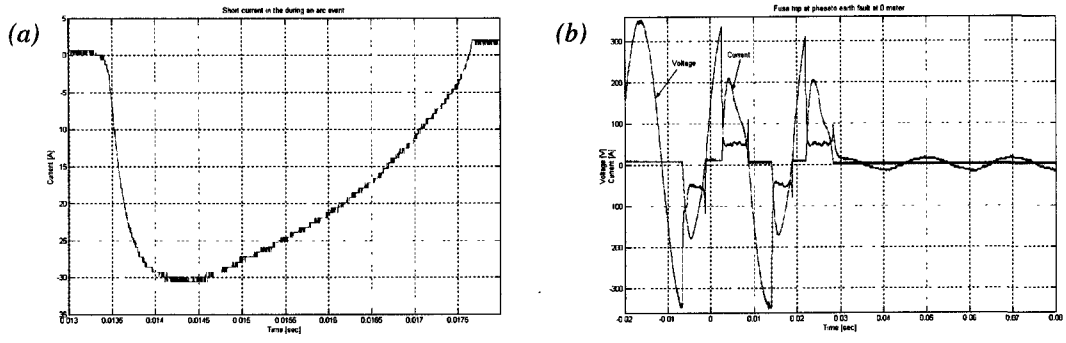

Figure 5-8 (a) Current behaviour during an arc event, (b) fuse trip caused by an arc event.

A low voltage arc result in a short circuit for a short time span, typically three to five milliseconds, depending on the condition of the fault. The current will rise to a certain value which is limited by the total system impedance. After its peak, the current starts to drop along with the voltage as illustrated in Figure 5-8a. The characteristics from appendix L show that fuses that can handle high currents for short times. Even a ten-ampere fuse can handle sixty amperes at ten milliseconds. Although the fuse will not blow due to the short existence of the high current, the fuse does get slightly damaged and the thermal resistance drops with every short circuit current. Eventually, if the fault develops and the arc returns in multiple succeeding cycle, the fuse will blow resulting in a low voltage fault as shown Figure 5-8b.

5.3 Spark effect

5.3.1 Behaviour

Before an arc ignites, discharges/sparks occur in the insulating oil impregnated paper material. This behaviour seems to happen in the higher voltage range, the large amplitude sparks seem to concentrate themselves in the tops of the sinusoidal waveform. The sparking seems to be initiated by the presence of moisture or from carbon particles that have been left over from a previous arc. Sparking continues to breakdown the insulation material and cause partial discharge pulses to propagate along the cable. These pulses can make it possible to detect the sparking which may even be used for localisation of the fault.

5.3.2 Causes of spark effect

The cause of sparking is difficult to determine exactly, but tracking seems the most likely cause of this phenomenon. In the event of tracking a conductive path is created across the surface of the insulation material. This is usually made up of carbon particles mixed with moisture. Carbon is highly conductive and even if there is not a path formed, they can change the field stresses significantly. For tracking to occur, an outside influence on the material is needed, for example, an organic substance or moisture. The moisture will create a conductive path that increases the leakage current that heats the surface. The heat will then cause evaporation of the moisture, which will cause interruptions in the moisture film (a dry band). This in itself increases field stresses and will create sparking between the separating moisture films. The heat generated by the sparks will cause carbonisation and volatilisation of the insulation and leads to permanent carbon track or particles on the surface [15].

Even after the moisture has disappeared, sparking continues, which is probably the cause of remaining carbon particles and/or tiny patches of moisture in the insulation. The effect of sparking can be reduced, or disappear after an arc strikes. The heat of the arc will evaporate all moisture in the insulation. However, the heat of the arc will create carbon particles and damages the insulating material further, although the blast of the arc will clear some of the carbon particles.

In low voltage cable, a less likely cause of sparking are the discharges that come from cavities in the insulation material, such discharges are very common in high voltage environments. When the gas in the cavity breaks down, the surface of the insulation provide instantaneous cathode and anode [15]. Some of the electrons will have enough energy to break down the surface of the insulating material. The erosion will roughen and then penetrate the insulation surface. This process continues until the insulation completely breaks down.

The discharge process is highly unlikely in a low voltage cable as the electrical field stresses are far too low to cause this kind of behaviour, yet moisture vapour may cause the breakdown voltage to be low enough in the cavities to allow sparking.

5.3.3 Detection method

The spark phenomena can be detected using the same technique as well for the measuring of partial discharges in high voltage cables. The principle is based upon separating the earth shield of the distribution cable and using a coaxial cable to detect high frequency pulses near the fault location. To keep a path for the large power frequency (50/60 Hz) currents, a solid connection has to be made between the earth shields. Figure 5-9 illustrates the set-up of this method. The measurement can be affected by external high frequency signals. Depending on the connection of the coaxial cable, a small loop is created which can pick up external signals.

The coaxial cable has a relatively low impedance for high frequencies as compared to the impedance of the 50Hz connection because of its inductivity. The 50Hz connection has a low impedance for low frequencies and is considered a short cut for 50/60Hz current, but a high impedance for high frequencies ($j\omega L$) related to currents during sparking. Any discharges, which are high frequency pulses, prefer to travel through the coaxial cable. Installing a 50-ohm resistor at the other end of the coaxial cable prevent reflections. The signal can be measured using a recording device, e.g. an oscilloscope.

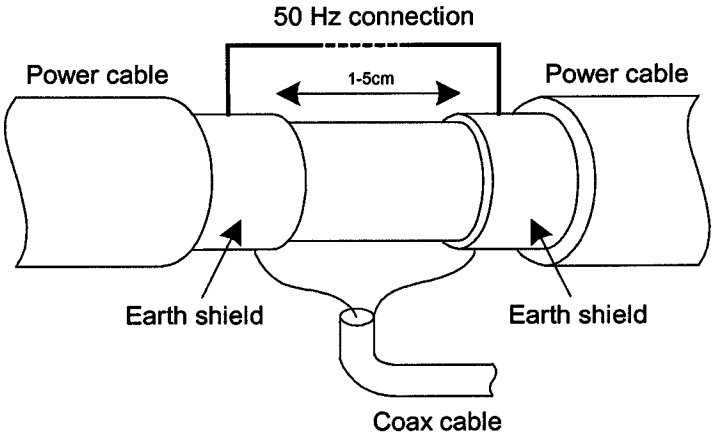

Figure 5-9 Circuit for spark detection in low voltage cable.

Figure 5-10 explains the principle of pulse reflection and transmission in more detail. A pulse travelling through a cable can be seen as two charges with opposite polarity travelling between two conductors or between conductor and earth sheath. The charge(s) will travel close to the edge of the conductor and earth shield. When a pulse travelling down the cable (1) reaches a change in impedance (2), reflection (3) and transmission will be the result (4 and 5). The reflection and transmission factors can be calculated using equations 3-9 and 3-10 on page 19.

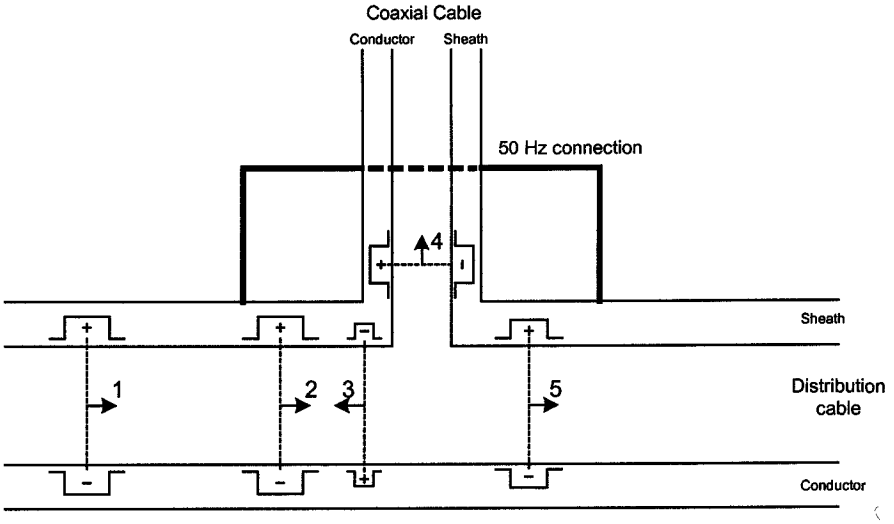

Figure 5-10 Illustration of pulse travelling down a low voltage distribution cable in combination with the spark detection circuit [17].

A part of the pulse will be transmitted to the coaxial cable and the continuing part of the distribution cable. The system that shows part of the spark pulse that propagates into the coaxial measuring cable connected to the scope can be simplified as illustrated Figure 5-9.

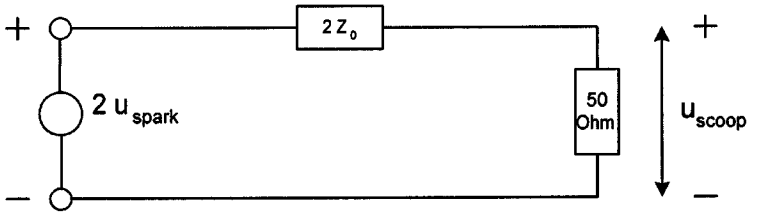

Figure 5-9 Simplified representation of spark detection circuit.

5.3.4 Results of sparking

The sparking is measured using the technique described in chapter 5.3.3. The cable sample is connected to the supply cable by means of connection leads. The sparking is measured on the paper cable sample near the fault location. This may introduce noise and additional reflection from the pulses generated by the sparking.

The data taken during sparking, shows that the spark phenomenon is concentrated at voltages above 200V or below –200V. The measured discharge amplitude varies randomly but tends to have maximum amplitude of about 500mV, occurring at the peak values of the supply voltage. Figure 5-10 shows the sparking with reference to the applied voltage. There are a large number of discharge signals occurring in one cycle, accompanied by reflections. This is caused by the open end of the paper cable sample and the connection leads. Appendix M figure M.2 shows more examples, one is taken at a higher sample rate (10 MHz) rate to make sure the complete frequency spectrum of the discharges was recorded. Another test was conducted at a sample frequency of 500 MHz, but the results were not any different to figure M.2 appendix M. The difference in sample rate does not make a huge difference in detecting the main discharges and therefore a 500 kHz sample rate is sufficient. Increasing the sample rate up to 100 Mhz will increase sensitivity to detect smaller pulses, however the used test set up can cause much distortion because of reflections and oscillations.

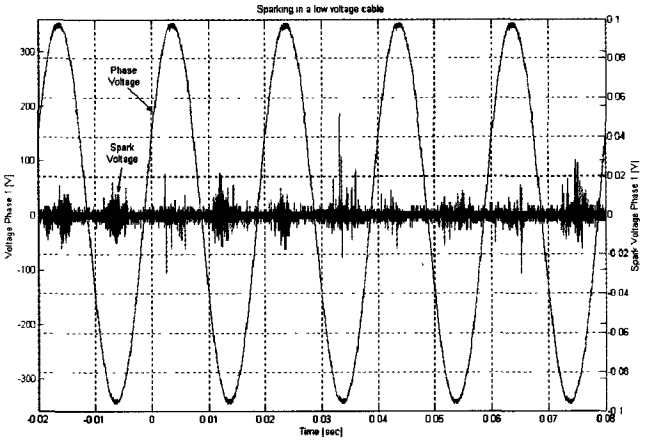

Figure 5-10 Measurement of sparking on a PILC cable with the reference voltage of phase L1, sampled at 500 kHz.

To calculate the measured spark voltage back to the value it has near the fault the following applies [17]:

$$u_{spark} = \frac{Z_{50ohm} + 2Z_0}{Z_{50ohm}} u_{scoop} \qquad (5\text{-}5)$$

In which Z_0 can be calculated using equation 3-4 (for the test net work Z_0=77ohm). Applying equation 5-5 a 300mV measured voltage (U_{scoop}) results in a spark voltage of 1,2V. Calculating the charge of the pulse can be accomplished with equation 5-6, in which t_0 the pulse width. For different pulse widths the charge is given in Table 5-1

$$q = \frac{t_0 \, u_{spark}}{Z_0} \qquad (5\text{-}6)$$

Table 5-1 Charge for different pulse widths using equation 5-6, in which 4000ns is measured and the others are used as reference values.

Pulse width [ns]	Charge [pC]
4000	36000
1000	9000
200	1800

The results from Table 5-1 show that charge is much larger than compared to a partial discharge as most of the sparking pulses are around pulse widths of 4000ns. This confirms that sparking has much higher discharge currents, which makes the tracking theory explained in chapter 5.3.2 much more likely.

The intensity of the sparking depends mainly on the amount of moisture together with the presence of carbon particles at the fault point. As the sparking causes the moisture to evaporate, the intensity will slowly decrease until there is hardly any sparking left as Figure 5-11 shows. Sparking can continue for a long time although its reoccurrence is adhoc and dependant on moisture left in the cable. The result of sparking can cause serious damage to the cables insulation as it slowly 'eats' the insulation away.

It is difficult to determine exactly whether the sparking happens between the oil impregnated paper insulation and the earth sheath or between the sheets of insulated paper.

Even though sparking is detectable, the amplitude of the discharges is too low to enable them to be detected at longer distances in a low voltage network. The number of T-joints in a low voltage circuit is much higher, than for example, in a medium voltage circuit. This causes pulse amplitude decline at every T-joint to a level where the signal does not exceed the noise amplitude. Furthermore it would only be applicable to the earth sheath of the cable making detection of phase to phase sparking impossible.

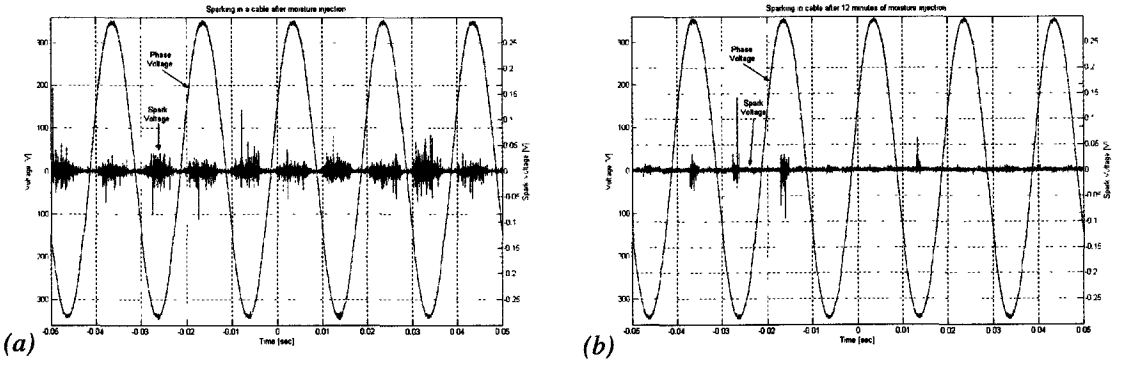

Figure 5-11(a) Sparking after moisture injection. (b) Sparking 12 minutes after moisture injection.

5.3.5 Results before and after arcing

To see if there is a relationship between the sparking and the ignition of an arc, data was taken of the sparking before and after an arc e.g. Figure 5-12. Although this figure suggests that there is sparking occurring before and after a low voltage arc, the figures in appendix N show a different fault with different results in sparking. During the event there is no sparking happening at all before the arc occurs. After the arc extinguishes the sparking starts for a number of periods after which it disappears or has a very low intensity.

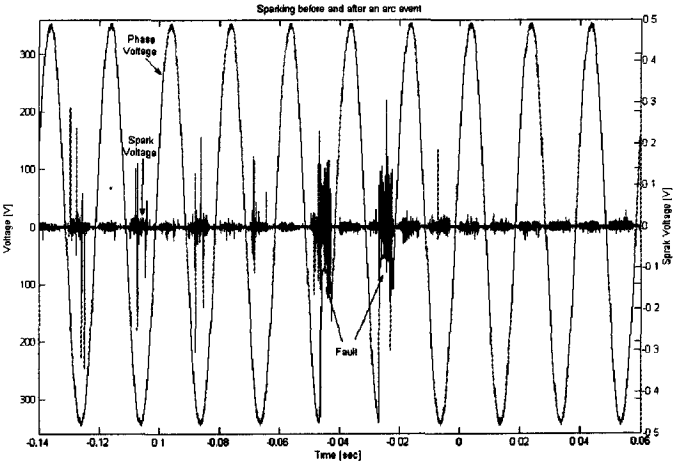

Figure 5-12 Measurement of sparking on a PILC cable with the reference voltage phase L1.

The same applies for figure N.2 where there is no relation between the arcing and the discharges recorded caused by the sparking. Even over longer time scales as figure N.3 shows there is not a direct relationship of spark intensity or magnitude to the ignition of an arc.

From the acquired data it can be concluded that there is no simple correlation between the sparking and the ignition of an arc. Sparking consistently occurs when there is enough moisture/pollution at the fault location. The chance of arc ignition seems to be not correlated to the sparking and both phenomena must be seen separated phenomena. However sparking does indicate the presence of water for a developing fault thus indicating an active fault, this could make sparking an interesting event to detect.

5.4 Fault location using arc voltage

Using the voltage and current measurements and cable properties gathered during the simulated arc, the fault can be located in the circuit. In most cases the resistance, inductance and capacitance values per kilometre of a cable are supplied by the cable manufacturer. The accuracy depends on how well the arc voltage is modelled.

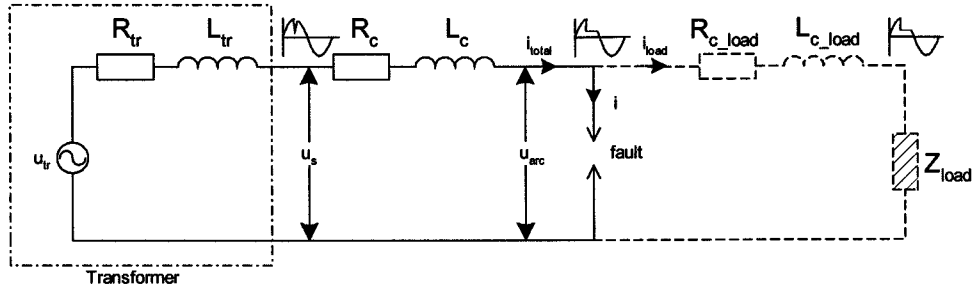

Figure 5-13 Schematic illustration of supply system with an arc fault.

Figure 5-13 gives a schematic illustration. The feeding and returning cores resistance and inductance have been taken together in R_c, L_c, R_{c_load}, L_{c_load}. Taking the feeding and returning impedance of the cable together introduces an error for a phase to earth fault as the return impedance through earth is difficult to determine and usually consist of other paths than just the earth sheath of the cable. Using Kirchoff's voltage law the supplied voltage should be equal to the sum of the voltages over all other components. In the model there is no load current flowing and the measured current at supply side is the arc current *i*.

$$u_s = i\,R_c + L_c\,\frac{di}{dt} + u_{arc} \tag{5-7}$$

For a data array equation 5-7 can be written in a matrix form as in equation 5-8. Where n is the start sample and $n+m$ is the end sample. This results in three unknown values R_c, L_c and u_{arc}. Both the cable resistance (R_c) and the cable inductance (L_c) are constant, although temperature increase of the conductor as a result of the large short circuit current can influence these values a little bit. The arc voltage u_{arc} will vary over time as explained in chapter 5.2.1.

$$\begin{bmatrix} u_s(n) \\ u_s(n+1) \\ \cdot \\ \cdot \\ u_s(n+m) \end{bmatrix} = \begin{bmatrix} i(n) & i'(n) & 1 \\ i(n+1) & i'(n+1) & 1 \\ \cdot & \cdot & \cdot \\ \cdot & \cdot & \cdot \\ i(n+m) & i'(n+m) & 1 \end{bmatrix} \begin{bmatrix} R_c \\ L_c \\ u_{arc} \end{bmatrix} \tag{5-8}$$

There are two ways of implementing equation 5-8. The first one is taking three data points and calculates the values for R_c, L_c and u_{arc}. This approach is used in script program impedanceURL.m. Calculating all three values over a period of time. If there is heavy over sampling of the signal, it is advisable to either bring the sample frequency down or to take more samples further apart. This will also keep the samples independent of each other and reduce the effect of bit noise.

Another approach is to estimate a value for the arc voltage from data gathered during the fault when the arc extinguishes and a distortion is created in the supply voltage. The distortion in voltage is shown in Figure 5-14. At the extinguishing point a peak in voltage occurs due to the behaviour of the arc voltage caused by the stop in current flow.

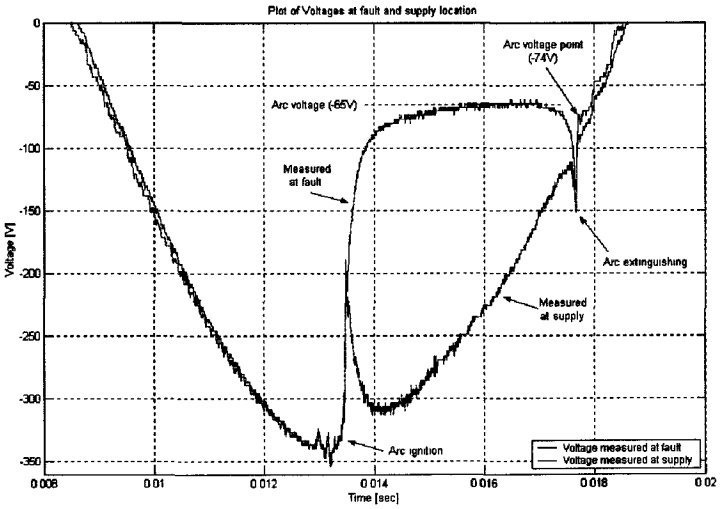

Figure 5-14 The effect of arc ignition and extinguishing on the supply voltage at 500 metres.

Just after the distortion, the voltage drops to the supply voltage. At this point the supply voltage equals the arc voltage and the arc voltage can be determined as Figure 5-14 shows. This method can result in a significant deviation from the real value. In the case of Figure 5-14 the minimum arc value is –65V and the determined arc voltage is –74V, leading to a 14% error. In reality though, the error is less because the determined arc voltage is used for the whole time span of the fault. Since the arc voltage is lower than the –74V at certain points, the average arc voltage will be much closer to –74V.

Implementing a pre defined arc voltage instead of the sampled arc voltage equation 5-8 will result in a two dimensional matrix as in equation 5-9.

$$\begin{bmatrix} R_c \\ L_c \end{bmatrix} = \begin{bmatrix} i(n) & i'(n) \\ i(n+o) & i'(n+o) \end{bmatrix}^{-1} \begin{bmatrix} (u_s(n) - u_{arc}) \\ (u_s(n+o) - u_{arc}) \end{bmatrix} \tag{5-9}$$

The following example shows how to implement a two and three dimensional matrix on a low voltage arc and will show the difference in accuracy. Data acquired from a simulated phase to neutral/earth fault at 500 metres is used for this example. The specification for the supply cable involved can be found in Table 4-3, which will be referred to for further calculations. Calculations are made using the software package MATLAB® 6, which can handle large data files. Appendix O contains the source code used for the following programs:

- **Execute.m** loads acquired data files, calculates fast Fourier transformation of the signals and makes basic impedance calculations.
- **Arc.m** analyses the data for arcs and determines the start and end time of arc(s), and it calculates arc voltage and arc current.
- **ImpedanceURL.m** executes equation 5-8 to calculate the arc voltage, cable resistance and impedance over time.
- **ImpedanceRL.m** executes equation 5-9 to calculate the cable resistance and inductance over time, using the pre defined u_{arc} value.
- **ChiURL.m** calculates the constant values for the cable resistance, cable inductance and arc voltage using the chi squared distribution as in equation 5-12.
- **ChiRL.m** calculates the constant values for the cable resistance and cable inductance using the chi squared distribution as in equation 5-12, using the pre defined u_{arc} value.

Solving matrixes numerically can cause some problems. In some cases a matrix is singular (determinant=0) or near singular, meaning that the matrix does not have an inverse. In MATLAB this

will result in an error and an infinite value, zero value, or inaccurate data. This leads to unusable data that will need to be filtered out. Filtering out can best be achieved by giving a maximum value to the cable resistance, since the cable has a length of 500 metres (one way) it means that the cable resistance cannot exceed 8 Ohms as Table 4-3 shows. The same principle can be applied for the inductance of the cable.

Differentiating the current can cause a problem as it acts as a noise amplifier. The way numerical differentiating works is by taking the difference between two samples and dividing by the sample time as in equation 5-10. To overcome this problem either the noise can be filtered out and the signals can be smoothed, or linear interpolation can be applied to the signal. The acquired equation from the linear interpolation can then be differentiated. Alternatively the equation 5-8 can also be integrated.

$$i'(n) = \frac{i(n+1) - i(n)}{t(n+1) - t(n)} \tag{5-10}$$

Due to the incomplete mode, and also measuring accuracy, R_c and L_c also depends on the chosen samples. These values can be averaged, however, the weight factors are unknown. In order to obtain these values, a more objective method is used: the "least square method" as applied in 5-12 assumes that all measured samples have equal absolute accuracy.

$$\chi^2 = \sum_n \delta(n)^2 = \sum_n (R_c i(n) + L_c i'(n) + u_{arc} - u_s(n))^2 \tag{5-11}$$

The most likely values of the parameters R_c, L_c and u_{arc} are those where χ^2 reaches a minimum. To determine the minimum the partial derivative can be taken for R_c, L_c and u_{arc}. These can be written in a matrix, equation 5-12. For the method of a assumed arc voltage, equation 5-12 would result in a 2x2 matrix.

$$\begin{pmatrix} \sum i(n)^2 & \sum i(n)i'(n) & \sum i(n) \\ \sum i(n)i'(n) & \sum i'(n)^2 & \sum i'(n) \\ \sum i(n) & \sum i'(n) & \sum 1 \end{pmatrix} \begin{pmatrix} R_c \\ L_c \\ u_{arc} \end{pmatrix} = \begin{pmatrix} \sum u_s(n)i(n) \\ \sum u_s(n)i'(n) \\ \sum u_s(n) \end{pmatrix} \tag{5-12}$$

The results of using equation 5-11 during the complete arc event time can be found in Table 5-2, together with the fault analysis for R_c and L_c. These results suggest that the performance of using an assumed arc voltage gives a more accurate result. However when the arc time window is made smaller and some of the start and end samples are ignored or given a lower weight, the results for using three variables (ChiURL.m) becomes significantly more accurate. The model is assuming a constant arc voltage, but in reality the arc voltage varies over time, this assumption causes the large error in calculation. Until there is a more accurate way of describing the arc voltage as a function of the arc current, the best result will be reached if the time window is made smaller during the arc event. It is then necessary to place the window at a time span where the arc voltage is almost constant to keep the error to a minimum.

In general working with an assumed arc voltage, which can be acquired from voltage waveform, gives a better result when using the complete number of samples during the arc event. When using a time span where the arc voltage is almost constant, the preferred method is using three variables (ChiURL.m) as no assumption needs to be made. In theory it should be possible to achieve an error better than 5%. In reality this will mainly depend on how accurately the data is supplied on the cable circuits resistance, inductance and length.

Another factor to consider is the nature of the used supply cable, the resistance is far bigger than the inductance, which makes the inductance negligible. This is reflected in the calculations, as the error in inductance is greater than with the resistance. Therefore the resistance was used to calculate the fault location. In practice the inductance will need to be taken into account for distribution cables, as they too have low resistance (and low impedance values). The fault distance can then be calculated from both parameters.

The result of working with three variables (ChiURL.m) will be more accurate if the arc voltage can be described as a function of the current. However this would also introduce a problem; if the circuit is fed from two sides for example, the current is only measured on one side, ignoring current fed from the other feeder(s). This method would be invalid, as the arc voltage is a function of both currents fed from the different supplies. To solve this problem, current could be measured at both feeders, which would require two recording devices. However when equation 5-8 is used, this problem does not occur as the arc voltage is determined by either a constant or a pre defined value.

Plots of the calculated arc voltage, cable resistance and inductance at a 500 metres fault can be found in appendix P, figures P.1 and P.3. For the calculations in impedanceRL.m an arc voltage of –60V was chosen for solving the cable resistance and impedance. To determine the constant values for the cable resistance and cable inductance the first 15 samples and the last 5 samples were ignored to increase accuracy. The reason for taking more samples at the start of the arc event is because the arc voltage changes are strongest here. A good guide for this is the current shape, as a sharp *di/dt* will result in variations in arc voltages. After the constant values have been calculated they can be filled in equation 5-8 to calculate the arc voltage. Results can be found in appendix P figures P.2 and P.4, which show that the arc voltage can be modelled fairly accurately.

Both methods are independent of the measuring location if voltage and current are measured at the same point. Therefore measuring at different locations at the same time will allow better fault location in circuits with many T-joints.

Table 5-2 Result of calculated distance on simulated phase neutral fault.

Program	R_c [Ohm]	L_c [mH]	Location using R_c and Table 4-3 [metres]	Error[2] R_c [Ohm]	Error[2] L_c [mH]
ChiURL.m at 0 metres	-0,3	0,09	19	0,08	0,06
ChiRL.m[1] at 0 metres	0,1	0,09	6	0,04	0,02
ChiURL.m at 200 metres	1,82	0,2	117	0,4	0,04
ChiRL.m[1] at 200 metres	3,3	0,2	211	0,2	0,05
ChiURL.m at 500 metres	6,0	0,4	385	0,4	0,05
ChiRL.m[1] at 500 metres	8,3	0,4	532	0,2	0,07

[1]Using an assumed arc voltage of –60 volt [2]Using chi square method

The process of determining the fault location becomes more difficult for circuits with multiple cable sections. Using transformation ratios, the different cable types can be brought back to one type of cable as the following example explains.

Example:

A circuit consists of three-cable sections all connected in series. All sections have different diameters, giving them different resistance values. Table 5-3 shows the conductor area, cable length and resistance value for each section.

Table 5-3 Properties of cable sections.

Circuit	Conductor area [mm^2]	Length [metres]	Resistance [μΩ/m]
Section 1	400	250	78
Section 2	185	475	164
Section 3	240	150	125

To calculate the sections back to the cable used in section one, the following equation can be applied

$$ratio_{Cable1->Cable2} = \frac{R_{cable2}}{R_{cable1}} \tag{5-13}$$

Taking the 400mm^2 cable as a reference cable the ratio factors can be calculated using equation 5-13

$$ratio_{185->400} = \frac{164}{78} = 2{,}1 \qquad ratio_{240->400} = \frac{125}{78} = 1{,}6$$

Using the ratio factors the cable lengths can be recalculated to the 400mm^2 reference size. Resulting in:

$$L_{185->400} = ratio_{185->400} \times 475 = 1001\ metres$$

$$L_{250->400} = ratio_{240->400} \times 150 = 241\ metres$$

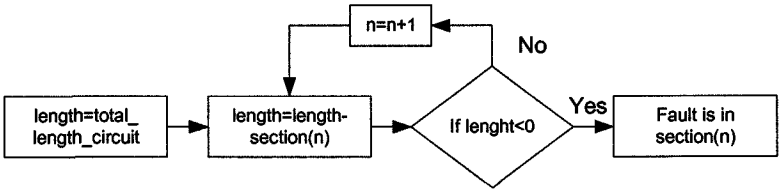

Figure 5-15 Flow diagram how to determine in which section the fault is.

Using the impedance calculations a resistance of 100 milli Ohm is calculated representing a distance of 1285 metres of 400mm^2 cable. To calculate the fault distance back into real values, it is necessary to take the fault distance minus the length of section one. This is explained in the flow diagram in Figure 5-15. For this example it will result in the following:

$$1285 - 250 - 1001 = 34\ metres$$

The above shows that the fault is in section three. To transfer the calculated value back to its real value (normalised to 400mm^2), the number of metres must be divided through the ratio factor of the cable. The result in a cable length will be 21 metres of the start of section three, or 746 metres from the start of section one. The same can be applied for the inductance.

Even though it is possible to make fault location calculations, there will always be a small error in the fault distance. In a low voltage network this can have some consequences, as there are a large number of T-joints. As Figure 5-16 shows the real fault is in one of the branches, but the calculated fault might be anywhere with the error of calculation or at different point along the circuit that match the calculated distance. This makes fault finding particularly difficult.

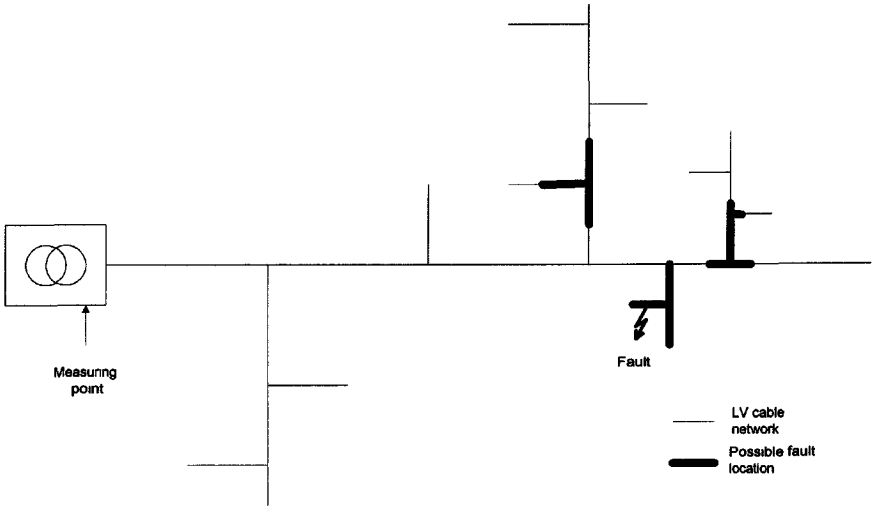

Figure 5-16 Effect of error on fault location in a low voltage network.

5.5 Conclusion

Arcs are unpredictable phenomena, literature is widely available on this phenomena, although assumptions still need to be made to calculate the arc conductance. Determining the conductance of a low voltage arc without measuring the arc voltage directly or making assumptions is virtually impossible, as the arc conductance mainly depends on the plasma generated during the fault. During ignition, the arc conductance behaves linear to the current, but at the point where the maximum current has been reached, this changes in non linear behaviour, which makes it impossible to determine the exact arc conductance after the maximum arc current is reached. However, it is possible to determine the arc voltage by means of using the transient created in the supply voltage during the extinguishing of an arc, which gives some confirmation on the arc conductance.

Before a fuse blows and a low voltage fault is created. There are two incipient phenomena that can be detected, sparking and arcing. Sparking occurs constantly when there is moisture at the fault point and only occurs in the upper part of the sinusoidal voltage. The intensity is dependent on the quantity of moisture in the cable. Arcing occurs as well when there is the presence of moisture in the cable, however the ignition of the arc looks random and does not seem have any reference to the intensity of the sparking.

Sparking is hard to detect due the high frequencies that need to be captured, making recording equipment expensive. From a practical point of view the pulses generated by the sparking are of such a low magnitude that due to reflection of T-joints they will not be detectable at the supply location. However sparking does indicate moisture penetration in a cable and as this event occurs over long time periods, it can be used to determine if a cable is developing a fault (if it can be detected at the supply).

From both phenomena, arcing is the most promising to detect. With low cost recording equipment an arc can be detected in the phase voltage(s) and when current is recorded, a fault location can be calculated. There are two options of impedance calculation, namely using three variables, cable resistance, cable inductance and arc voltage, or using two variables, cable resistance and cable inductance, in which the arc voltage is are defined. Both methods give accuracies better than 10%. Using three variables is the preferred option as no assumptions need to be made. However, the two variable method performs better when calculation over the complete fault time. Therefore it is recommended to use both solution methods, as this will allow for comparing the results.

Although the impedance calculations are reasonably accurate, problems could occur in a real circuits, as it is difficult to know exactly what the return impedance is through earth, in the event of a phase to the earth fault.

6 Recommendations

6.1 Modify existing resources

London has about 15.000 low voltage substations of which 6000 are equipped with a remote terminal unit (RTU). This unit records various properties in the substation, including all three phase voltages and currents. Any abnormality in the recorded properties will cause the unit to communicate with a main computer in the control room through a low speed radio modem (300 BAUD). The main computer can only communicate with one RTU at a time, due to the fact that communication devices allow only one connection.

In principle it is possible to modify the program of these units and allow them to detect any characteristics that could indicate a low voltage fault. However, the sampling rate of the micro controller is low, losing resolution and making fault detecting more difficult. Furthermore, the recorded data needs to be sent to a main computer for analysis, as the current micro controller is not fast enough. This will be virtually impossible as there is a lack of bandwidth making transfer times too long for the RTU to upload the information. This will clog up the system though, as the main computer can only communicate with one RTU at the time. The RTU is still an option to look further into, and to see if it would be possible to do onboard processing.

6.2 New prototype low voltage fault detection

Building a fault detecting recorder is another option to consider. Using a micro controller it is possible to develop a low cost solution. However there are a number of specifications that the micro controllers need to meet:

- High clock frequency (>20 MHz) to allow sampling of data at 20 kHz and above, and still keep enough processing speed available to process data.
- At least six A/D converters with sampling at 8-bits or at 10-bits.
- Be able to communicate with a modem.
- Have the memory capacity to be able to record sufficient data.

A processor that can handle these specifications is the *Microchip* PIC18F452 micro controller. This micro controller runs at a clock frequency of 40 MHz with 1536 byte RAM, 8x 10 bit A/D converters and 2x D/A converters. Using a development board and wide range of source code examples supplied by the manufacturer *Microchip*, development time can be kept to a minimum. The total cost of this development board would be around £150 (quoted June, 2002).

Using this micro controller it should be possible to calculate the fault location onboard, the device needs to be able to communicate with a modem for remote communications to allow data to be sent back to a main server for possible further analysis.

To measure the supplied voltage a resistance/capacitance bridge divider can be used although it is preferred to use isolation transformers to keep the distribution circuit strictly separated from the recording device from a safety aspect.

To compensate for any load current, the load current together with the phase shift can be recorded constantly or every 30 minutes, depending on the available process time and memory. The recorded waveform can then be subtracted form the current during a fault, making fault location more accurate. This introduces a problem though, as short circuit currents are many times higher than the load current, meaning that the termination of the current transformer must be set for large circuit currents, resulting in resolution loss as the A/D converters range is from zero to five volts. A way to get around this problem is by using an A/D converter with a higher bit ratio e.g. 10 bit instead of 8 bit. Another option is to use two A/D converters to measure the same signal at different sensitivities, or by using relays to switch terminating resistor values when measuring the load current. Side effect of using relays is the large time of switching.

In substations equipped with a Remote Terminal Unit (RTU), the recorder could be installed next to the RTU, giving the RTU a signal in event of a fault. The RTU can then contact (at 300 BAUD connection) the server in the control room to update the circuit status. This would save installing a cellular modem unit.

As the unit is recording the voltage and current waveforms, it is possible to calculate the power factor and half-hourly load data. This would make the device highly flexible and still be a low cost solution. Also the D/A converter that is built into the micro controller can be used for pulse echo measurement to locate the fault more accurately.

For internal communications within the substations between multiple units, a different *Microchip* processor can be used which could support the CAN 2.0B wireless network.

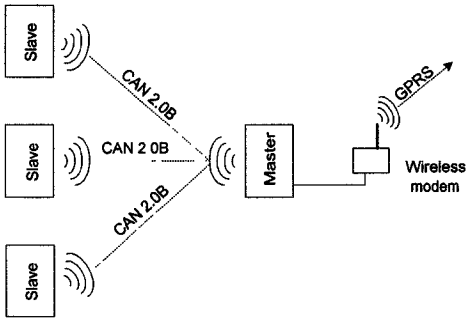

Figure 6-1 Representation of multiple units monitoring different circuits in a substation, communication with one master unit.

A rough schematic is given in Figure 6-2. In which X_1 and X_2 are voltage resistor dividers to bring the measured voltage down. The dividing factor depends on the maximum resolution of the A/D converter. To increase the frequency, response capacitors need to be placed parallel to the resistors, keeping in mind that both X_1 and X_2 have the same RC times. The component Y can either be one terminating resistance or a number of different resistors controllable through relays. It is important that the cables going to the bus-bar are fused as close as possible to the bus-bar to give maximum protection.

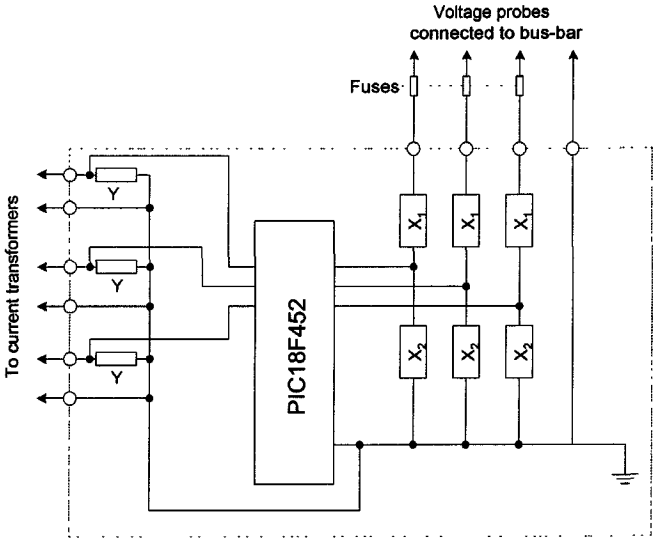

Figure 6-2 General schematic prototype disturbance recorder.

A long term view on fault location in low voltage networks would be the installation of multiple units in a cable circuit at various points for example in link boxes. These units could be modified to detect faults and fire a pulse during the fault to make a pulse echo localisation. As multiple units are installed on the circuit, the effect of attenuation of the pulse due to T-joint becomes less of an issue. After the localisation of the fault, units could communicate with each other using the distribution cable via a modem. A master unit in the substation would then make a decision and transfer the data to a server fault database.

7 Conclusion

The results acquired show that there are two incipient phenomena existing before a fuse blows and a low voltage fault is created. The first is a spark phenomenon, which occurs due to the moisture penetration in the oil impregnated paper insulation. Sparking will slowly 'eat' the insulating material away until there is no moisture or until there is other pollution left for sparking to occur. The second phenomenon is the arc caused by the breakdown of the insulation. Arcing causes significant damage to the cable leaving carbon particles behind while clearing the fault from most moisture content for a limited period of time.

Arc phenomena are an unpredictable event occurring when the insulation suddenly breaks down. The behaviour is mainly dependent on the maximum current flowing through the arc, which determines the arc conductance and therefore the arc voltage. When the arc ignites, the voltage will quickly drop to a minimum threshold value and will slowly rise when the current starts to drop. The rise and drop in arc voltage is subjected to a hysteresis effect causing different values for the voltage during ignition and extinguishing of an arc. Large current arcs tend to extinguish themselves quicker and are less repetitive in early development stages of a fault compared to low current arcs. This is caused due to their volatile behaviour, which clears the fault location of all moisture, and the blasts will leave less carbon particles behind. Large current arcs will do more damage to the cable and are more likely to cause a permanent fault in a shorter time span. They also tend to have lower arc voltages, as the arc conductance is mainly dependent on the arc current.

Although the spark phenomenon indicates moisture has penetrated the cable and a fault is developing, it does not seem to have a direct correlation to the ignition of an arc and is not incipient to the ignition of an arc. Therefore the arc phenomenon needs to be seen as a random event. As sparking continues for a longer time period it can be interesting to monitor it. The discharges caused by the sparking are detectable when measuring close to the spark event. However due to the large number of T-joints on a low voltage network detection of these discharges is difficult or impossible. The T-joints cause significant attenuation for discharge pulses.

At present there are only a few methods available to conduct fault location on low voltage networks and most of them work on the basics of pulse reflection. This method does not allow fault detection on the branches of a distribution cable and the number of T-joints limit the range in which fault can be localised. The results from the simulated test show that fault location is actually possible with a reasonable accuracy (within 10%) using fault impedance calculations.

In reality one of the major problems to overcome is the lack of information on cable circuits as many of them consist of dozens of different type of cables sections and joints. The fault location given by the impedance calculations can also be related to different cables in the circuit as there are many branches, which will cause alternative fault locations.

With the current status of technology it is relatively easy to develop a low cost device that can detect and analyse low voltage arcs before they result in a low voltage fault, making the monitoring and localisation of low voltage circuits affordable. Even though technology can help locating low voltage faults, pinpointing of a fault in low voltage networks remains difficult.

8 Suggestions for future work

The results of this report give concrete answers to the behaviour of low voltage faults and form the base of further studies in how to prevent and solve low voltage fault. There are some areas in which more studies and tests can be done:

- **Live test:** Testing of simulated faults on a 500 metres long PILC or CONSAC distribution network with a 500kVA or larger supply transformer. This will allow verification of the effect of large current arcs and to check if the sparking can be detected on a distance at 500 metres with and without any T-joints. Also it will give a better insight into how the arc voltage behaves on a low resistance and inductance cable at large currents.
- **Effect of closed fault:** Investigate the effect on voltage and behaviour of an arc phenomena and the spark phenomena in the event of an in closed fault in the cable, for example a buried cable. This can be accomplished by sealing of the moisture injection hole. The expectation using equation 5-2 is that the arc voltage will rise as the arc conductance will decrease due to less cooling power . This should be related to the lower cooling power and thus increasing the arc resistance.
- **Model of arc:** A model of the arc as a function of the current would be needed to make fault location more accurate. If it would be possible, the most ideal result would be determining the k in equation 4-1.
- **Effect of supply voltage:** Conduct test with a 110 Volt (American) system to investigate if arcing and sparking occurs at this voltage.
- **Acquire real data:** Gather more data on real field faults to calculate the fault location and with the help of a pulse reflection device and/or by digging up the cable location to check the calculations.
- **Long term faults:** Investigate if there are relationships between sparking and arcing over a long time span, preferably from the start of a developing fault. Measuring the number of arcs during this time span to acquire a more detailed picture into the fault development process. Investigate how long before a cable fails, sparking and arcing occur.
- **Loaded cables:** Conduct tests with loaded circuits to investigate the effect of loads on the arc event to verify why some results from the field have distortions after an arc.
- **Transients:** Investigate if there are detectable transients at ignition and extinction of an arc that can be used for fault location. For now it seems that it is likely to have transients at the both ignition and extinguishing events.
- **Low costs prototype:** Development of a low cost recording device that meets the specifications for detecting low voltage arcs and calculating the fault distance.
- **Tune algorithms:** Improve the performance of the computer algorithms that determine and calculate the arc voltage, cable resistance and cable inductance. Improve chi-squared distribution by conducting more calculation into the correlation between the calculated parameters.

9 References

[1] *Tijhuis, A.G.*
Elektromagnetisme 2
Eindhoven (the Netherlands): Eindhoven University of Technology
1999
Lecture book 5F080

[2] *Moore, G.F.*
Electric Cables Handbook
Third Edition
Liverpool: Blackwell science, 1997
ISBN 0-632-04075-0

[3] *Neimanis, R*
On estimation of Moisture Content in Mass Impregnated Distribution Cables
Stockholm, Kugl Tekniska Hogskolan
Stockholm, 2001
Doctoral Dissertation, ISSN 1100-1593

[4] *Jones, E.W.P*
The great dielectric phenomenon
Power Engineering Journal, January 1989: p. 33-37

[5] *Clegg, B.*
Underground Cable Fault Location
Maidenhead, England: BCC Electrical Engineering and Training Consultancy, 1998
ISBN 0-95-325609

[6] *Kreuger, F.H.*
Industrial High Voltage
Delft University Press, 1992
ISBN 90-6275-562-3

[7] *Overbeek, H.H.*
Elektriciteitsopwekking -transport en –distributie, deel II
Eindhoven, the Netherlands: Eindhoven University of Technology
1992
Lecture book

[8] *Kraus J.D.*
Electromagnetics
Singapore: McGraw-Hill Inc., 1991
ISBN 0-07-112666-x

[9] *Oyegoke, B. and Hyvönen, P. and Aro, M.*
Dielectric Response Measurements as Diagnostic Tool for Power Cable Systems, Literature Review
Espoo, Finland: Helsinki University of Technology
Espoo 2001
ISBN 951-22-5396-8

[10] *Gale, P.F.*
Cable-fault location by impulse-current method
PROC. IEE Vol. 122, Bo 4, April 1975

[11] *Gale, P.F.*
Voltage dips due to transitory low voltage cable faults
International Conference on Sources and Effects of Power System Disturbances.
IEE, London, UK; 1974; xii+272 pp. p.36-40.

[12] *Kleiner, C.T.*
An Electrical surge arrestor (ESA) model for computer-aided design and evaluation
IEEE publication
Anaheim, California, 1978

[13] *van de Sluis, L. and Rutgers, W.R.*
The Comparison of Test Circuits with Arc Models
IEEE Transactions on Power Vol.10, No. 1, January 1995

[14] *Brownse J.R.*
The Electrical Arc as a Circuit Element
Journal of electrochemical society, January 1955

[15] *Kuffel, E. and Zaengl, W.S. and Kuffel, J.*
High Voltage Engineering Fundamentals. 2th ed.
Oxford: Butterworth-Heinemann, 2000
ISBN 0 7506 3634 3

[16] *Orr, J.A. and Emanuel, A.E.*
On the Need for Strict Second Harminc Limits
IEEE Transaction on power delivery, Vol. 15 (July 2000), No. 3, p. 9

[17] *Steennis, E.F.*
Metingen van partiële ontladingen in hoogspanningskabels
Eindhoven (the Netherlands): Eindhoven University of Technology
1981
Msc. Thesis67-971

Appendix A : Specification PILS Cable

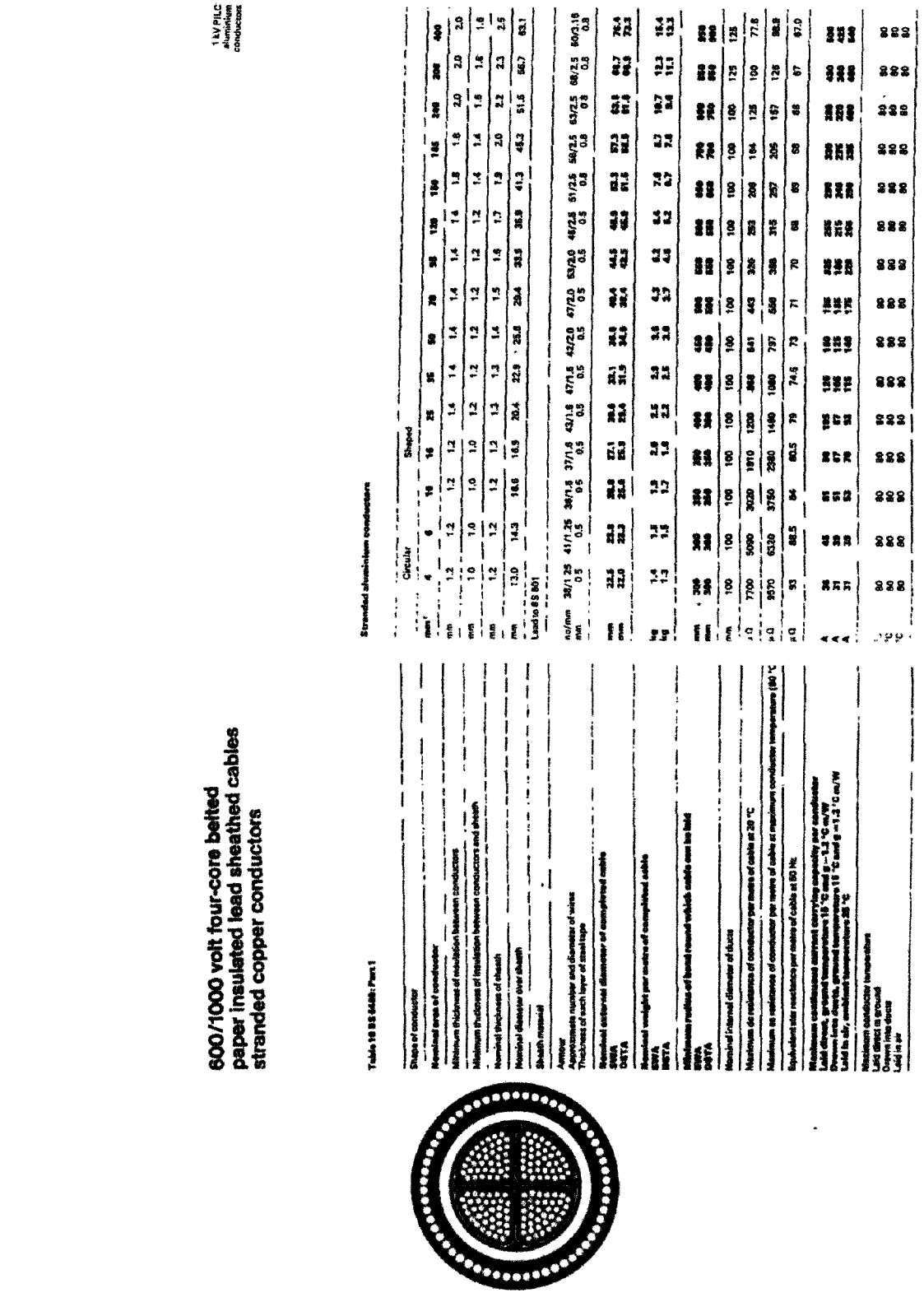

1 kV PILC aluminium conductors

600/1000 volt four-core belted paper insulated lead sheathed cables stranded copper conductors

Stranded aluminium conductors

Table 19 BS 6480: Part 1

Shape of conductor		Circular				Shaped																
Nominal area of conductor	mm²	4	6	10	16	25	35	50	70	95	120	150	185	240	300	400						
Minimum thickness of insulation between conductors	min	1.2	1.2	1.2	1.2	1.4	1.4	1.4	1.4	1.4	1.4	1.4	1.8	1.8	2.0	2.0	2.0					
Minimum thickness of insulation between conductors and sheath	mm	1.0	1.0	1.0	1.0	1.2	1.2	1.2	1.2	1.2	1.2	1.2	1.4	1.4	1.6	1.6	1.6					
Nominal thickness of sheath	mm	1.2	1.2	1.2	1.2	1.3	1.3	1.4	1.5	1.6	1.7	1.8	2.0	2.2	2.3	2.5						
Nominal diameter over sheath	mm	13.0	14.3	16.6	16.9	20.4	22.9	25.8	29.4	33.5	36.9	41.3	45.2	51.6	56.7	63.1						
Sheath material	Lead to BS 801																					
Armour																						
Approximate number and diameter of wires	no/mm	38/1.25	41/1.25	38/1.6	37/1.6	43/1.6	47/1.6	42/2.0	47/2.0	53/2.0	48/2.5	51/2.5	56/2.5	63/2.5	66/2.5	80/2.16						
Thickness of each layer of steel tape	mm	0.5	0.5	0.5	0.5	0.5	0.5	0.5	0.5	0.5	0.5	0.8	0.8	0.8	0.8	0.8						
Nominal external diameter of completed cable																						
SWA	mm	22.5	23.8	26.8	27.1	30.6	33.1	36.8	40.4	44.5	48.8	53.3	57.3	63.8	69.7	76.4						
SWTA	mm	22.0	23.3	25.6	25.9	29.4	31.9	34.9	38.4	42.5	46.8	51.5	55.5	61.8	66.8	73.3						
Nominal weight per metre of completed cable																						
SWA	kg	1.4	1.6	1.9	2.0	2.5	3.0	3.6	4.3	5.2	6.4	7.6	8.7	10.7	12.3	15.4						
SWTA	kg	1.3	1.5	1.7	1.8	2.3	2.6	3.0	3.7	4.5	5.2	6.7	7.6	8.8	11.1	13.3						
Minimum radius of bend around which cable can be laid																						
SWA	mm	300	300	300	300	400	400	400	500	550	550	550	700	700	800	800						
SWTA	mm	300	300	300	300	400	400	400	500	550	550	550	700	700	800	800						
Nominal internal diameter of ducts	mm	100	100	100	100	100	100	100	100	100	100	100	100	100	125	125						
Maximum dc resistance of conductor per metre of cable at 20 °C	μΩ	7700	5090	3020	1910	1200	868	641	443	320	253	206	164	125	100	77.6						
Maximum ac resistance of conductor per metre of cable at maximum conductor temperature (90 °C	μΩ	9570	6330	3750	2380	1490	1080	797	550	398	315	257	205	157	126	96.9						
Equivalent star resistance per metre of cable at 50 Hz	μΩ	53	88.5	84	80.5	79	74.5	73	71	70	68	69	69	68	67	67.0						
Maximum continuous current carrying capacity per conductor																						
Laid direct, ground temperature 15 °C and $g = 1.2$ °C m/W	A	36	46	61	80	105	128	160	196	225	260	299	330	380	430	504						
Ducts in ducts, ground temperature 15 °C and $g = 1.2$ °C m/W	A	31	39	51	67	87	106	135	166	195	215	248	275	320	360	425						
Laid in air, ambient temperature 25 °C	A	31	39	53	70	93	118	148	175	225	266	306	335	400	460	540						
Maximum conductor temperature																						
Laid direct in ground	°C	80	80	80	80	80	80	80	80	80	80	80	80	80	80	80						
Ducts into ducts	°C	80	80	80	80	80	80	80	80	80	80	80	80	80	80	80						
Laid in air	°C	80	80	80	80	80	80	80	80	80	80	80	80	80	80	80						

Appendix B : Specification CONSAC Cable

ESI Standard 09-8 — **Solid aluminium conductors**

Shape of conductor		Shaped							
Nominal area of conductor	mm²	70	95	120	150	185	240	300	
Minimum thickness of insulation between conductors	mm	1.4	1.4	1.4	1.8	1.8	2.0	2.0	
Minimum thickness of insulation between conductors and sheath	mm	1.2	1.2	1.2	1.4	1.4	1.8	1.8	
Nominal thickness of sheath	mm	1.1	1.2	1.4	1.5	1.7	2.0	2.2	
Nominal diameter over sheath	mm	23.4	26.6	29.4	32.7	36.0	41.1	45.3	
Nominal thickness of PVC oversheath	mm	1.9	2.1	2.2	2.3	2.5	2.7	2.8	
Nominal external diameter of completed cable	mm	27.6	31.2	34.2	37.8	41.5	47.1	51.4	
Nominal weight per metre of completed cable	kg	1.2	1.5	1.9	2.3	2.8	3.6	4.3	
Minimum radius of bend round which cable can be laid	mm	480	500	560	600	650	750	860	
Nominal internal diameter of ducts	mm	100	100	100	100	100	100	100	
Maximum dc resistance of conductor per metre of cable at 20 °C	μΩ	443	320	253	206	164	125	100	
Maximum dc resistance of sheath (neutral conductor) per metre at 20 °C	μΩ	386	310	242	206	164	126	100	
Maximum ac resistance of conductor per metre of cable at maximum conductor temp	μΩ	551	398	315	257	205	157	126	
Equivalent star reactance per metre of cable at 50 Hz	μΩ	70.5	69.0	66.5	66.5	66.5	66	67.5	
Maximum continuous current carrying capacity per conductor									
Laid direct, ground temperature 15 °C and g = 1.2 °C m/W	A	185	230	250	290	320	370	420	
Drawn into ducts, ground temperature 15 °C and g = 1.2 °C m/W	A	160	190	210	235	265	310	350	
Laid air, ambient temperature 25 °C	A	185	205	235	270	310	370	425	
Maximum conductor temperature									
Laid direct in ground	°C	80	80	80	80	80	80	80	
Drawn into ducts	°C	80	80	80	80	80	80	80	
Laid in air	°C	80	80	80	80	80	80	80	

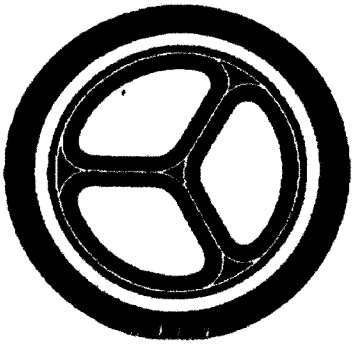

Appendix C : Current Transformer Specifications

LEM

LEM US UE 0.34 1000 Current Transformer Specification

Nominal Input Current	**1000 Amperes**
Continuous Input Current	**1200 Amperes**
Overload	**x20 Nominal Input Current for 1 second**
Output Signal	**0.34V AC at Nominal Input Current**
Ratio	**2941:1**
Typical Accuracy	**±1 %**
Maximum Error	**±2% of reading**
Load Impedance	**1 kΩ min. for specified accuracy**
Accuracy at 2kHz	**±2% at 200 Amperes**
Phase Error at 2kHz	**<0.5°**
Phase Error	**In range 100A to 1200A < 1°**
Frequency range	**40Hz to 5kHz (fundamental)**
Safety Class	**Class III as per IEC1010-1**
Dielectric Strength	**3kV, 50Hz for 1 minute**
Temperature Range	**-10°C to +50°C**
Max. Working Voltage	**600V Category III as per IEC1010-1**
Jaw Aperture	**43mm**
Dimensions	**90 x 205 x 40mm**
Weight	**0.485kg**
Colour	**Blue / grey**
Output	**1½m cable, type FM2R**
	S1- White
	S2- Blue

Generic Test Result

Current (A)	Amplitude Error(%)	Phase Error(°)	Test Frequency
5	-2.1	from	50Hz
10	-1.5	2	50Hz
20	-0.8		50Hz
50	-0.3	to	50Hz
100	+0.4		50Hz
500	+0.6		50Hz
1000	+0.8	0.5	50Hz

LEM HEME LIMITED
PENKETH PLACE
MEDWAY PARK, SKELMERSDALE
LANCASHIRE WN8 9PX UNITED KINGDOM
Registered in England
Company Number 1378145
Registered Office Penketh Place Skelmersdale
TEL 01695 20020
FAX 01695 50279
www.lem.com

Appendix D : Phase to earth/neutral fault

The following conditions have been used to calculate the short circuit currents for phase to neutral fault including the arc impedance:

$$\begin{aligned} \underline{U}_R &= \underline{U}_1 + \underline{U}_2 + \underline{U}_0 \\ \underline{U}_S &= a^2\,\underline{U}_1 + a\,\underline{U}_2 + \underline{U}_0 \\ \underline{U}_T &= a\,\underline{U}_1 + a^2\,\underline{U}_2 + \underline{U}_0 \end{aligned} \qquad \text{(D-1)}$$

$$\begin{aligned} \underline{I}_R &= \underline{I}_1 + \underline{I}_2 + \underline{I}_0 \\ \underline{I}_S &= a^2\,\underline{I}_1 + a\,\underline{I}_2 + \underline{I}_0 \\ \underline{I}_T &= a\,\underline{I}_1 + a^2\,\underline{I}_2 + \underline{I}_0 \end{aligned} \qquad \text{(D-2)}$$

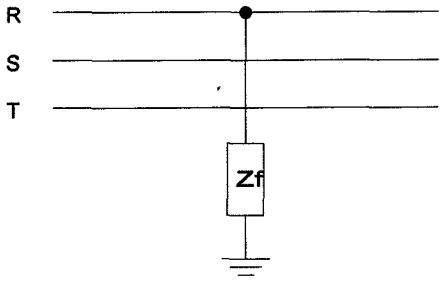

Figure D.1 Illustration of phase to earth fault.

$$\begin{aligned} \underline{U}_1 &= \underline{E}_b - \underline{I}_1\,\underline{Z}_1 \\ \underline{U}_2 &= -\underline{I}_2\,\underline{Z}_2 \\ \underline{U}_0 &= -\underline{I}_0\,\underline{Z}_0 \end{aligned} \qquad \text{(D-3)}$$

In which $\underline{E}_b = \dfrac{U_n}{\sqrt{3}}$ and $a = e^{j\frac{2}{3}\pi}$

Conditions for the 1-phase fault

$$\underline{I}_S = \underline{I}_T = 0$$

$$\underline{U}_R = \underline{I}_R\,\underline{Z}_f$$

In which $\underline{Z}_f$ is the impedance of the low voltage arc. The load current in phase R is not taken into account and therefore I_R will only include the fault current through $\underline{Z}_f$.

Using (D-1), (D-2) and (D-3):

$$\underline{I}_S = \underline{I}_T \rightarrow a^2\,\underline{I}_1 + a\,\underline{I}_2 + \underline{I}_0 = a\,\underline{I}_1 + a^2\,\underline{I}_2 + \underline{I}_0$$

$$(a^2 - a)\,\underline{I}_1 = (a^2 - a)\,\underline{I}_2 \Rightarrow \underline{I}_1 = \underline{I}_2$$

$$\underline{I}_S = 0 \rightarrow a^2\,\underline{I}_1 + a\,\underline{I}_1 + \underline{I}_0 = 0 \Rightarrow \underline{I}_0 = \underline{I}_1$$

Next the relation to Z_f needs to be determined:

$$\underline{U}_R = \underline{U}_1 + \underline{U}_2 + \underline{U}_0 = \underline{I}_R\,\underline{Z}_f = 3\,\underline{I}_1\,\underline{Z}_f$$

$$\underline{E}_b - \underline{I}_1\,\underline{Z}_1 - \underline{I}_1\,\underline{Z}_2 - \underline{I}_1\,\underline{Z}_0 = 3\,\underline{I}_1\,\underline{Z}_f$$

$$\underline{I}_1 = \frac{\underline{E}_b}{\underline{Z}_1 + \underline{Z}_2 + \underline{Z}_0 + 3\,\underline{Z}_f} = \underline{I}_2 = \underline{I}_0$$

$$\underline{I}_R = \frac{3\,\underline{E}_b}{\underline{Z}_1 + \underline{Z}_2 + \underline{Z}_0 + 3\,\underline{Z}_f}$$

Assuming that $\underline{Z}_1$=$\underline{Z}_2$ the 1-phase short circuit current can be described as followed:

$$\underline{I}_k = \frac{\sqrt{3}\,U_n}{2\,\underline{Z}_1 + \underline{Z}_0 + 3\,\underline{Z}_f} \qquad \text{(D-4)}$$

Appendix E : Phase to Phase

The following conditions have been used to calculate the short circuit currents for phase to phase fault including the arc impedance:

$$\underline{I}_R = 0 \Rightarrow \underline{I}_0 = -\underline{I}_1 - \underline{I}_2 \Rightarrow \underline{I}_0 = 0$$

$$\underline{I}_S = -\underline{I}_T \Rightarrow (a^2 + a)(\underline{I}_2 + \underline{I}_1) + 2\underline{I}_0 = 0$$

$$\Rightarrow \underline{I}_0 = 0, \quad \underline{I}_2 = -\underline{I}_1 \qquad \text{(E-1)}$$

$$\underline{U}_S - \underline{U}_T = \underline{I}_S \, \underline{Z}_f \qquad \text{(E-2)}$$

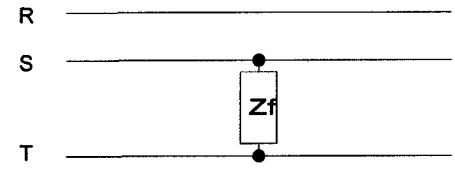

Figure E.1 Illustration of phase to phase fault.

Using equation D-1 and E-2

$$a^2 \underline{U}_1 + a\underline{U}_2 + \underline{U}_0 - a\underline{U}_1 - a^2 \underline{U}_2 - \underline{U}_0 = \underline{I}_S \, \underline{Z}_f$$

$$(a^2 - a)(\underline{U}_1 + \underline{U}_2) = \underline{I}_S \, \underline{Z}_f$$

With D-3

$$\underline{E}_b - \underline{I}_1 \underline{Z}_1 - \underline{I}_1 \underline{Z}_2 = \frac{j \underline{I}_S \underline{Z}_f}{\sqrt{3}}$$

$$\underline{I}_1 = \frac{-j\frac{\sqrt{3}}{3}\underline{I}_S \underline{Z}_f + \underline{E}_b}{\underline{Z}_1 + \underline{Z}_2} \quad \text{and} \quad \underline{I}_2 = \frac{j\frac{\sqrt{3}}{3}\underline{I}_S \underline{Z}_f - \underline{E}_b}{\underline{Z}_1 + \underline{Z}_2}$$

$$\underline{I}_S = (a^2 - a)\underline{I}_1 = -\sqrt{3}\, j \underline{I}_1 \quad \text{and} \quad \underline{I}_T = (a - a^2)\underline{I}_1 = \sqrt{3}\, j \underline{I}_1$$

$$\underline{I}_S = -\left(\frac{\underline{I}_S \underline{Z}_f + j U_n}{\underline{Z}_1 + \underline{Z}_2}\right) = \frac{-j U_n}{\underline{Z}_1 + \underline{Z}_2 + \underline{Z}_f}$$

Assuming that $\underline{Z}_1 = \underline{Z}_2$ the 2-phase short circuit current can be described as followed:

$$|\underline{I}_{k2}| = \left|\frac{U_n}{2\underline{Z}_1 + \underline{Z}_f}\right| \qquad \text{(E-3)}$$

For the phase voltages the following applies:

$$\underline{U}_R = \underline{U}_1 + \underline{U}_2 = \underline{E}_b$$

$$\underline{U}_S = \underline{U}_T + \underline{I}_S \, \underline{Z}_f = \frac{a^2 + a}{2}\underline{E}_b + \underline{I}_S \, \underline{Z}_f = -\frac{\underline{E}_b}{2} + \underline{I}_S \, \underline{Z}_f$$

Appendix F : Short circuit calculations for typical substations

General short circuit equations (with Z_f=0):

$$X_{tr} = \frac{\varepsilon}{100}\frac{U_{sec}^{\ 2}}{S_n} \quad \text{(F-1)}$$

$$\underline{I}_{k1} = \frac{3\,\underline{E}_b}{\underline{Z}_1 + \underline{Z}_2 + \underline{Z}_0} \quad \text{(F-2)}$$

$$\underline{I}_{k2} = \frac{\sqrt{3}\,\underline{E}_b}{\underline{Z}_1 + \underline{Z}_2} \quad \text{(F-3)}$$

$$\underline{I}_{k3} = \frac{\underline{E}_b}{\underline{Z}_1} \quad \text{(F-4)}$$

$$S_k = I_k\, U_b\, \sqrt{3} \quad \text{(F-5)}$$

Table F-1 Short circuit values for test network at 500 metres.

Short circuit parameters	Value
I_{k1} [kA] using F-2	2,3
I_{k2} [kA] using F-3	2,2
I_{k3} [kA] using F-4	2,6
S_k [MVA] (3 phase) using F-5	1,84

Note: $\underline{Z}_0$=1.5 $\underline{Z}_1$ and $\underline{Z}_1$= $\underline{Z}_2$ for the PILC cable and $\underline{Z}_0$=$\underline{Z}_1$ and $\underline{Z}_1$= $\underline{Z}_2$ for the transformer [7].

Table F-2 Specifications isolating transformer.

Details Transformer	Value
Nominal Power (S_n) [kVA]	750
Primary Voltage (U_{pri}) [kV]	11
Secondary Voltage (U_{sec}) [V]	415
Primary Current (I_{pri}) [A]	N/A
Secondary Current (I_{sec}) [A]	N/A
Reactance (x) [%]	5
X_{tr} [mOhm] using F-1	11.5
Coil configuration	Delta/Star

Table F-3 Cable properties specified for 185mm^2 4-core PILC distribution cable.

Plastic cable properties 20°C	Value
Resistance (R_c) [mOhm/km]	164
Inductance[1] (ωL_c) [mOhm/km]	68
Capacitance phase to phase ($C_{c\_p\text{-}p}$) [nF/km]	N/A
Capacitance phase to earth ($C_{c\ p\text{-}earth}$) [nF/km]	N/A
Discharge current ($I_{c\_p\text{-}p}$) [A]	N/A
Discharge current ($I_{c\_p\text{-}earth}$) [A]	N/A

[1] Factory specification

Appendix G : Phase to earth fault at 500 metres

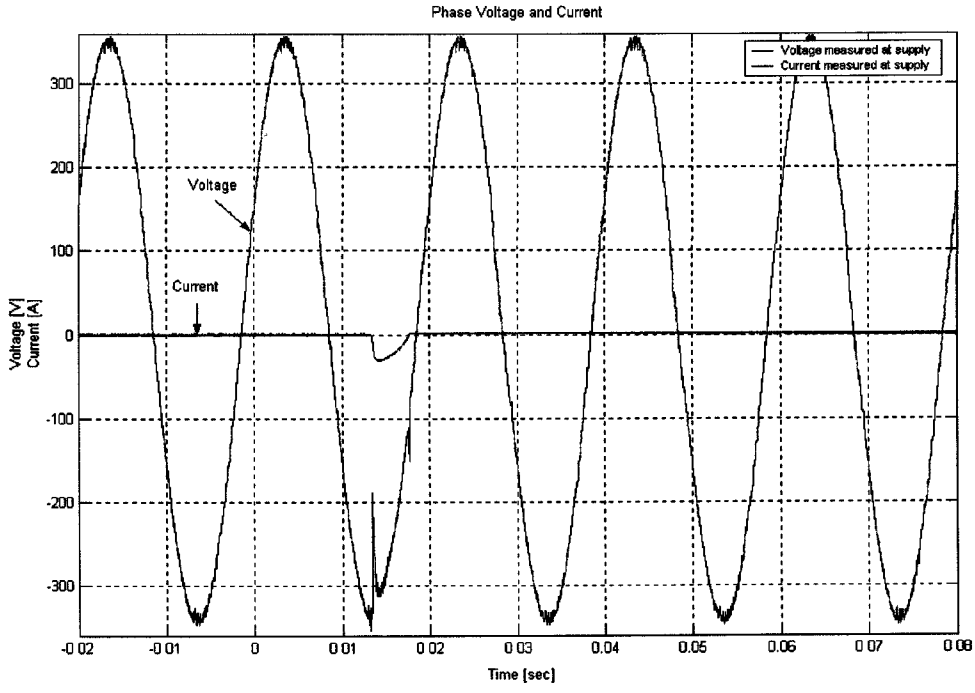

Figure G.1 Current and voltage measured at supply side before, during and after a low voltage using a PILC cable sample.

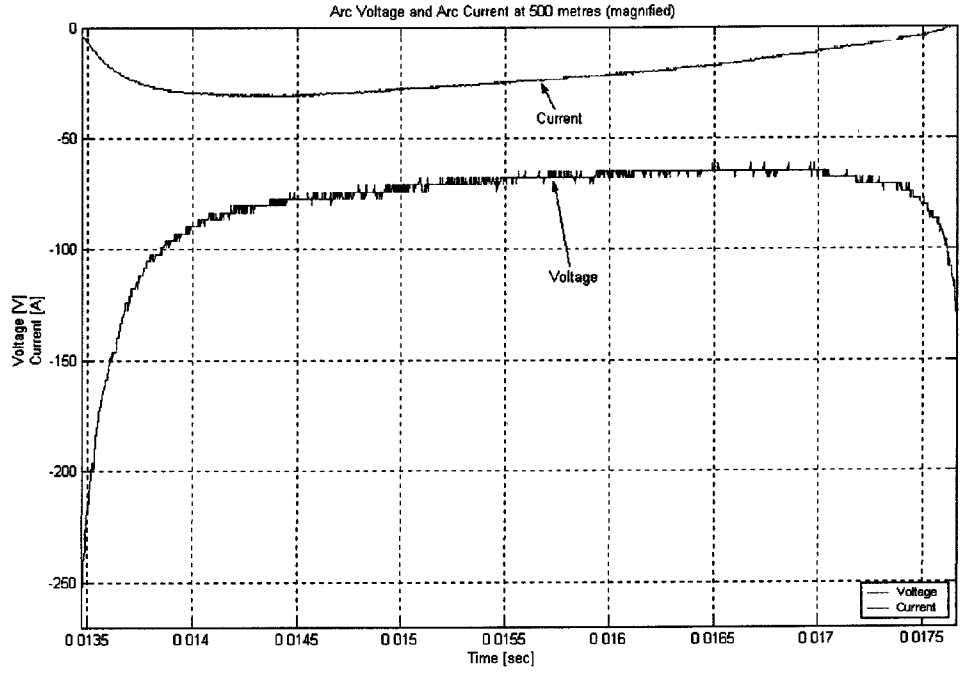

Figure G.2 Arc current and arc voltage magnified measured at fault location using a PILC cable sample.

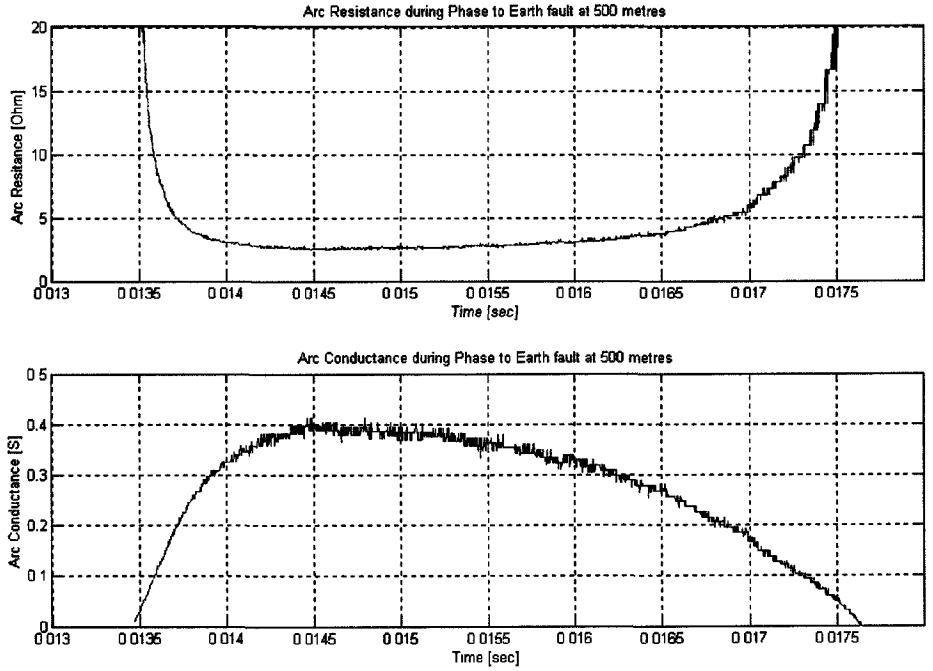

Figure G.3 Arc resistance and arc conductance using a PILC cable sample.

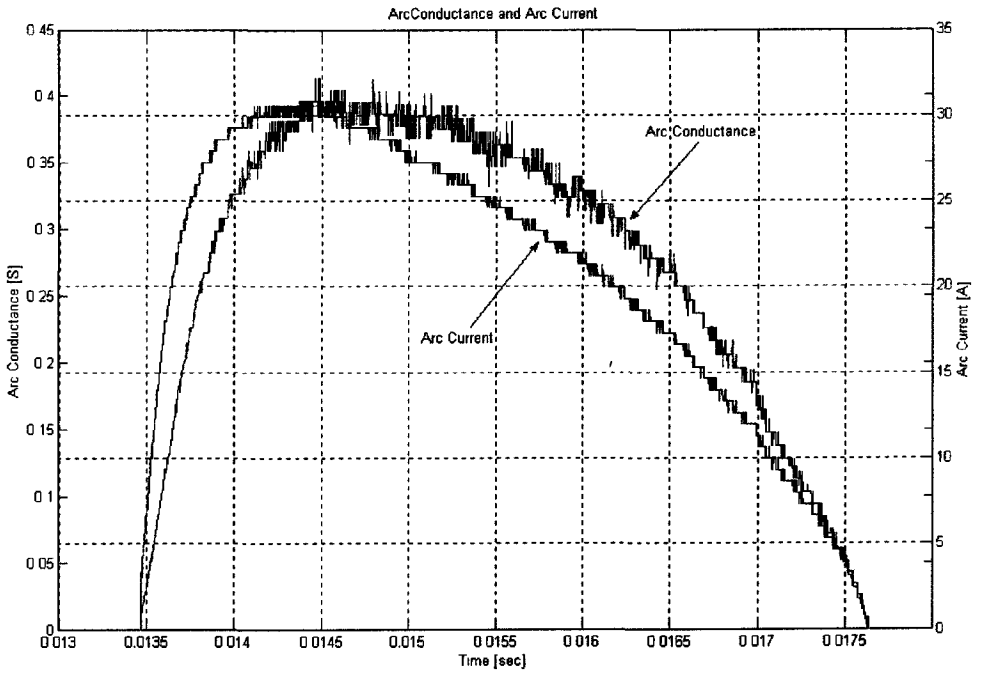

Figure G.4 Arc conductance and arc current using a PILC cable sample.

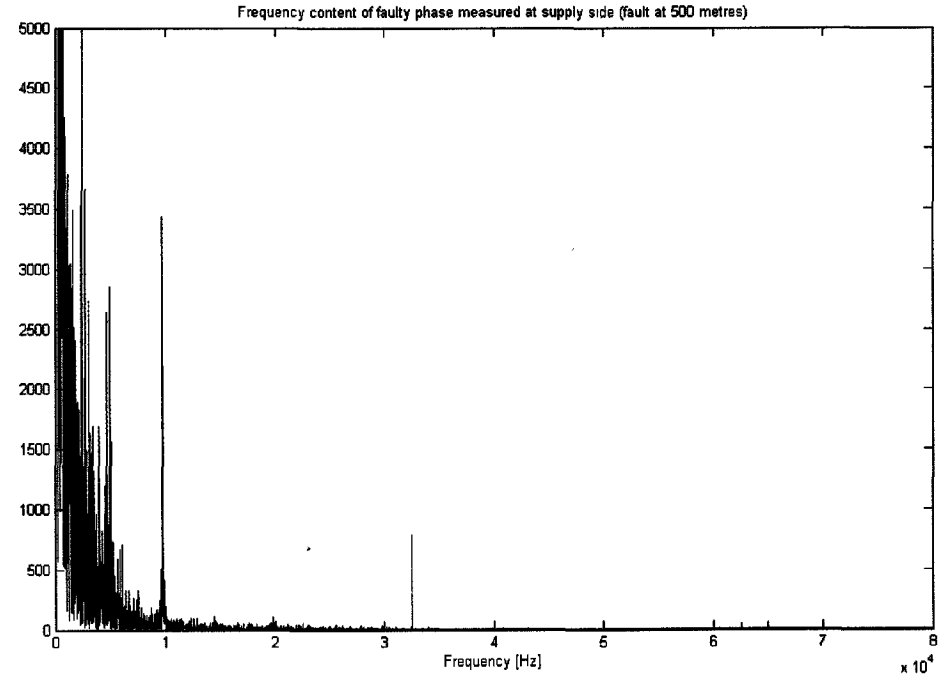

Figure G.5 Fast Fourier transformation of voltage from figure G. (magnified to show influence 9. KHz).

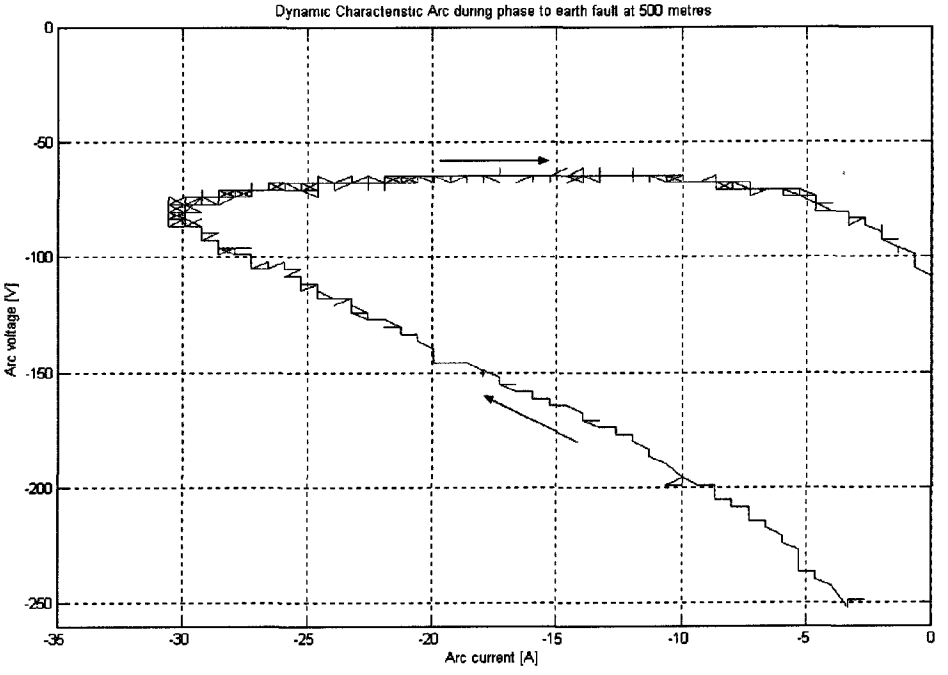

Figure G .6 Arc current versus arc voltage from figure G.2.

Appendix H : Phase to earth fault at 200 metres

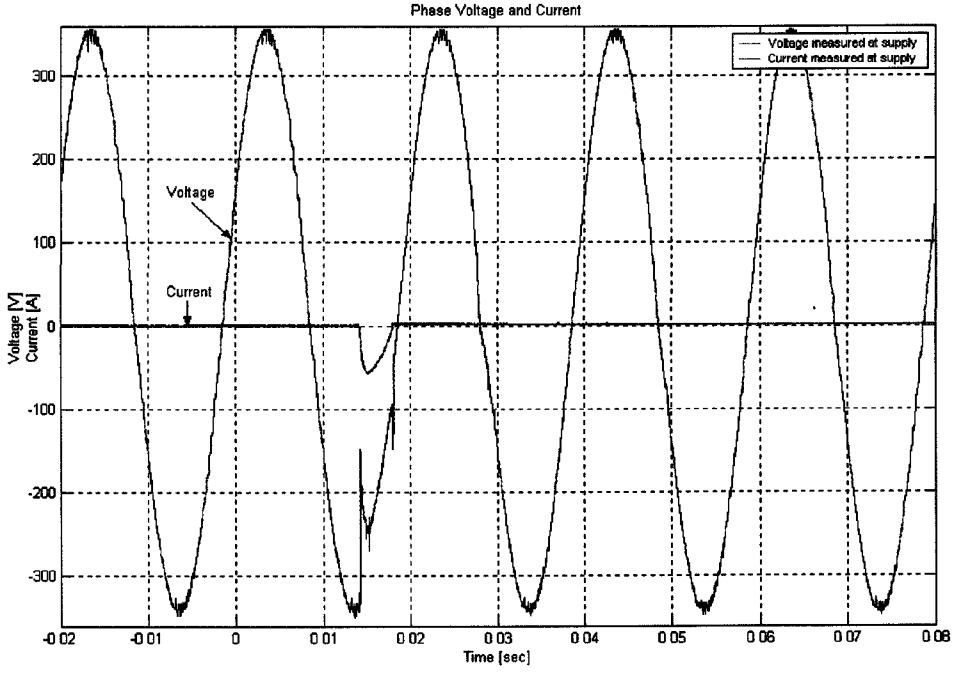

Figure H.1 Current and voltage measured at supply side before, during and after a low voltage using a PILC cable sample.

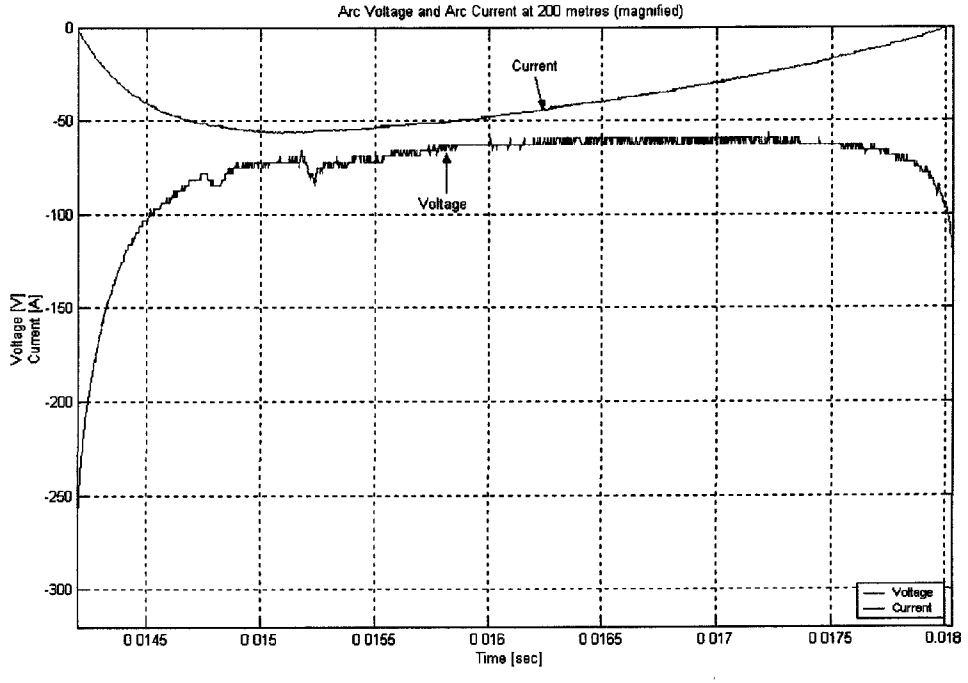

Figure H.2 Arc current and arc voltage magnified measured at fault location using a PILC cable sample.

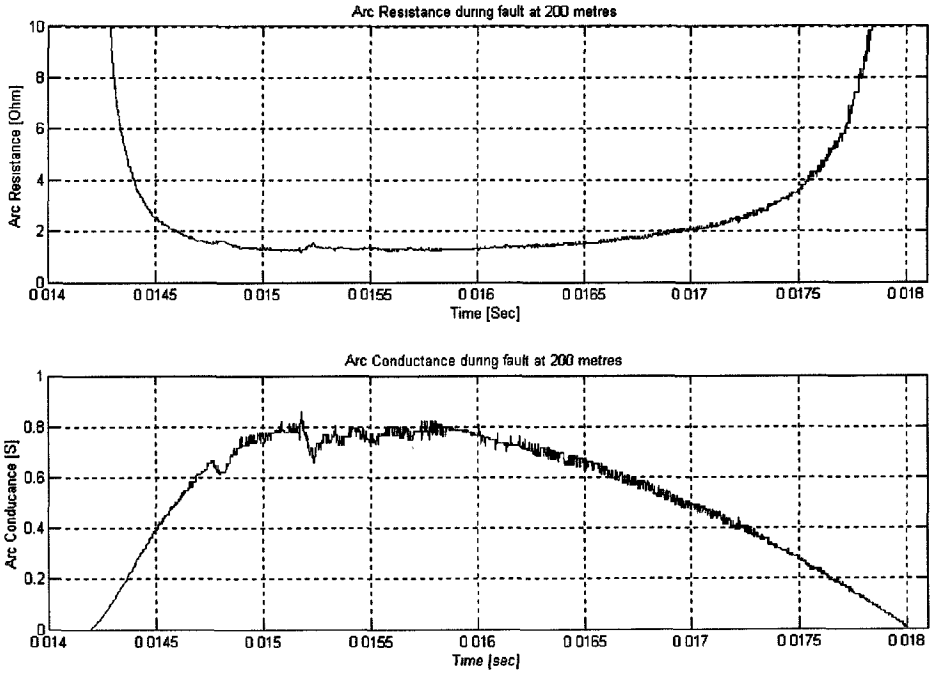

Figure H.3 Arc resistance and arc conductance using a PILC cable sample.

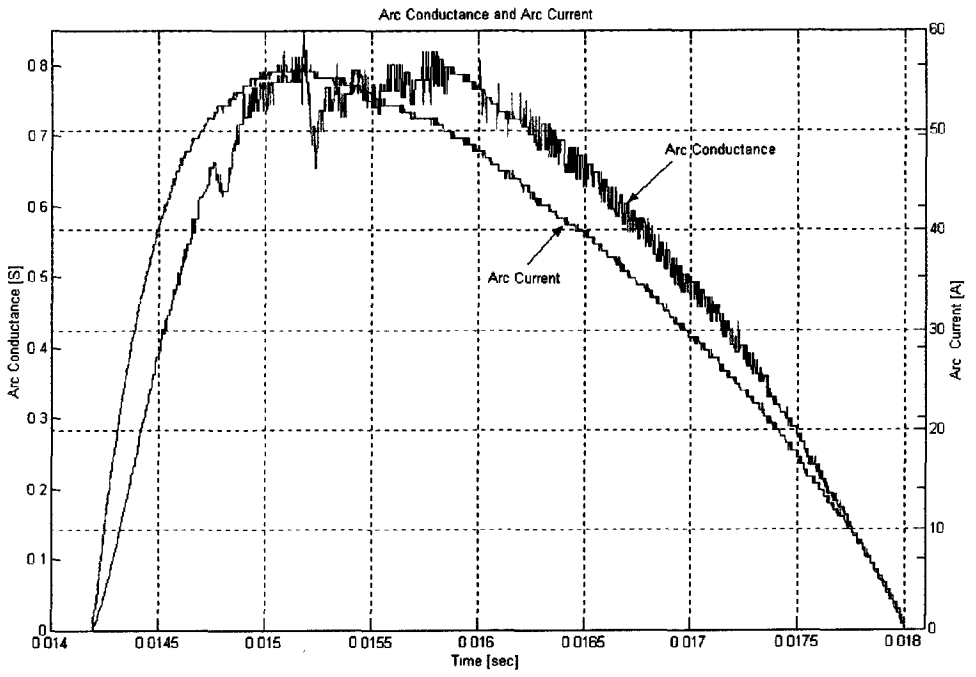

Figure H.4 Arc conductance and arc current using a PILC cable sample.

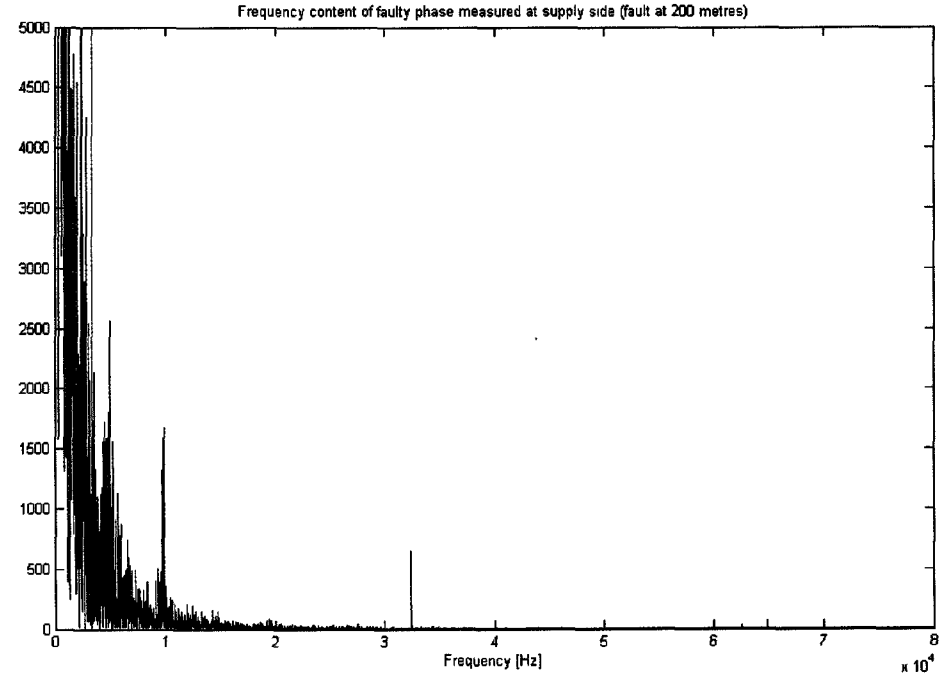

Figure H.5 Fast Fourier transformation of voltage from figure H.1(magnified to show influence 9. KHz).

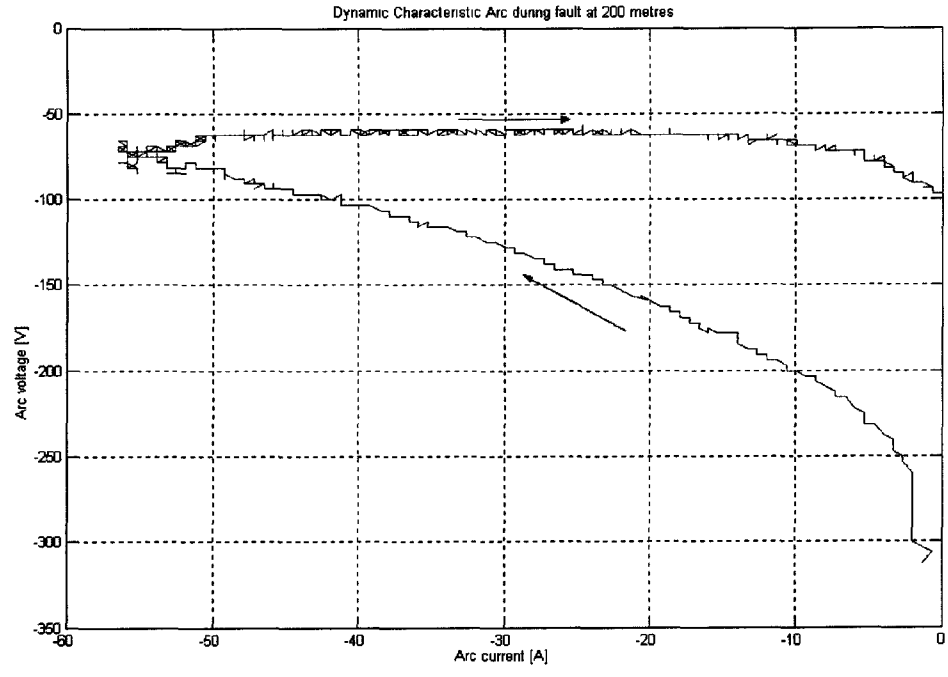

Figure H.6 Arc current versus arc voltage from figure H.2.

Appendix I : Phase to earth fault at 0 metres

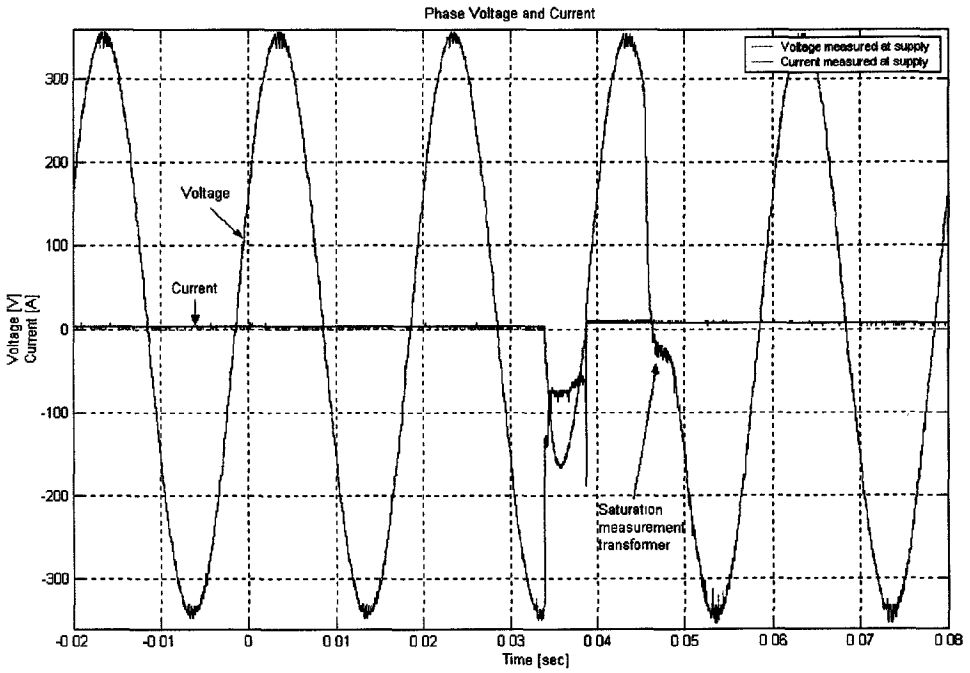

Figure I.1 Current and voltage measured at supply side before, during and after a low voltage using a PILC cable sample.

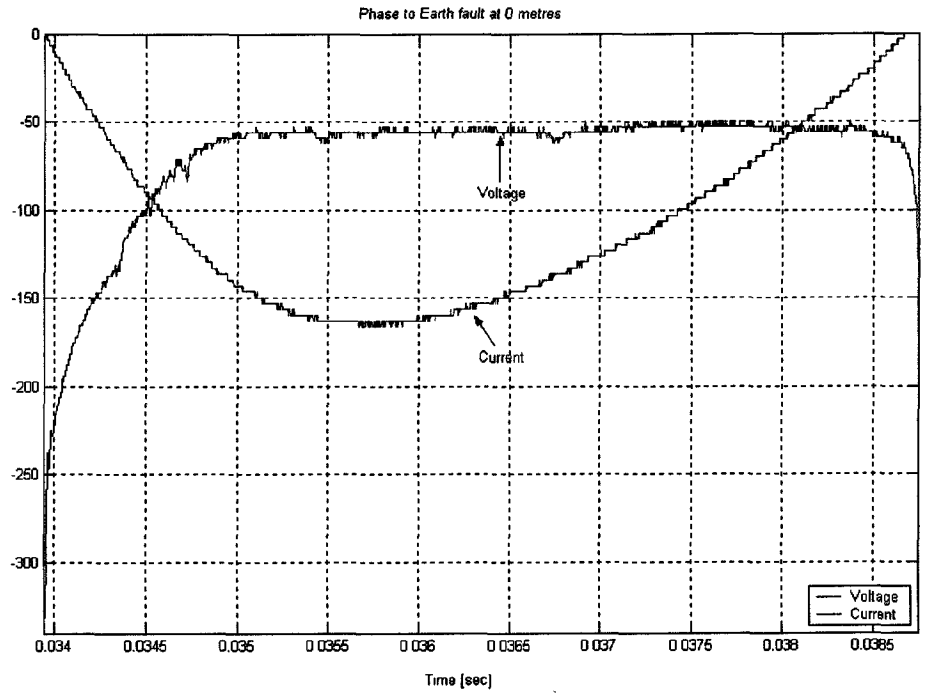

Figure I.2 Arc current and arc voltage magnified measured at fault location using a PILC cable sample.

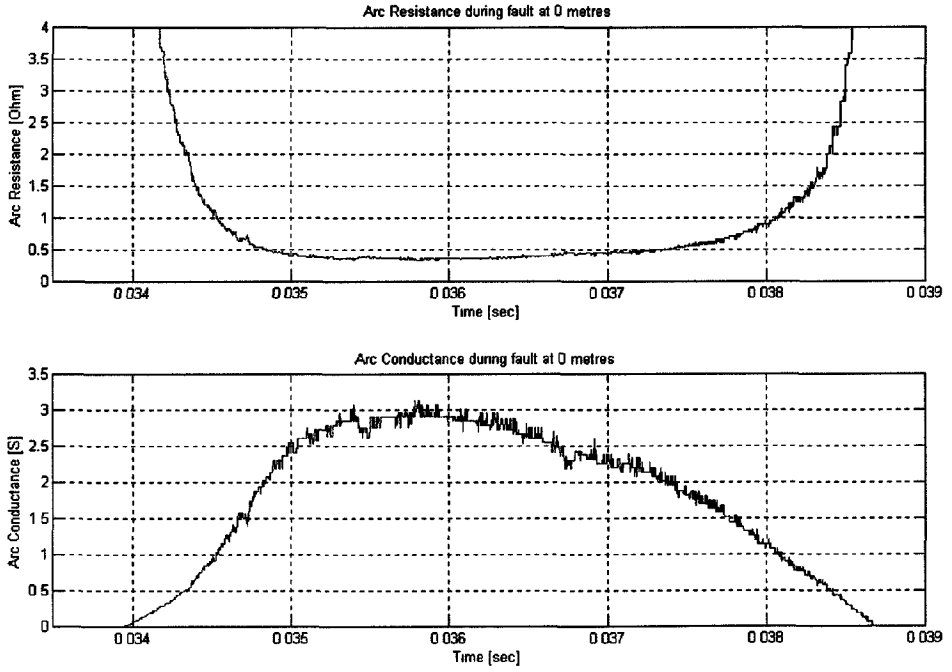

Figure I.3 Graph of arc resistance and arc conductance using a PILC cable sample.

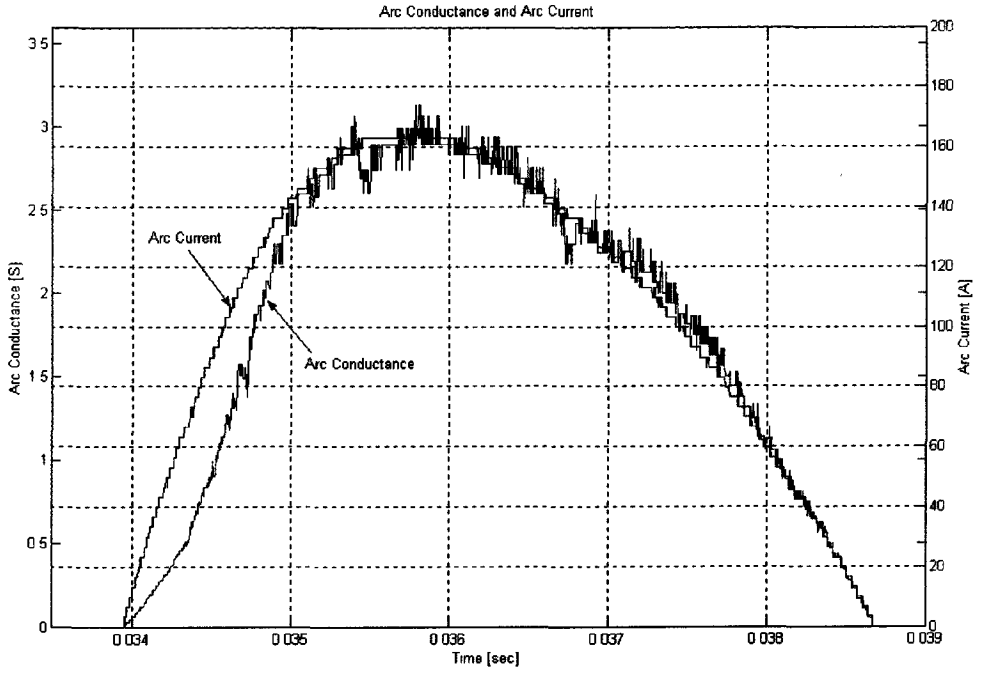

Figure I.4 Arc conductance and arc current using a PILC cable sample.

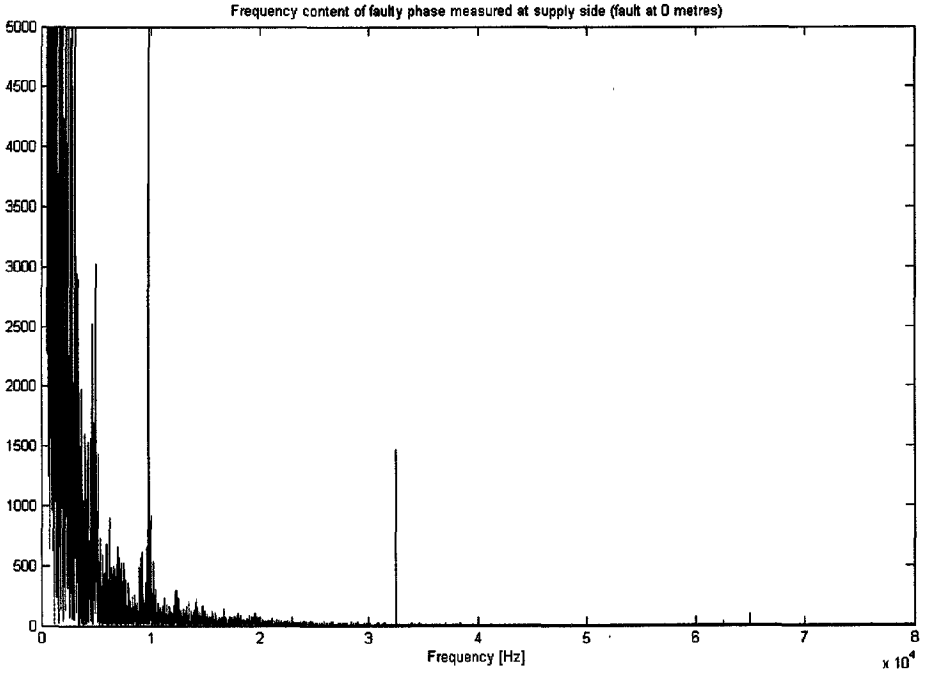

Figure I.5 Fast Fourier transformation of voltage from figure I.1(magnified to show influence 9. KHz).

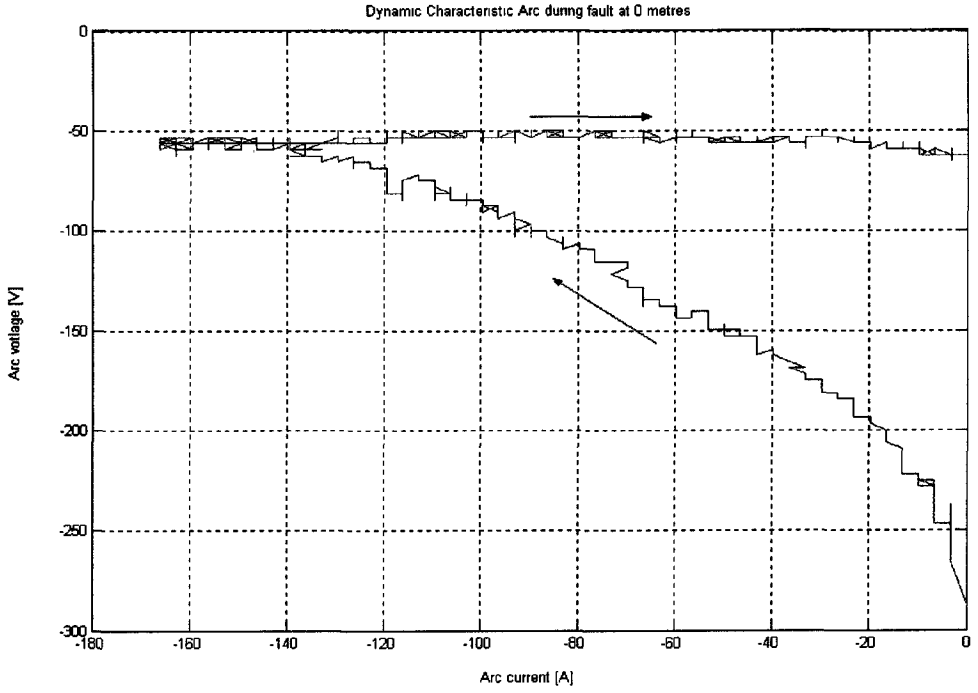

Figure I.6 Arc current versus arc voltage from figure I.2.

Appendix J : Phase to Phase fault at 500 metres

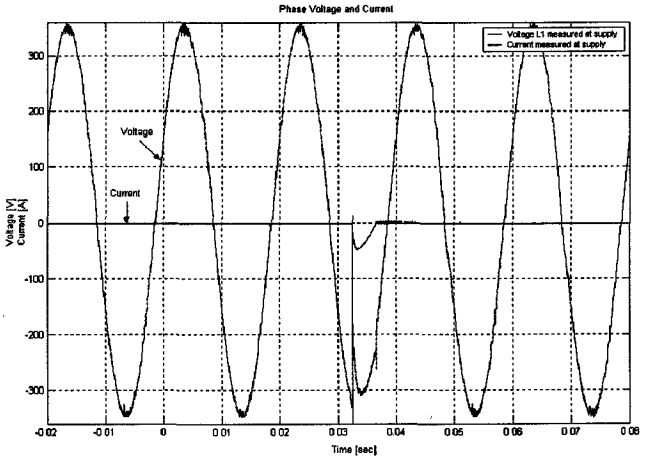

Figure J.1a Current and voltage measured at supply side before, during and after a low voltage using a PILC cable sample.

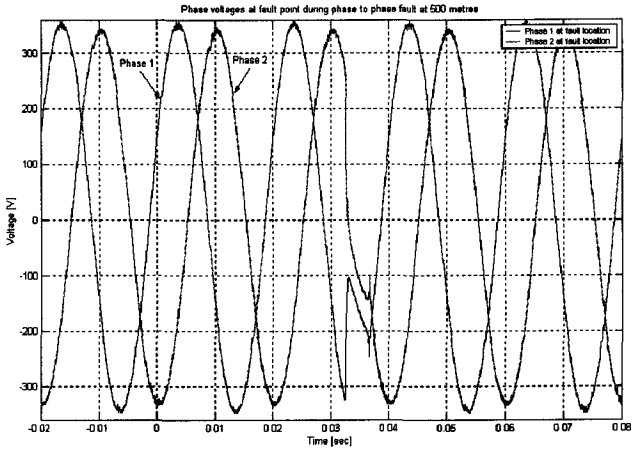

Figure J.1b Current and voltage measured at fault location.

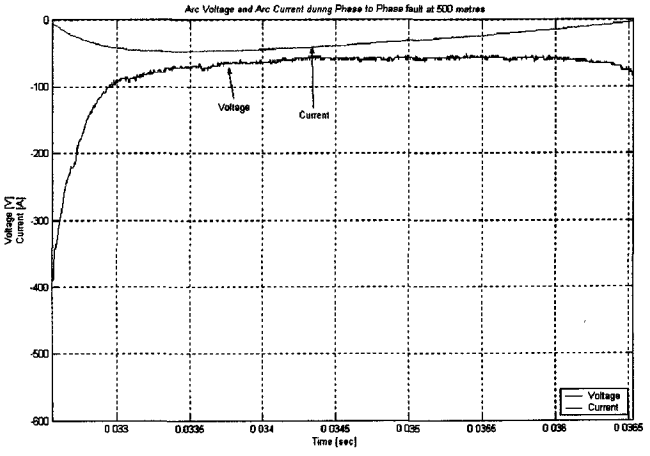

Figure J.2 Graph of arc current and arc voltage magnified for a PILC cable.

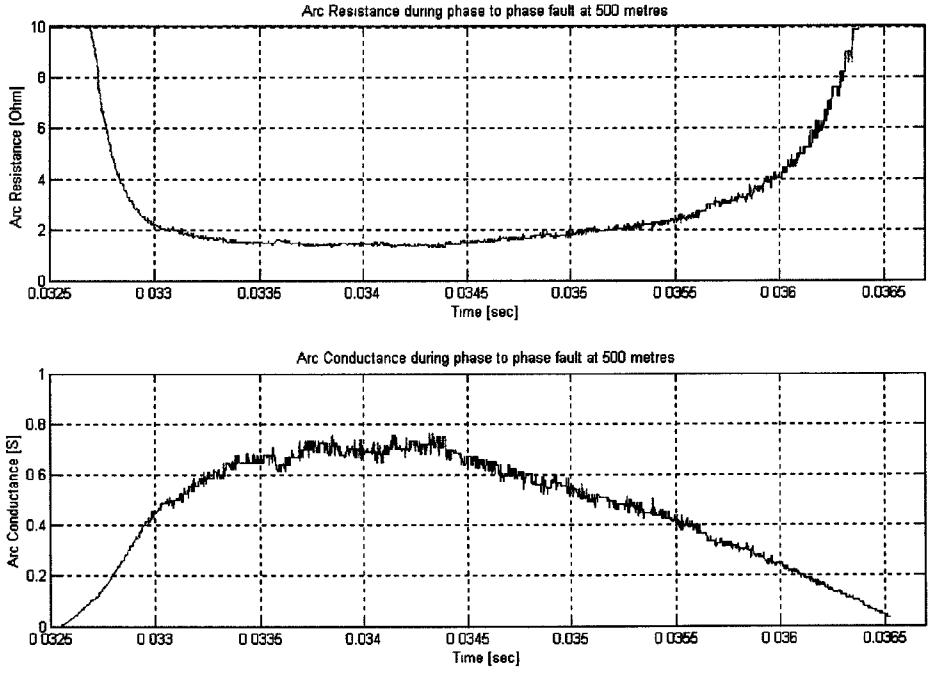

Figure J.3 Arc resistance and arc conductance using a PILC cable sample.

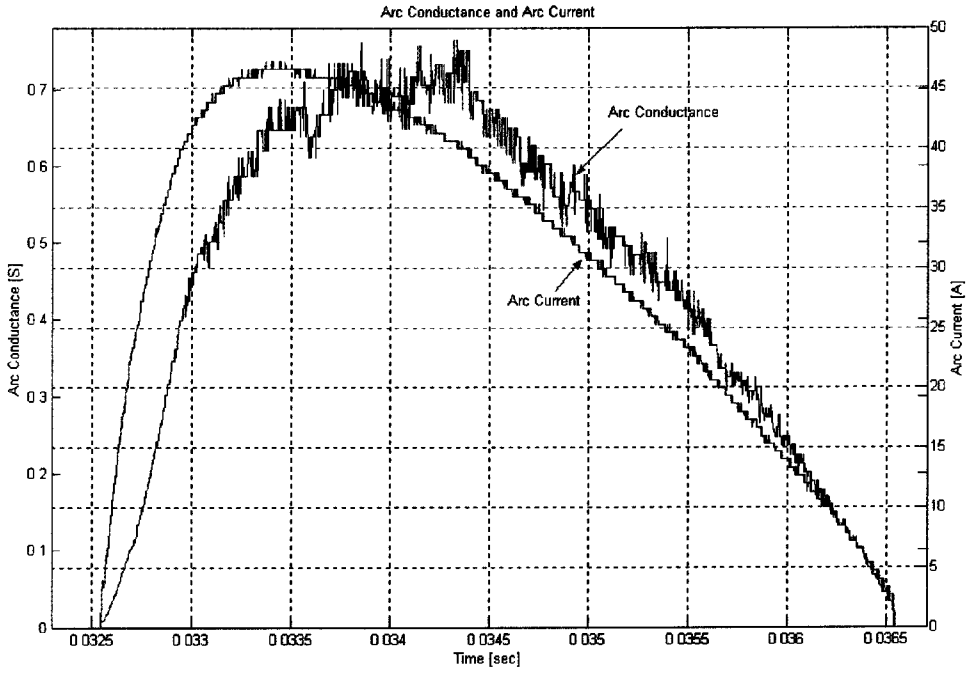

Figure J.4 Arc conductance and arc current using a PILC cable sample.

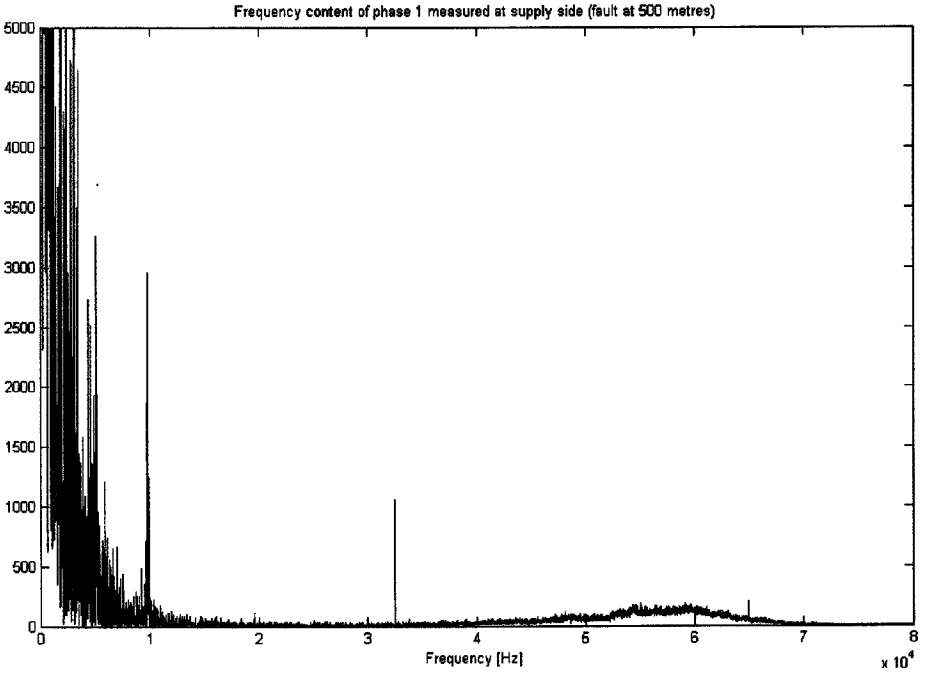

Figure J.5 Fast Fourier transformation of voltage from figure J.1 (magnified to show influence 9. KHz).

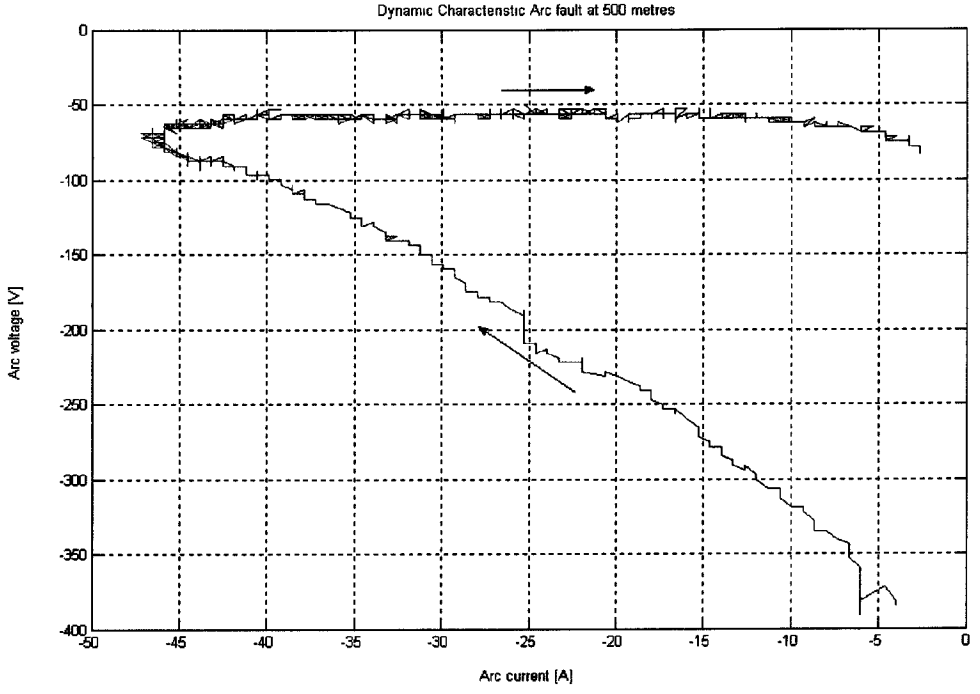

Figure J.6 Arc current versus arc voltage from figure J.2.

Appendix K : Flowchart fault development

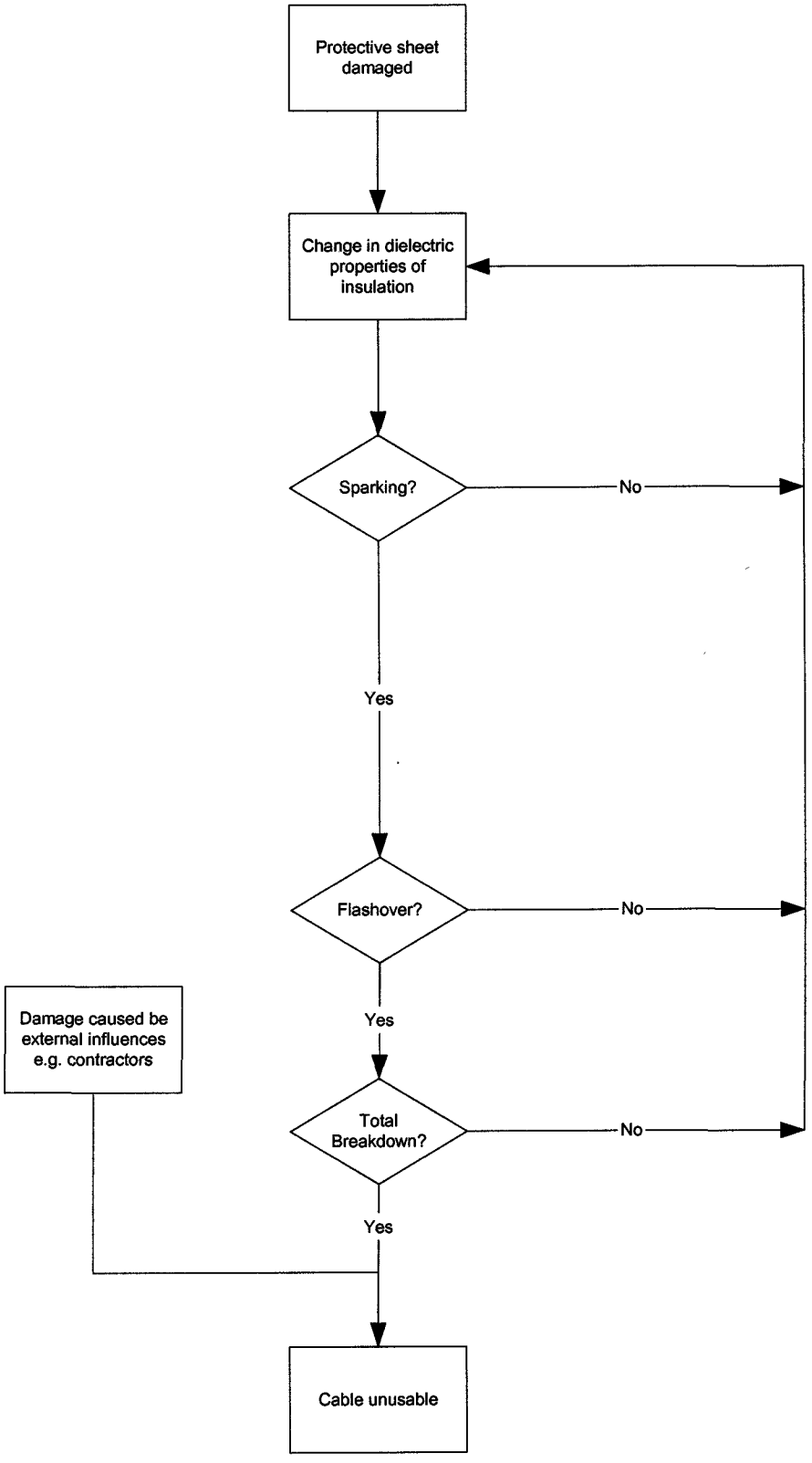

Appendix L : Fuse Characteristics

Bussmann

Industrial HRC Fuse — NSD

13.8 x 58.7mm, BS88: Part 6, IEC 269-1
Offset Blade Tags

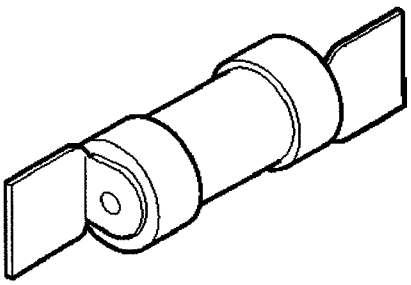

CATALOG SYMBOL: NSD
INDUSTRIAL HRC FUSE
OFFSET BLADE TAGS
PACKAGE QUANTITY: 20
80kA INTERRUPTING RATING
MOUNTS IN CAMLOC OR SAFELOC SERIES HOLDERS

Dimensional Data:

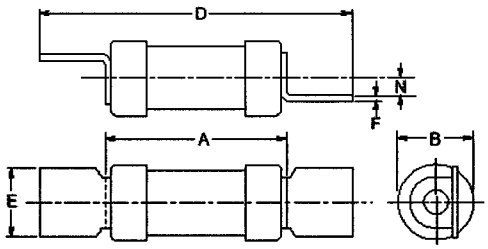

Time-Current Characteristic Curve (Full Size Curves Available)

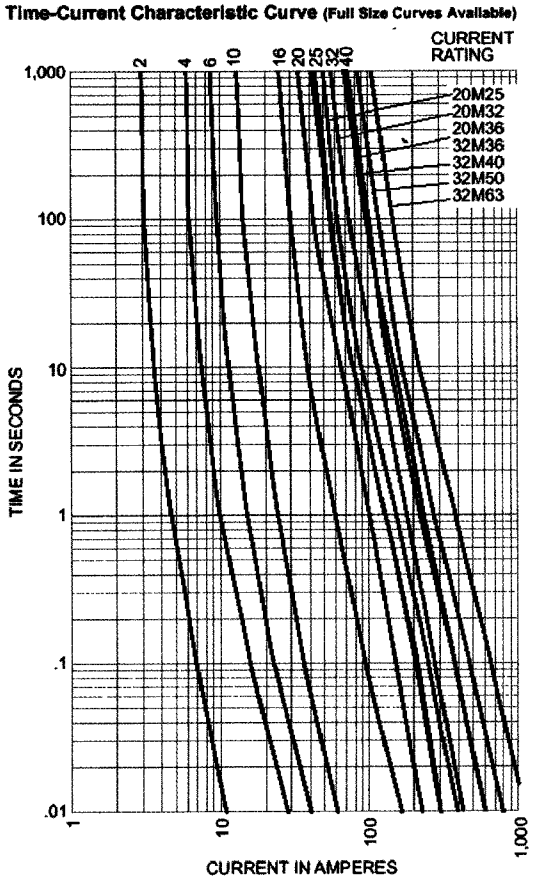

Electrical Characteristics

Catalog Number	Ampere Rating	I²T (Amp² Seconds) Pre-Arcing	Total At 415V	Total At 550V	Nom Watts Loss	Rated Voltage	Dimensions (Inches/mm) A	B	D	E	F	N
NSD2	2	1.3	4.6	5	0.9	550AC	34.6	54 13 8	58 5	12 7	.03 .8	14 3 5
NSD4	4	8	27	30	1.4							
NSD6	6	29	100	115	1 8							
NSD10	10	120	400	490	2.1							
NSD16	16	120	470	730	1.8							
NSD20	20	260	1070	1700	1.8							
NSD25	25	560	2300	3550	2							
NSD32	32	710	3000	5000	2 9							
NSD20M25	20M25	570	2350	—	1.2	415AC	34.6	69 17 5				
NSD20M32	20M32	770	3000	—	0.95							
NSD20M36	20M36	1150	5000	—	0.88							
NSD32M36	32M36	1150	5000	—	2.4							
NSD32M40	32M40	1500	6000	—	1.9							
NSD32M50	32M50	2700	8700	—	1 4							
NSD32M63	32M63	5000	13,550	—	1.0							

COOPER Bussmann
12-28-98
SB98107 Rev. A

Form No NSD
Page 1 of 1
BIF Doc #4100

Appendix M : General Sparking

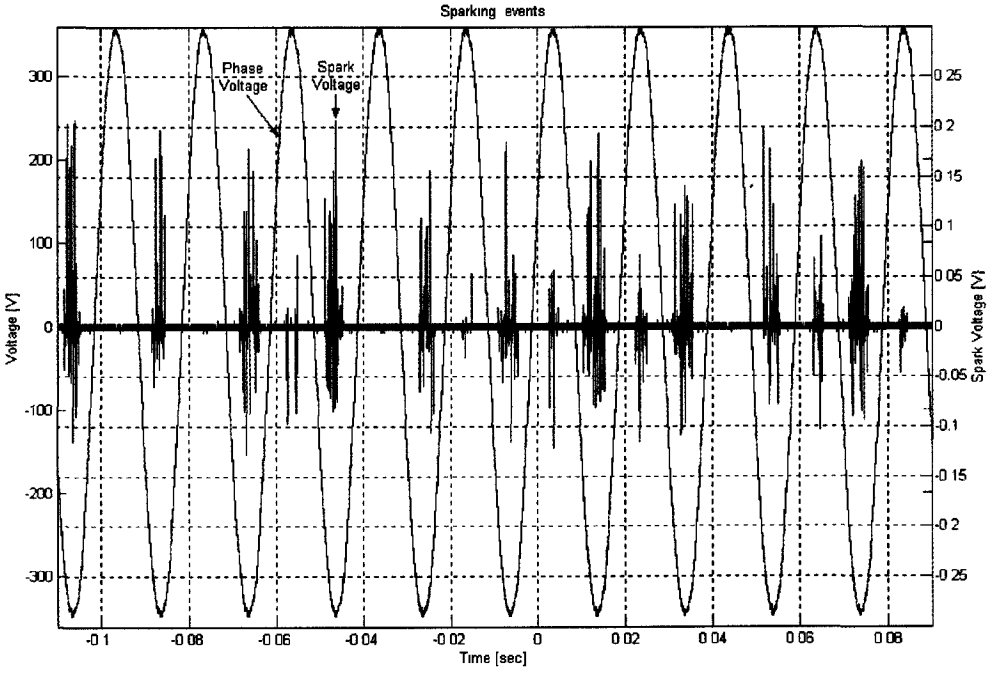

Figure M.1 Discharges caused by sparking at a 500 kHz sample frequency.

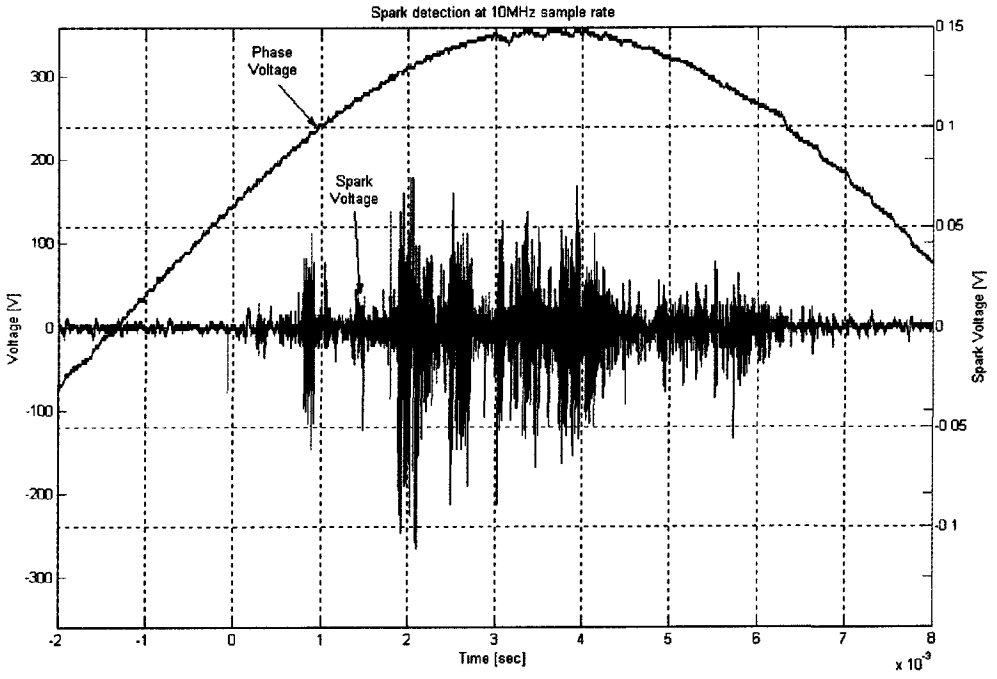

Figure M.2 Discharges caused by sparking at a 10 MHz sample frequency in a positive cycle.

Appendix N : Sparking before and after an arc

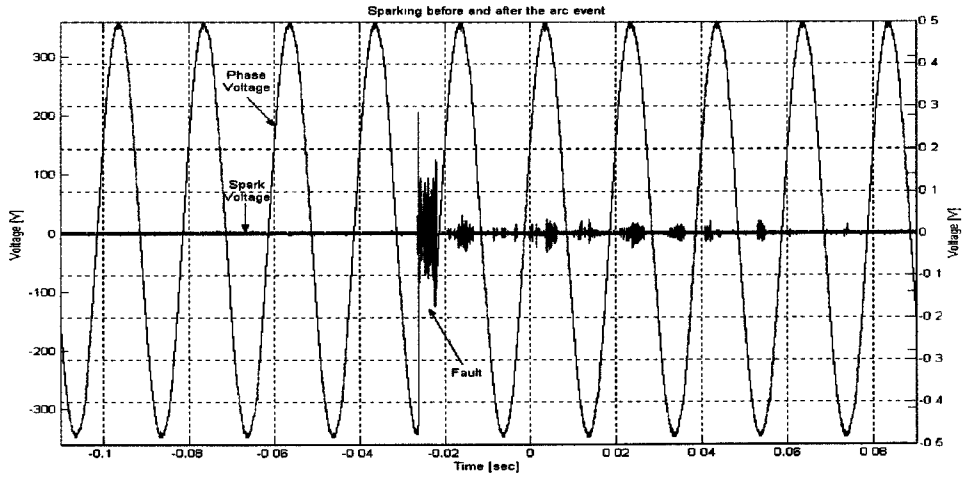

Figure N.1 Discharges caused by sparking before and after an arc event.

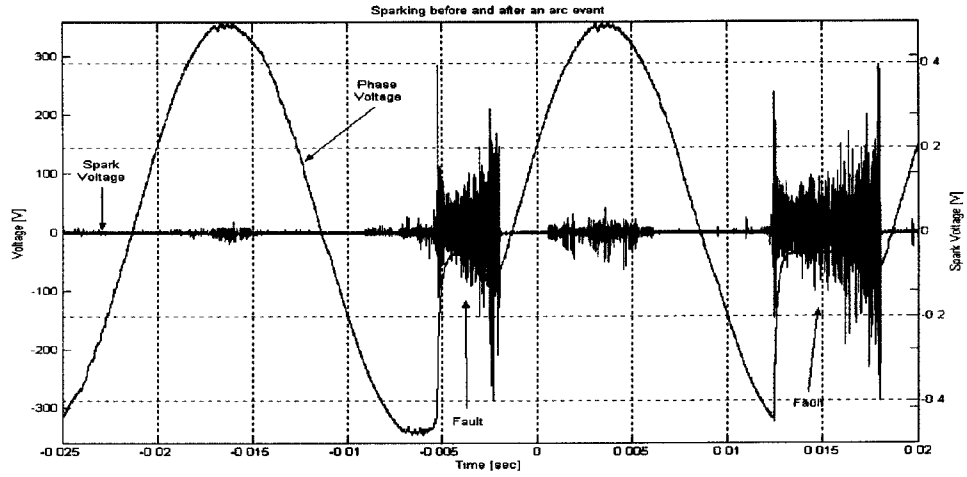

Figure N.2 Discharges caused by sparking before and after a multiple arc event.

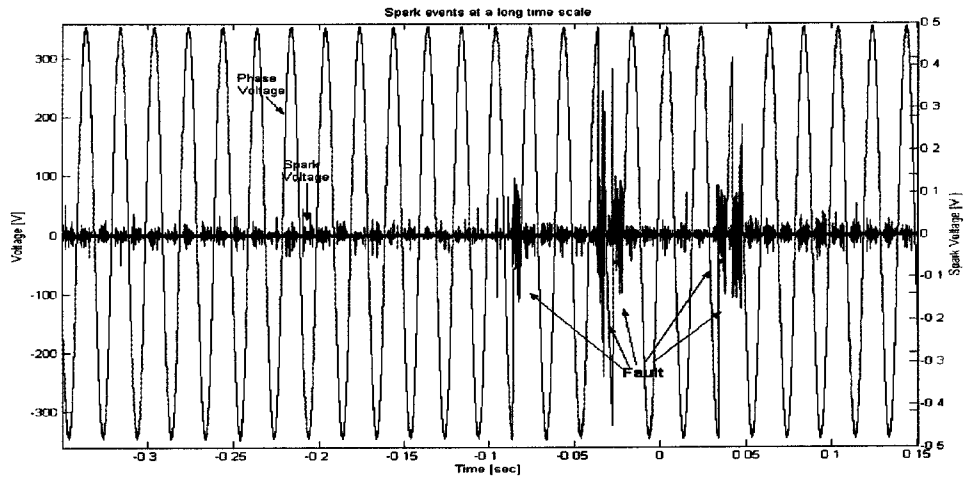

Figure N.2 Discharges caused by sparking before and after a multiple arc event on a long time scale.

Appendix O : MATLAB source code

Execute.m

```
%Note Datanumber may only vary between 0 and 9
name = input('Enter Datanumber: ','s');
sensitivity=0.047;
convert=21.555;
%Loading datafiles
file1=['sc1.00' name '.txt'];
file2=['sc2.00' name '.txt'];
file3=['sc3.00' name '.txt'];
file4=['sc4.00' name '.txt'];
load(file1)
load(file2)
load(file3)
load(file4)
%Name and scale variables
t=sc1(:,1);
u1=sc1(:,2);
u2=sc2(:,2);
u2=u2.*convert;
u3=sc3(:,2);
u3=u3.*convert;
i=sc4(:,2)/sensitivity;
%Calculate resistance
r1=abs(u1./i);
r2=abs(u2./i);
r3=abs(u3./i);
%Calculate sample frequency
n=length(u1);
if t(1)<0       %check for delay time
  sample_t=(-t(1)+t(n))/n;
else
  sample_t=(t(1)+t(n))/n;
end
sample_f=1/sample_t;
f=sample_f*(0:n/2)/n;
%Fast fourrier spectrum
y1=fft(u1);
p1=y1.*conj(y1)/n;
y2=fft(u2);
p2=y2.*conj(y2)/n;
y3=fft(u3);
p3=y3.*conj(y3)/n;
```

Arc.m

```
%~~~~ Determines Arc voltage and Arc current from data ~~~~%
close all;
sysvol=u2;
arcvol=u1;
test=u2;
arccur=i;
deviation_high=20;          %sets the first trigger for start of fault, which should be less sensitive then
deviation_low
deviation_low=4;            %sets the trigger for end of fault
upperbound=20;              %sets positive voltage limit for fault
lowerbound=-20;             %sets negative voltage limit for fault
leftbound=10;               %sets the minimum number of points for an arc to exist
rightbound=5000;            %sets the maximum number of points for an arc to exist
cur_bound=2;                %sets the limit under which the current will be set to zero, to filter out a/d
converter noise
adjust_piek1=0;             %trims the arc voltage on the start side to remove any spikes
adjust_piek2=7;             %trims the arc voltage on the end side to remove any spikes
number_points=3;            %specifies how many point are taken to average the signal to the fault
count=0;
count_h=0;
count_l=0;
for j=1:n
 sysvol(j)=0;
 test(j)=0;
 arccur(j)=0;
 arcvol(j)=0;
end
count=0;
%check voltage for arc disturbance
deviation=deviation_high;
for j=(number_points+1):n
%average
        average=0;
        for a=1:number_points
            average=average+abs(u2(j-a));
        end
        average=average/a;
%end average
%---Start fault finding---%
    if u2(j)<0
         if count_l>=1
                deviation=deviation_high;
                count_l=0;
             end
     count_h=1;
     fault_voltage=abs(u2(j))+deviation;
     if (fault_voltage<average)&(u2(j)<lowerbound)
         if u2(j)<0
          count=count+1;
          fault(count)=j;
          deviation=deviation_low;
          test(j)=u2(j);
```

```
        else
        %deviation=deviation_high;
        end
     end
    else
    end
    if u2(j)>0
     if count_h>=1
                deviation=deviation_high;
                count_h=0;
              end
     count_l=1;
     fault_voltage=abs(u2(j))+deviation;
     if (fault_voltage<average)&(u2(j)>upperbound)
         if u2(j)>0
          count=count+1;
          fault(count)=j;
          deviation=deviation_low;
          test(j)=u2(j);
         else
         %deviation=deviation_high;
         end
     else
     end
    end
end
g=1;
check=1;
while g<count
 if u2(fault(g))<0                                                                    %negative voltage arc
     fault_start=fault(g+adjust_piek1);                                               %set start point arc
     while (u2(fault(g+1))<0)&(g<count-1)&(check==1)&(fault(g+1)-fault_start<rightbound)  %check for end
           for j=fault_start:fault(g+1)
            if u2(j)<0
             check=1;
             else
             check=0;
            end
           end
            g=g+1;
     end
     fault_end=fault(g-1-adjust_piek2);                                               %set end point arc
    if  (fault_end-fault_start>leftbound)%&(fault_end-fault_start<rightbound)%check  if  voltage  disturbance  is  long
enough to be an arc
       for h=fault_start:fault_end
          sysvol(h)=u2(h);
          arcvol(h)=u1(h);                                                            %start filling arc array
          arccur(h)=i(h);
     end

  end              '
     g=g+1;
 else                                                                                 %positive voltage arc
     fault_start=fault(g+adjust_piek1);                                               %set start point arc
     while (u2(fault(g+1))>0)&(g<count-1)&(check==1)&(fault(g+1)-fault_start<rightbound)  %check for end
         for j=fault_start:fault(g+1)
            if u2(j)>0
             check=1;
             else
             check=0;
            end
           end
          g=g+1;
          %temp(g)=u2(fault(g+1));
     end
     fault_end=fault(g-1-adjust_piek2);                                               %set end point arc
     if  (fault_end-fault_start>leftbound)%&(fault_end-fault_start<rightbound)%check  if  voltage  disturbance  is  long
enough to be an arc
       for h=fault_start:fault_end
           sysvol(h)=u2(h);                                                           %start filling arc array
           arcvol(h)=u1(h);
           arccur(h)=i(h);
      end
     end
     g=g+1;
 end
%filters current to get rid of bit error
%for j=1:n
% if (arccur(j)>cur_bound)|(arccur(j)<(-cur_bound))
%     arccur(j)=i(j);
%else
%     arccur(j)=0;
%end
%end
cirvol=sysvol-arcvol;
%calculates arc resistance
arcr=arcvol./arccur;
arcy=arccur./arcvol;
end
```

ImpedanceURL.m

```
%~~~~ Calaculates the systems impedance ~~~~%

% Includes arc voltage in matrix %

delay_scoop=abs(t(1));                                  % Detect delay time setting on LeCroy 9344
wo=2*pi*50;                                             % Angular frequancy
ts=t(2)-t(1);                                           % Determine sample time
fs=1/ts;                                                % Calculate sample frequency
sample=50;                                              % Set factor to bring sample frequency down
max_r=20;                                               % Set maximum value to resitance to ignore fault data
max_l=2;                                                % Set maximum value to inductance to ignore fault data
%--- Load Data into matrix ---%
load(:,1)=sc2(:,2);
load(:,2)=sc3(:,2);
load(:,3)=sc4(:,2);
%--- Bring Sample frequency down ---%
data=load(1:sample:end,:);
fs_matlab=fs/sample;
ts_matlab=ts*sample;
%--- Start scaling data to real values ---%
n=length(data);                                         % Determine number of samples
us_L1=data(:,1).*21.55;                                 % Source voltage Phase 1 scaled
us_L2=data(:,2).*21.55;                                 % Source voltage Phase 2 scaled only of use for Ph-Ph fault
us_pp=us_L1-us_L2;                                      % Source voltage Phase Phase difference
i_arc=data(:,3)./0.047;                                 % (arc)Current scaled
%--- Filter current for bit error when current zero ---%
cur_bound=2;                                            % Set factor for current to be filtered
for j=1:n
    if (i_arc(j)>cur_bound)|(i_arc(j)<(-cur_bound))
       i_arc(j)=i_arc(j);
    else
      i_arc(j)=0;
    end
end
%--- Start Matrix calculations ---%
idiff=diff(i_arc)/(ts_matlab*wo);                       % Differentiate current
nd=length(idiff);                                       % Determine number of samples
for k=3:nd
    km=k-2;                                             % Index for matrix
    us1=us_L1(k);                                       % In case of Ph-Ph fault use us_pp
    us2=us_L1(k-1);
    us3=us_L1(k-2);
    i1=i_arc(k);
    i2=i_arc(k-1);
    i3=i_arc(k-2);
    id1=idiff(k);
    id2=idiff(k-1);
    id3=idiff(k-2);
    um=[us1;us2;us3];
    im=[i1 id1 1;i2 id2 1; i3 id3 1];
    result=im\um;                                       %Using Gaussian elimination instead of normal inverse
command
    imp(km,:)=result';
end
ta=(t(3*sample:sample:end));                            % Calculate time index
%--- Determine Rs and Ls ---%
rs=imp(:,1);
ls=imp(:,2);
u_arc=imp(:,3);
%--- Filter out singular errors caused in matlab to certain extend ---%
jj=length(imp);                                         % Determine length of matrix
for j=2:jj-10
%--- Filter Rs
    if ((rs(j)>max_r)  | (rs(j)<=0.01))                 %give resistance maximum value to ignore faulty data
       if ((rs(j-1)<20) & (rs(j+10)<20))
           rs(j)=rs(j-1);
       else
           rs(j)=0;
    end
       end
%--- Filter Ls
    if (ls(j)>max_l | ls(j)<0)                           %give inductance maximum value to ignore faulty data
        if ((ls(j-1)<2) & (ls(j+10)<2))
        ls(j)=ls(j-1);
    else
            ls(j)=0;
        end
    end
%--- Filter Uarc
    if (u_arc(j)<-360 | u_arc(j)>0) & (rs(j)~=0)
        if (u_arc(j-1)>-360)
        u_arc(j)=u_arc(j-1);
    else
            u_arc(j)=0;
        end
    end
end
%--- Plot calculated data ---%
clf
subplot(411),plot(t,u1)
axis([-0.02 0.08 -360 360])
grid
ylabel('Voltage [V]')
title('Results of impedance calculations using impedance2.m')
subplot(412),plot(ta,rs)
axis([-0.02 0.08 0 20])
ylabel('Cable resisance [Ohm]')
grid
subplot(413),plot(ta,ls)
axis([-0.02 0.08 0 0.5])
ylabel('Cable inductance [H]')
```

```
grid
subplot(414),plot(ta,u_arc)
axis([-0.02 0.08 -560 0])
ylabel('Arc voltage [V]')
xlabel('Time [sec]')
grid
```

ChiURL.m

```
%~~~~ Calaculates the systems impedance ~~~~%
delay_scoop=abs(t(1));                                  % Detect delay time setting on LeCroy 9344
wo=2*pi*50;                                             % Angular frequancy
ts=t(2)-t(1);                                           % Determine sample time
fs=1/ts;                                                % Calculate sample frequency
sample=50;                                              % Set factor to bring sample frequency down
%--- Load Data into matrix ---%
load(:,1)=sc2(:,2);
load(:,2)=sc3(:,2);
load(:,3)=sc4(:,2);
%--- Bring Sample frequency down ---%
data=load(1:sample:end,:);
fs_matlab=fs/sample;
ts_matlab=ts*sample;
%--- Start scaling data to real values ---%
n=length(data);                                         % Determine number of samples
us_L1=data(:,1).*21.55;                                 % Source voltage Phase 1 scaled
us_L2=data(:,2).*21.55;                                 % Source voltage Phase 2 scaled only of use for Ph-Ph fault
us_pp=us_L1-us_L2;                                      % Source voltage Phase Phase difference
i_arc=data(:,3)./0.047;                                 % (arc)Current scaled
ta=(t(3*sample:sample:end));                            % Calculated time index
%--- Filter current for bit error when current zero ---%
cur_bound=2;                                            % Set factor for current to be filtered
for j=1:n
    if (i_arc(j)>cur_bound)|(i_arc(j)<(-cur_bound))
       i_arc(j)=i_arc(j);
    else
      i_arc(j)=0;
    end
end
%--- Start Matrix calculations ---%
arc_start=350;                                          % Set start sample arc
arc_end=373;                                            % Set end sample arc
idiff=diff(i_arc)/(ts_matlab*wo);                       % Differentiate current
idiff(n)=0;                                             % Fill last sample lost in diff
nd=length(idiff);                                       % Determine number of samples
i2=i_arc.*i_arc;                                        % Current^2
i_id=i_arc.*idiff;                                      % Current times differentiated current
id2=idiff.*idiff;                                       % (Differentiated current)^2
us_i=us_L1.*i_arc;                                      % Supply voltage minus arc voltage times current
us_id=us_L1.*idiff;                                        % Supply voltage minus arc voltage times differentiated
current
sum_us=0; sum_i=0; sum_i2=0; sum_i_id=0; sum_id2=0;
sum_id=0; sum_n=0; sum_us_i=0; sum_us_id=0;
for k=arc_start:arc_end                                 % Index for matrix
    sum_n=sum_n+1;                                      % Calaculate sum of 1
    sum_us=sum_us+us_L1(k);                             % Calaculate sum of us_L1
    sum_i=sum_i+i_arc(k);                               % Calaculate sum of current
    sum_i2=sum_i2+i2(k);                                % Calaculate sum of current^2
    sum_i_id=sum_i_id+i_id(k);                          % Calaculate sum of differentiated current times current
    sum_id2=sum_id2+id2(k);                             % Calaculate sum of (differentiated current)^2
    sum_id=sum_id+idiff(k);                             % Calaculate sum of differentiated current
    sum_us_i=sum_us_i+us_i(k);                          % Calaculate sum of supply voltage time current
    sum_us_id=sum_us_id+us_id(k);                          % Calaculate sum of supply voltage time differentiated
current
end
um=[sum_us_i ;sum_us_id ;sum_us];                       % Setup matrix
im=[sum_i2 sum_i_id sum_i; sum_i_id sum_id2 sum_id; sum_i sum_id sum_n]; % Setup matrix
result=im\um;                                              % Using Gaussian elimination instead of normal inverse
command
r=result(1,:)                                           % Cable resistance
l=result(2,:)                                           % Cable inductance
arc_voltage=result(3,:)                                 % Arc voltage
chi=0;
n=0;
%--- Start Matrix calculations ---%
imin=inv(im);
chi=0;
for k=arc_start:arc_end
    chi=chi+((r*i_arc(k))+(l*idiff(k))+arc_voltage-us_L1(k))^2;
    n=n+1;
end
chi=chi/(n-3);
error=imin*chi;
error_r=sqrt(error(1,1))
error_l=sqrt(error(2,2))
error_u=sqrt(error(3,3))
```

ImpedanceRL.m

```
%~~~~ Calaculates the systems impedance ~~~~%
% Excludes arc voltage in matrix %
delay_scoop=abs(t(1));                                  % Detect delay time setting on LeCroy 9344
wo=2*pi*50;                                             % Angular frequancy
ts=t(2)-t(1);                                           % Determine sample time
fs=1/ts;                                                % Calculate sample frequency
sample=50;                                              % Set factor to bring sample frequency down
arc_vol=-60;                                            % Set arc voltage
max_r=20;                                               % Set maximum value to resitance to ignore fault data
max_l=2;                                                % Set maximum value to inductance to ignore fault data
%--- Load Data into matrix ---%
load(:,1)=sc2(:,2);
load(:,2)=sc3(:,2);
load(:,3)=sc4(:,2);
%--- Bring Sample frequency down ---%
```

```
data=load(1:sample:end,:);
fs_matlab=fs/sample;
ts_matlab=ts*sample;
%--- Start scaling data to real values ---%
n=length(data);                                          % Determine number of samples
us_L1=data(:,1).*21.55;                                  % Source voltage Phase 1 scaled
us_L2=data(:,2).*21.55;                                  % Source voltage Phase 2 scaled only of use for Ph-Ph fault
us_pp=us_L1-us_L2;                                       % Source voltage Phase Phase difference
i_arc=data(:,3)./0.047;                                  % (arc)Current scaled
%--- Filter current for bit error when current zero ---%
cur_bound=2;                                             % Set factor for current to be filtered
for j=1:n
    if (i_arc(j)>cur_bound)|(i_arc(j)<(-cur_bound))
       i_arc(j)=i_arc(j);
    else
      i_arc(j)=0;
    end
end
%--- Start Matrix calculations ---%
idiff=diff(i_arc)/(ts_matlab*wo);                        % Differentiate current
nd=length(idiff);                                        % Determine number of samples
for k=2:nd
    km=k-1;                                              % Index for matrix

    us1=us_L1(k);                                        % In case of Ph-Ph fault use us_pp
    us2=us_L1(k-1);

    i1=i_arc(k);
    i2=i_arc(k-1);

    id1=idiff(k);
    id2=idiff(k-1);

    um=[us1;us2];
    im=[i1 id1;i2 id2];

    result=im\(-arc_vol+um);                                 %Using Gaussian elimination instead of normal inverse
command
    imp(km,:)=result';
end
ta=(t(2*sample:sample:end));                             % Calculate time index
%--- Determine Rs and Ls ---%
rs=imp(:,1);
ls=imp(:,2);
%--- Filter out singular errors caused in matlab to certain extend ---%
jj=length(imp);                                          % Determine length of matrix
for j=2:jj-10
%--- Filter Rs
    if ((rs(j)>max_r)  | (rs(j)<=0.01))
       if ((rs(j-1)<20) & (rs(j+10)<20))
            rs(j)=rs(j-1);
        else
            rs(j)=0;
        end
    end

%--- Filter Ls
    if (ls(j)>max_l | ls(j)<0)
        if ((ls(j-1)<2) & (ls(j+10)<2))
        ls(j)=ls(j-1);
    else
            ls(j)=0;
        end
    end
  end

%--- Plot calculated data ---%
clf
subplot(311),plot(t,u1)
axis([-0.02 0.08 -360 360])
ylabel('Voltage [V]');
title('Results of impedance calculations using impedance.m');
grid
subplot(312),plot(ta,rs)
axis([-0.02 0.08 0 20])
ylabel('Cable resisance [Ohm]');
grid
subplot(313),plot(ta,ls)
axis([-0.02 0.08 0 0.5])
ylabel('Cable inductance [H]');
xlabel('Time [sec]');
grid
```

ChiRL.m

```
%~~~~ Calaculates the systems impedance ~~~~%
delay_scoop=abs(t(1));                                   % Detect delay time setting on LeCroy 9344
wo=2*pi*50;                                              % Angular frequancy
ts=t(2)-t(1);                                            % Determine sample time
fs=1/ts;                                                 % Calculate sample frequency
sample=50;                                               % Set factor to bring sample frequency down

%--- Load Data into matrix ---%
load(:,1)=sc2(:,2);
load(:,2)=sc3(:,2);
load(:,3)=sc4(:,2);

%--- Bring Sample frequency down ---%
data=load(1:sample:end,:);
fs_matlab=fs/sample;
ts_matlab=ts*sample;

%--- Start scaling data to real values ---%
```

```
n=length(data);                                          % Determine number of samples
us_L1=data(:,1).*21.55;                                  % Source voltage Phase 1 scaled
us_L2=data(:,2).*21.55;                                  % Source voltage Phase 2 scaled only of use for Ph-Ph fault
us_pp=us_L1-us_L2;                                       % Source voltage Phase Phase difference
i_arc=data(:,3)./0.047;                                  % (arc)Current scaled
ta=(t(3*sample:sample:end));                             % Calculated time index

%--- Filter current for bit error when current zero ---%
cur_bound=2;                                             % Set factor for current to be filtered
for j=1:n
    if (i_arc(j)>cur_bound)|(i_arc(j)<(-cur_bound))
       i_arc(j)=i_arc(j);
    else
      i_arc(j)=0;
    end
end

%--- Start Matrix calculations ---%
arc_start=340;                                           % Set start sample arc
arc_end=373;                                             % Set end sample arc
arc_vol=-60;                                             % Set assumed arc voltage
idiff=diff(i_arc)/(ts_matlab*wo);                        % Differentiate current
idiff(n)=0;                                              % Fill last sample lost in diff
nd=length(idiff);                                        % Determine number of samples
i2=i_arc.*i_arc;                                         % Current^2
i_id=i_arc.*idiff;                                       % Current times differentiated current
id2=idiff.*idiff;                                        % (Differentiated current)^2
us_i=(us_L1-arc_vol).*i_arc;                             % Supply voltage minus arc voltage times current
us_id=(us_L1-arc_vol).*idiff;                               % Supply voltage minus arc voltage times differentiated
current

%--- start summation
sum_i2=0; sum_i_id=0; sum_id2=0; sum_us_i=0; sum_us_id=0;
for k=arc_start:arc_end                                  % Index for matrix
    sum_i2=sum_i2+i2(k);                                 % Calaculate sum of current^2
    sum_i_id=sum_i_id+i_id(k);                           % Calaculate sum of differentiated current times current
    sum_id2=sum_id2+id2(k);                              % Calaculate sum of (differentiated current)^2
    sum_us_i=sum_us_i+us_i(k);                           % Calaculate sum of supply voltage time current
    sum_us_id=sum_us_id+us_id(k);                           % Calaculate sum of supply voltage time differentiated
current
end
um=[sum_us_i ;sum_us_id];                                % Setup matrix
im=[sum_i2 sum_i_id; sum_i_id sum_id2];                  % Setup matrix
result=im\um;                                               % Using Gaussian elimination instead of normal inverse
command
r=result(1,:)                                            % Cable resistance
l=result(2,:)                                            % Cable inductance

%--- Start Matrix calculations ---%
imin=inv(im);
chi=0;
for k=arc_start:arc_end
    chi=chi+((r*i_arc(k))+(l*idiff(k))+arc_vol-us_L1(k))^2;
    n=n+1;
end
chi=chi/(n-2);
error=imin*chi;
error_r=sqrt(error(1,1))
error_l=sqrt(error(2,2))
```

Appendix P : Results localisation calculations

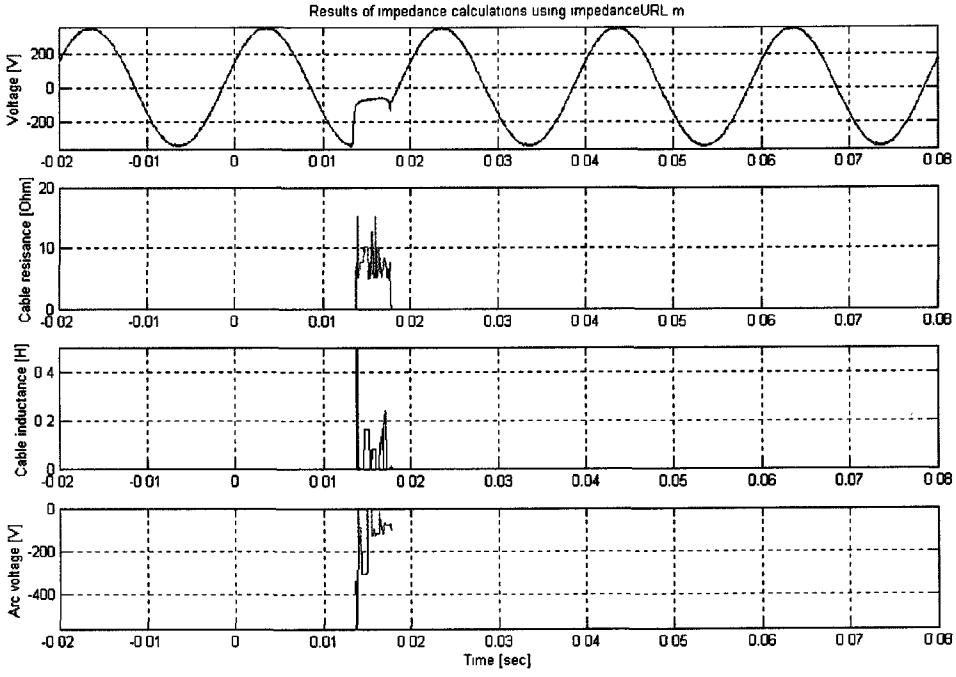

Figure P.1 Results after averaging and comparing the calculated arc voltage with the measured arc voltage.

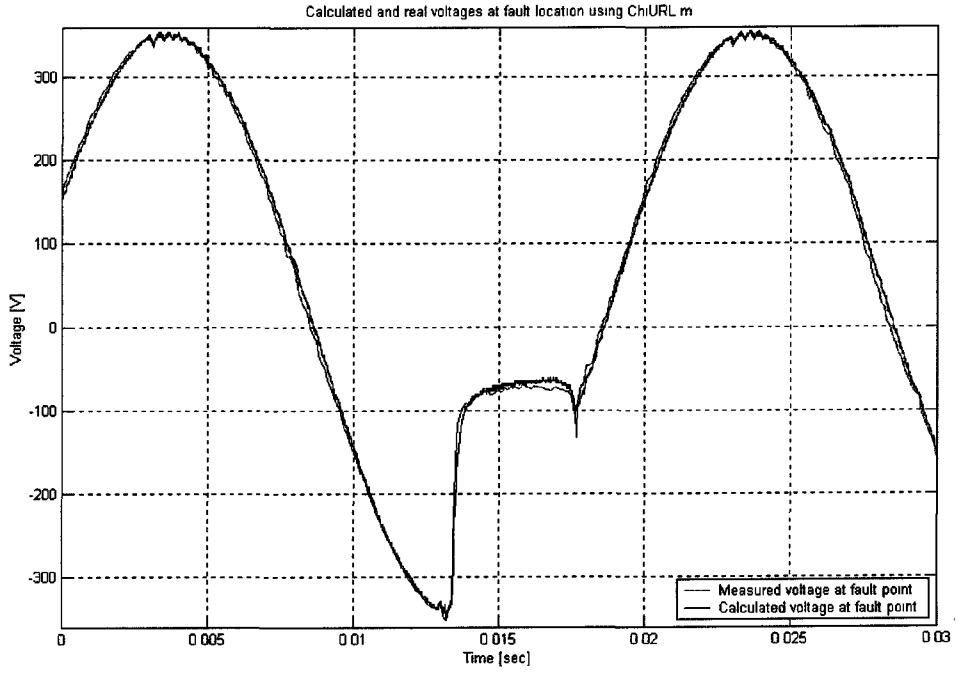

Figure P.2 Results of arc voltage calculations compared to the measured value.

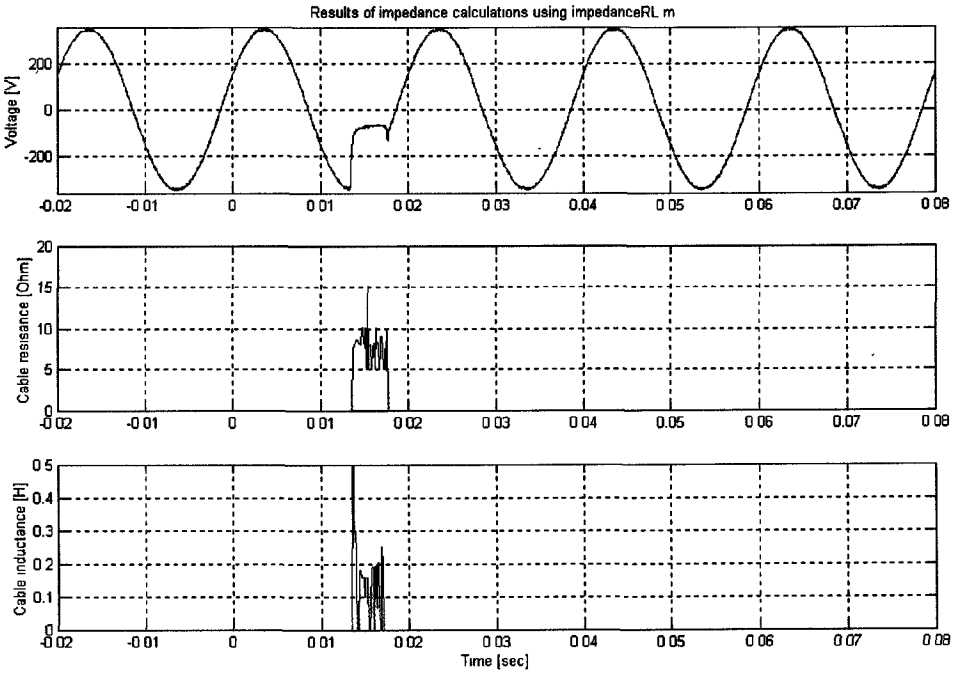

Figure P.3 Results of calculations.

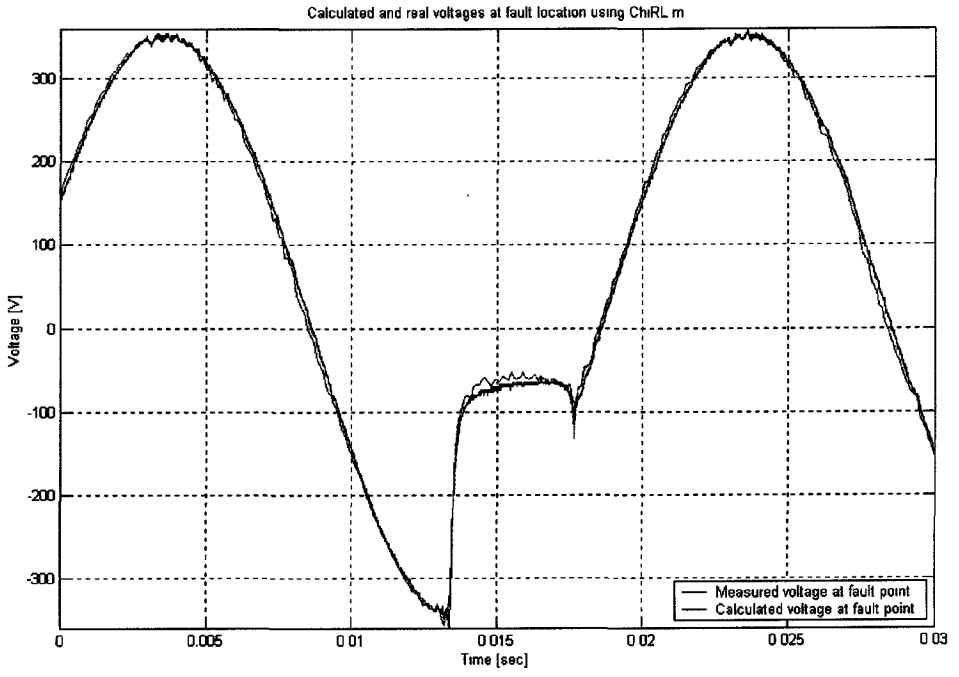

Figure P.4 Results of arc voltage calculations compared to the measured value.

Appendix Q : List of symbols

ε	*Relative permittivity, dielectric constant*	
C	*Capacitance*	*[F]*
C_0	*Characteristic capacitance*	*[F]*
C_c	*Cable capacitance*	*[F]*
g	*Arc conductance*	*[S]*
G	*Conductance*	*[S]*
I	*Current*	*[A]*
i	*Current*	*[A]*
i'	*Differentiated current*	
i_{arc}	*Arc current*	*[A]*
I_C	*Capacitive current*	*[A]*
I_c	*Charge/discharge current*	*[A]*
$i_{forward}$	*Forward waveform current*	*[A]*
I_{k1}	*Phase-earth short circuit Current*	*[A]*
I_{k2}	*Phase to phase short circuit current*	*[A]*
I_{k3}	*Three phase short circuit current*	*[A]*
I_R	*Resistive current*	*[A]*
$i_{reverse}$	*Reverse waveform current*	*[A]*
L	*Length of cable*	*[m]*
L	*Inductance*	*[H]*
m	*End sample*	
n	*Start sample*	
o	*Step in samples*	
P	*Power dissipation/losses*	*[W]*
P_0	*Cooling power*	*[VA]*
R	*Resistance*	*[Ohm]*
r	*Reflection coefficient*	
R_1	*Cable resistance of equipment*	*[Ohm]*
R_a	*Balance resistance*	*[Ohm]*
R_b	*Balance resistance*	*[Ohm]*
R_c	*Cable resistance*	*[Ohm]*
R_{fuse}	*Fuse resistance*	*[Ohm]*
R_{pm}	*Resistance per meter*	*[Ohm]*
R_x	*Resistance to fault*	*[Ohm]*
R_y	*Resistance to fault via healthy core*	*[Ohm]*
s	*Distance*	*[m]*
S_k	*Short circuit power*	*[VA]*
t	*Time*	*[sec]*
t_r	*Transmission coefficient*	
U	*Voltage*	*[V]*
u	*Voltage*	*[V]*
u_{arc}	*Arc voltage*	*[V]*
$u_{forward}$	*Forward waveform voltage*	*[V]*
$u_{reverse}$	*Reverse waveform voltage*	*[V]*
u_s	*Supply voltage [V]*	*[V]*
v	*Propagation speed*	*[m/sec]*
v_c	*Speed of light*	*[m/sec]*
W	*Energy*	*[J]*
W_{fuse}	*Energy*	*[Wh]*
x	*Transformer reactance*	*[%]*
X_{tr}	*Transformer impedance*	*[Ohm]*
Z_0	*Character impedance*	*[Ohm]*
$\underline{Z}_0$	*Zero sequence impedance*	*[Ohm]*
$\underline{Z}_1$	*Positive impedance*	*[Ohm]*
$\underline{Z}_2$	*Negative impedance*	*[Ohm]*
Z_f	*Fault impedance*	*[Ohm]*
δ	*Loss angle*	*[°]*
ε'	*Real frequency dependent relative permittivity*	
ε''	*Imaginary frequency dependent relative permittivity*	
τ	*Time constant arc*	*[sec]*
ω	*Angular frequency*	*[Rad/sec]*